

# **LAGRANGIAN SIMILARITY THEORY APPLIED TO DIFFUSION IN SURFACE LAYER OF THE ATMOSPHERE**

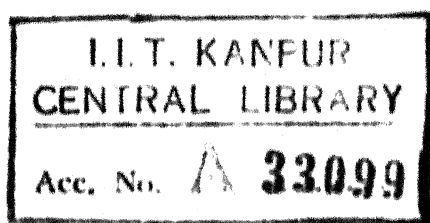
A Thesis Submitted  
In Partial Fulfilment of the Requirements  
for the Degree of  
DOCTOR OF PHILOSOPHY

By  
B. P. SWADAS

to the

**DEPARTMENT OF CIVIL ENGINEERING  
INDIAN INSTITUTE OF TECHNOLOGY KANPUR  
JULY 1974**

Thesis  
628.53  
SW11



5 MAR 1975

CE-1974-D-SWA-LAG



## SYNOPSIS

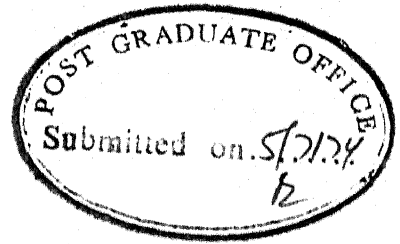
### LAGRANGIAN SIMILARITY THEORY APPLIED TO DIFFUSION IN SURFACE LAYER OF THE ATMOSPHERE

B. P. Swadas  
Department of Civil Engineering  
Indian Institute of Technology, Kanpur  
June, 1974

Diffusion models based on gradient-transfer theory or on statistical theory (such as of Bosanquet and Pearson, Sutton, Pasquill, etc.) are inadequate to rationally and completely describe the diffusion of pollutants released from a source in the surface layer of the atmosphere. Monin applied Lagrangian similarity theory to solve this problem. His work, however, did not cover practical ranges of investigation for the three - unstable, neutral and stable - conditions of the atmosphere, nor was tested on field data. Monin's approach has been extended in this work to cover all these ranges. Besides, unlike Monin's approach, where he assumed that the equations of motion represented boundaries of the plume, the author has proposed that the equations of motion be taken to represent the mean height of ensemble of particles. Equations have been derived mathematically relating mean vertical spread  $\bar{z}$ , mean downwind distance travelled  $\bar{x}$ , surface roughness length  $z_0$  and Monin-Obukhov stability length  $L$ . Solving these equations with the help of a digital computer, tables and graphs are presented to facilitate estimation of vertical spreads under given meteorological conditions.

The mathematical equations proposed were tested on field data from two comprehensive diffusion studies : one carried out in open unobstructed terrain, viz., Project Prairie Grass, O'Neill, Nebraska, U.S.A., and the other conducted in urban area of metropolitan St. Louis, Missouri, U.S.A. It was observed that there was a very close agreement in the observed vertical spreads and that computed by the proposed equations for both unstable as well as neutral conditions of the atmosphere for both the cases of low and high surface roughnesses. In comparison the extended Monin's approach gave smaller values of vertical spreads for both these stability conditions for both surface roughnesses, hence it may overestimate the concentration distribution. During stable atmospheric conditions, estimates of vertical spreads by both the approaches (Monin's as well as the proposed by author) were nearly equal, and generally agreed well with the observed spreads for  $\bar{z}/L \leq 0.1$ , beyond which the agreement was poor. Once the vertical spreads were estimated for any diffusion situation, concentration distribution could be easily computed assuming exponential distribution of particles.

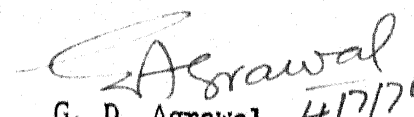
The mathematical models were also tested on limited data obtained from the city of Kanpur and they generally agreed well with the observed concentrations.




CERTIFICATE

Certified that the work presented in this thesis entitled 'Lagrangian Similarity Theory Applied to Diffusion in Surface Layer of the Atmosphere' by Shri B. P. Swadas has been carried out under my supervision and it has not been submitted elsewhere for a degree.

July, 1974.

  
G. D. Agrawal 4/7/74  
Professor  
Department of Civil Engineering  
Indian Institute of Technology  
Kanpur

POST GRADUATE OFFICE  
This thesis has been approved  
for the award of the Degree of  
Doctor of Philosophy (Ph.D.)  
in accordance with the  
regulations of the Indian  
Institute of Technology Kanpur  
Dated: 11/2/75 

Dedicated  
to  
the  
Lotus-feet  
of  
my Lord  
SWAMINARAYAN

## ACKNOWLEDGEMENTS

The author wishes to put on record his heartfelt appreciation to the following for helping to make this thesis possible :

Dr. G.D. Agrawal for his valuable guidance, inspiring suggestions, and encouraging advice throughout the course of research and thesis preparation.

Dr. A.V.S. Prabhakara Rao, Dr. Malay Chaudhuri, Dr. S.D. Bokil and Shri C. Venkobachar for their constant inspirations and encouragements.

All the members of the Environmental Engineering 'family' who, at some stage, have helped the author during his stay for the research work, with special reference to Sarvashri Subhash Verma, A.G.Menon and N. Sriramulu.

Dr. (Miss) A. Mani, Deputy Director-General (Instruments), Indian Meteorological Department, and Shri Surya Prakash, of Lucknow Met. office, for providing some balloons and giving all necessary information and help for this study.

Prof. R. S. Mehta, Vice-Chancellor, Sardar Patel University, Vallabh Vidyanagar, for his inspiring guidance and encouragement.

Management of Birla Vishvakarma Mahavidyalaya, Vallabh Vidyanagar, for deputation to pursue the study; and Ministry of Education, Government of India, for the financial support, made available under Quality Improvement Programme.

## TABLE OF CONTENTS

	PAGE
SYNOPSIS	
CERTIFICATE	
DEDICATION	
ACKNOWLEDGMENTS	
LIST OF TABLES	vi
LIST OF FIGURES	viii
1. INTRODUCTION	1
2. LITERATURE REVIEW	3
2.1 Transport of Pollutants in Air	3
2.2 Meteorological Elements Useful for Air Pollution Study	5
2.2.1. Basic Representation of Turbulent Motion	5
2.2.2. Boundary Layer	6
2.2.3. Vertical Wind Profile	6
2.2.3.1. Friction Velocity	6
2.2.3.2. Velocity Profile under Adiabatic Conditions	7
2.2.3.3. Wind Profile under Diabatic Conditions	9
2.2.4 Turbulent Fluctuations	13
2.2.4.1. Vertical Fluctuations	14
2.2.4.2. Lateral Fluctuations	15

2.2	Diffusion Theories	17
2.3.1.	The Gradient-Transfer Theory	18
2.3.1.1.	Limitations of Gradient-Transfer Theory	20
2.3.1.2.	Solution of Eq. (2.33)	22
2.3.2.	The Statistical Theory	25
2.3.2.1.	Sutton's Approach	26
2.3.2.2.	Pasquill's Method	28
2.3.2.3.	Concentration Distribution	33
2.3.3.	The Lagrangian Similarity Theory	35
2.4	Use of Lagrangian Similarity Theory to Estimate the Vertical Spread	38
3.	DEVELOPMENT OF A MATHEMATICAL MODEL FOR PREDICTION OF POLLUTANT CONCENTRATIONS	42
3.1	Importance of Mathematical Models	42
3.2	Earlier Models	43
3.2.1.	Bosanquet-Tearson Model	43
3.2.2.	Sutton's Model	45
3.2.3.	Pasquill's Method	45
3.2.4.	Model based on Lagrangian Similarity	46
3.3	Extension of Monin's Approach to Cover Practical Ranges of $z/L$ for All Conditions	47
3.3.1.	Unstable Atmosphere	48
3.3.2.	Stable Atmosphere	53
3.3.3.	Neutral Atmosphere	57
3.3.4.	Concentration Distribution by Monin's Approach	60
3.3.5.	Critical Appraisal of Monin's Approach	61

3.4	Objectives of this Study	62
3.5	Evolution of a Comprehensive Diffusion Model	63
3.5.1.	Estimation of Vertical Spread	63
3.5.1.1.	Neutral Atmosphere	66
3.5.1.2.	Unstable Atmosphere	71
3.5.1.3.	Stable Atmosphere	85
3.5.2	Estimation of Lateral Spread	92
3.5.3.	Estimation of Concentration Distribution	96
3.6	Closure	99
4.	VERIFICATION OF THE MATHEMATICAL MODEL ON AVAILABLE FIELD DATA	100
4.1	Dispersion Study at Project Prairie Grass	100
4.1.1.	Experimental Techniques	101
4.1.2.	Surface Roughness of IIG Site	102
4.1.3.	Stability Lengths for IIG Experiments	102
4.1.4.	Vertical Spreads at 100m from Source	103
4.1.5.	Vertical Spreads from Proposed Formulation	106
4.1.6.	Agreement of Observed and Computed Values of Vertical Spread	120
✓ 4.2	Dispersion Study at St. Louis	123
4.2.1.	Experimental Techniques	123
4.2.2.	Vertical Spreads	124
4.2.3.	Evaluation of Roughness Length	130



4.2.4.	Stability Lengths	137
4.2.5	Vertical Spread from Proposed Formulation	142
4.2.6	Agreement of Observed and Computed Values of Vertical Spread	148
5.	PROCEDURE FOR PREDICTION OF CONCENTRATIONS OF POLLUTANTS IN AIR UNDER DIFFERENT METEOROLOGICAL CONDITIONS	151
5.1	Micrometeorological Data	151
5.2	Zero-plane Displacement Length	152
5.3	Determination of Surface Roughness Length	153
5.3.1.	Instrumentation as Case One	153
5.3.2.	Instrumentation as Case Two and Case Three	155
5.4	Determination of Stability Length	155
5.4.1.	Instrumentation as Case One	155
5.4.2.	Instrumentation as Case Two	157
5.4.3.	Instrumentation as Case Three	157
5.5	Estimation of Vertical Spread	158
5.6	Estimation of Lateral Spread	159
5.7	Estimation of Concentration Distribution	164
6.	FIELD STUDIES DONE AT KANPUR	165
6.1	Introduction	165
6.2	Planning of Pollution Studies	166
6.3	Materials and Methods	167
6.3.1.	The Source	167
6.3.2.	Vertical Temperature Measurements	169

6.3.2.1.	Materials	169
6.3.2.2.	Methods	170
6.3.3.	Measurement of Wind Velocity	173
6.3.4.	Measurement of Sulphur-Dioxide Concentrations	174
6.4	Results and Discussions	174
6.4.1.	Zero-plane Displacement Length	174
6.4.2.	Surface Roughness Length	175
6.4.3.	Micrometeorological Measurements	176
6.4.4.	Calculation of Vertical Spread	179
6.4.5.	Calculation of Lateral Spread	180
6.4.6.	Computation of Concentrations	181
6.4.7.	Discussion of Results	183
7.	CONCLUSIONS	185
	APPENDICES	189
	REFERENCES	194

# LIST OF TABLES

TABLE		PAGE
2.1	Roughness Lengths of Various Surfaces	8
3.1	The Values of $z_{\max}/(-L)$ and Corresponding values of $b\bar{x}/(-L)$ , for Different $z_0/(-L)$ , by using Eqs. (3.4) and (3.6), for Unstable Atmospheric Conditions	51
3.2	The Values of $z_{\max}/L$ and Corresponding Values of $b\bar{x}/L$ , for Different $z_0/L$ , by using Eq. (3.13), for Stable Atmospheric Conditions.	55
3.3	The Values of $z_{\max}/z_0$ and corresponding Values of $\bar{x}/z_0$ , from Eq. (3.16), for Neutral Atmospheric Conditions, taking $b = 1.2$	58
3.4	The Values of $\bar{z}/z_0$ and Corresponding Values of $\bar{x}/z_0$ , from Eq. (3.32), for Neutral Atmospheric Conditions	69
3.5	The Values of $\bar{z}/(-L)$ and Corresponding Values of $k^2\bar{x}/(-L)$ , for Different $z_0/(-L)$ , by using Eqs. (3.42) - (3.43) and (3.47), for Unstable Atmospheric Conditions	86
3.6	The Values of $\bar{z}/L$ and Corresponding Values of $k^2\bar{x}/L$ , for Different $z_0/L$ , using Eq. (3.58), for Stable Atmospheric Conditions	93
4.1	Standard Deviations of Vertical Spread at 100 m and Stability Lengths $L$ for PPG Experiments	104
4.2	Comparison of Standard Deviations of Vertical Spread as Calculated from Proposed Formulation	109

## TABLE

## PAGE

4.3	Comparison of Standard Deviations of Vertical Spread as Calculated from Extension of Monin's Approach	112
4.4	Standard Deviations of Vertical Spread at 100 m, as Calculated by Proposed Formulation	116
4.5	Standard Deviations of Vertical Spreads at 100 m, as Calculated from Extended Monin's Approach	117
4.6	Stability Categories of McElroy and Pooler	125
4.7	Summary of Dispersion Data and Meteorological Indices for St. Louis Dispersion Study	126 ✓
4.8	Evaluation of $z_0$ from Half-Hourly Wind Data, using Eq. (4.5)	132
4.9	Mean and Standard Deviation of $z_0$	134
4.10	Average Values of $\sigma_\theta$ for Four Stability Categories	138
4.11	Stability Lengths for Four Stability Categories	142
6.1	Details of Chimney of Riverside Power-House, Kanpur	168
6.2	Particulars of Boilers of Riverside Power-House, Kanpur	168
6.3	Wind Speed and Vertical Temperatures for Kanpur Study	178
6.4	Values of Stability Parameters for Kanpur Study	179
6.5	Vertical Spread $\bar{z}$ for Kanpur Study	179
6.6	Lateral Spreads $\sigma_y$ for Kanpur Study	180
6.7	Pollutant Concentration Values for Kanpur Study	182

# LIST OF FIGURES

FIGURE		PAGE
2.1	Comparison of the Results of the St. Louis (McElroy and Pooler, 1968b) Experiments with those Summarized by Tasquill and Gifford (1961)	32
3.1	Major Elements of the Urban Air Pollution Problem Connected with Mathematical Modelling	44
3.2	Plot of $z_{\max}/(-L)$ Vs. $bk\bar{x}/(-L)$ , for Different Values of $z_0/(-L)$ , as given by Eqs. (3.4) and (3.6), for Unstable Atmospheric Conditions	52
3.3	Plot of $z_{\max}/L$ Vs. $bk\bar{x}/L$ , for Different Values of $z_0/L$ , as given by Eq. (3.13), for Stable Atmospheric Conditions	56
3.4	Plot of $z_{\max}/z_0$ Vs. $\bar{x}/z_0$ , as given by Eq. (3.16), for Neutral Atmospheric Conditions, taking $b=1.2$	59
3.5	Plot of $\bar{z}/z_0$ Vs. $\bar{x}/z_0$ , as given by Eq. (3.32), for Neutral Atmospheric Conditions	70
3.6	Plot of $\bar{z}/(-L)$ Vs. $k^2\bar{x}/(-L)$ for Different Values of $z_0/(-L)$ , as given by Eqs. (3.42)-(3.43) and (3.47), for Unstable Atmospheric Conditions	87
3.7	Plot of $\bar{z}/L$ Vs. $k^2\bar{x}/L$ for Different Values of $z_0/L$ , as given by Eq. (3.58), for Stable Atmospheric Conditions	94
4.1	Comparison of Vertical Spread at 100m from a Source, $z_0=0.008m$	119
4.2	Comparison of Vertical Spread at St. Louis	144
4.3	Comparison of Vertical Spread at St. Louis	145

4.4	Comparison of Vertical Spread at St. Louis	146
4.5	Comparison of Vertical Spread at St. Louis	147
5.1	Plot of $\bar{x}/z_0$ Vs $\bar{z}/z_0$ for Unstable Atmosphere	160
5.2	Plot of $\bar{x}/z_0$ Vs $\bar{z}/z_0$ for Stable Atmosphere	161
5.3	Relation between the Ratio of Half-width of Maximum Fluctuations the r.m.s. Value and the Sampling Time $\tau$ (After Hino, 1968b)	163

## Chapter One

### 1. INTRODUCTION

This God-made space ship Earth is enveloped with a thin and frail veil of air that is pre-requisite to the life. For too long men have treated the atmosphere as a sink, dumping vast quantities of effluents into it, oblivious to the fact that the air is not an unlimited resource and that the ability of air to cleanse itself of poison is not infinite.

Of all the threats to our environment, air pollution is potentially the most dangerous, because whereas we may replenish soil or purify water before use, we breathe the air as it comes to us - and each day it comes to us more heavily laden with the by-product wastes of our industrialized society.

Abundant evidence has established that air pollution adversely affects man and his environment. It is a definite factor in human and animal morbidity and mortality. It damages vegetation, accelerates corrosion and deterioration of materials, soils property, and interferes with the comfortable enjoyment of life and property. It affects climate, reduces visibility and solar radiation and contributes to safety hazards. In spite of the overwhelming evidence of deleterious effects of air pollution, complete elimination of the sources of air pollution is not possible at the present or in the foreseeable future. It is woven throughout the fabric of our daily lives.

Major proportion of our present-day air pollution is contributed by urbanization and industrialization. The pace of urbanization is very

great among both the developed as well as the developing countries. This has increased the levels of air pollutants, and it will continue to do so unless something is done about it. The existing sources of air pollution should be judiciously controlled and the future development should be rationally planned. The effects of air pollution are obviously proportional to the concentrations of pollutants prevailing in the ambient air. The concentrations, among other things, will largely depend on the ability of the atmosphere to disperse the pollutants. Thus, to prescribe a degree of control in any air pollution control programme one must take into consideration the dispersion characteristics of the atmosphere. This has led to the search for an adequate mathematical model of diffusion pattern of air pollutants over the urban areas. Quite a few diffusion theories have been proposed for individual sources, either instantaneous or continuous.

The study reported herein is concerned with the application of the Lagrangian similarity theory to predict the spreads of the pollutants in the field. Both the adiabatic and diabatic stability conditions of the atmosphere are studied.

The effects of the variation of aerodynamic roughness on the spread, and hence on the concentration, of pollutants have also been studied.



## Chapter Two

### 2. LITERATURE REVIEW

#### 2.1 Transport of Pollutants in Air

Just as in the case of a polluted stream or river, a polluted air environment undergoes self-purification. The self-purification of a stream is primarily the result of biological action and dilution. In the atmosphere, several self-purification mechanisms, such as sedimentation of particulate matter, washing action of rain, photochemical reactions, absorption by vegetation, soil, etc., are at work along with the dilution of pollutants. Unlike stream pollution, where the water flow confines within certain finite boundaries, the spread of air pollutants is three dimensional and may not confine within finite boundaries. The general area into which pollutants released from a source move is specified by the wind direction, which itself changes from time to time.

The dilution of air pollutants in the atmosphere is of prime importance in the prevention of undesirable levels of pollution, and it is due to two physically separable processes of advection and diffusion (Monin, 1959a). Advection brings about the transport of pollutants due to mean wind. Other things being equal, the concentration of a pollutant downwind from a source varies inversely with the wind speed (Hewson, 1955). Diffusion transfers the pollutant from regions of higher concentration to regions of lower concentration, and proceeds by two different processes of molecular diffusion and eddy dispersion. Molecular diffusion, caused by Brownian motion of molecules, is several thousands of times slower than

4

eddy diffusion or dispersion, which is due to the transport by fluid eddies. Hence, in atmospheric diffusion problems molecular diffusion is often neglected (Sutton, 1953).

Atmospheric turbulence produces eddy dispersion, and the study of atmospheric diffusion problems has closely followed developments in the study of turbulence in general.

Atmospheric turbulence is classified as mechanical or thermal as they are produced primarily by shearing stress or by convection (Wanta, 1968). While both types are often present in combination, one or the other may dominate under particular meteorological conditions. Mechanical turbulence prevails in stable air, whereas in unstable air thermal turbulence generally predominates.

Turbulence increases with increase of wind shear, surface roughness and instability (Gifford, 1968). High winds and unstable thermal stratification favour rapid diffusion, whereas inversion conditions of the atmosphere along with light winds impede the diffusion of pollutants.

It is not particularly difficult to describe qualitatively the concept of the diffusion of air pollutants in the atmosphere, but it is more difficult to express these facts quantitatively in a form so that predictions can be made. Many theories have been proposed to predict the downwind concentration of pollutant in terms of source strength and meteorological parameters. Meteorological conditions are obviously of prime importance in such predictions. The existing concepts regarding such parameters and the major theories for interpretation of transport of pollutants are briefly reviewed in the following sections.

## 2.2 Meteorological Elements Useful for Air Pollution Study

An exhaustive discussion of the meteorological elements useful for the air pollution study has been given by Sutton (1953), Priestley (1959), and Lumley and Panofsky (1964). Matveev (1967) has also discussed the topics in great details, with special reference to contributions of Russian research workers on the topic.

### 2.2.1. Basic Representation of Turbulent Motion

Sutton (1953) describes the components of velocity measured at a point  $(x, y, z)$  by  $u, v, w$ . In turbulent flow all three components are functions of time as well as of position. The mean velocity, with components  $\bar{u}, \bar{v}, \bar{w}$ , is defined at a fixed point and at a time  $t_0$  by

$$\begin{aligned}\bar{u} &= \frac{1}{T} \int_{t_0 - \frac{1}{2}T}^{t_0 + \frac{1}{2}T} u \, dt \\ \bar{v} &= \frac{1}{T} \int_{t_0 - \frac{1}{2}T}^{t_0 + \frac{1}{2}T} v \, dt \\ \bar{w} &= \frac{1}{T} \int_{t_0 - \frac{1}{2}T}^{t_0 + \frac{1}{2}T} w \, dt\end{aligned}\tag{2.1}$$

where  $T$  is an arbitrary interval called the period of sampling.

A fluctuation, or eddy velocity,  $u', v', w'$ , is defined as the difference between the total velocity at any instant and the mean velocity, so that

$$\begin{aligned}u' &= u - \bar{u} \\ v' &= v - \bar{v} \\ w' &= w - \bar{w}\end{aligned}\tag{2.2}$$

### 2.2.2. Boundary Layer

Following Prandtl's boundary layer theory (Goldstein, 1938; Rouse, 1959), the atmosphere near the earth's surface is divided into the planetary boundary layer close to the surface, and above this, the free atmosphere. In the planetary boundary layer (upto 1 to 1.5 km) the character of motion is considerably influenced by the underlying surface and turbulent friction (Matveev, 1967). The diurnal variations in the meteorological elements are pronounced in this layer.

Within the boundary layer, a surface layer of the atmosphere (50 - 200 m) is distinguished (Sutton, 1953), in which the eddy transport of heat and the eddy viscosity stress can be considered constant (i.e. independent of height) to a sufficient accuracy (Prandtl and Tietjens, 1934).

The laws governing processes in the surface layer are very different from those operating elsewhere in the atmosphere (Matveev, 1967). The state of the surface layer is very closely related to the state of the active layer of the earth's surface. Meteorological elements undergo sharp variations in height and time. The vertical gradients of the meteorological elements are one or two orders larger than aloft (Priestley, 1959).

### 2.2.3. Vertical Wind Profile

#### 2.2.3.1 Friction Velocity

The assumptions that the lowest layer of the atmosphere can be regarded as part of a fully developed turbulent boundary layer and that

the eddy shearing stress is invariant with height in the surface layer of the atmosphere, provided the basis to define the friction velocity,  $u_*$ , (Goldstein, 1938) as

$$u_* = (\tau/\rho)^{1/2} \quad (2.3)$$

where  $\tau$  is the constant eddy shearing stress and  $\rho$  is the density of air. The friction velocity, (constant with height), depends on the nature of the surface and magnitude of the mean velocity (Lumley and Panofsky, 1964).

#### 2.2.3.2 Velocity Profile under Adiabatic Conditions

For adiabatic conditions of the atmosphere, following the classical experiments of Nikuradse (Priestley, 1959), the variation of mean wind velocity  $\bar{u}$  with height  $z$  from the earth's surface, is given by

$$\bar{u} = \frac{u_*}{k} \ln z + \text{constant} \quad (2.4)$$

where  $k$  is Von Karman's constant and is approximately equal to 0.4.

The equation is also written in the forms (Sutton, 1953) :

$$\bar{u} = \frac{u_*}{k} \ln \frac{z}{z_0} \quad (2.4a)$$

$$\text{or} \quad \bar{u} = \frac{u_*}{k} \ln \frac{z + z_0}{z_0} \quad (2.4b)$$

where  $z_0$  is the roughness length (the height above surface at which  $\bar{u} = 0$ ) which is related to the size of the proturbenances, and varies from a fraction of a centimetre over smooth surfaces like mudflats, ice, etc. to several metres over urban areas. In Table 2.1, some values of  $z_0$  are listed.

TABLE 2.1  
ROUGHNESS LENGTHS OF VARIOUS SURFACES

Type of Surface	$z_0$ , cm	Reference
Smooth mud flats, ice	0.001	Sutton (1953)
Mown grass, upto 4.5 cm	0.2 - 2.4	Priestley (1959)
Long grass, upto 60 - 70 cm	3.7 - 9.0	Priestley (1959)
Air field	2.5	Matveev (1967)
Urban areas		
Copenhagen	3000	Davenport (1961)
Tokyo suburbs	3000	Davenport (1961)
Reading	700	Pasquill (1970a)
London	2300	Pasquill (1971)

The roughness length,  $z_0$ , cannot be interpreted as a function only of the surface elements directly below the anemometers. In fact the roughness parameters, as suggested by O'Brien (1965), may vary considerably according to the influence of upstream topography. He obtained  $z_0$  by least-square analysis of the wind-profile data near the surface of the earth. To get roughness length,  $z_0$ , Anisimova et al. (1965) use Eq. (2.4a) at two heights with half-hourly average values of wind velocities, thus give

$$\ln z_0 = \frac{u_2 \ln z_1 - u_1 \ln z_2}{u_2 - u_1} \quad (2.5)$$

For very rough surfaces, as found in urban localities, the height  $z$  in Eq. (2.4) is taken as  $(z-d)$  where  $d$  is an arbitrary zero-plane

displacement length (Sutton, 1953). A simple method of approximating  $z_0$  and  $d$  has been given by Kutzbach (1961, quoted by Hanna, 1969). If  $\Lambda$  is the ratio of the total area of a given region to the area of the buildings in that region, and  $h$  is the average height of the buildings, then Kutzbach suggests the laws :

$$\frac{d}{h} \approx \Lambda^{-0.3} \quad (2.6a)$$

$$\frac{z_0}{h} \approx \Lambda^{-1.1} \quad (2.6b)$$

The parameter  $\Lambda$  varies from 2 to 10 for cities, consequently, if  $h$  is about 10 m, the roughness length  $z_0$  is between 0.5 and 2m and the displacement length  $d$  is between 6m and 9m.

### 2.2.3.3 Wind Profile under Diabatic Conditions

When the air is being heated or cooled from below, the effects of thermal stratification and buoyancy have also to be considered, so that at least one more basic parameter is required before the wind profile can be specified (Priestley, 1959). Richardson (1926) number has been used for this purpose (Batchelor, 1953). The Richardson number,  $Ri$ , is a dimensionless ratio of buoyancy forces to inertia forces in the atmosphere. Thus

$$Ri = \frac{g}{T} \frac{(\partial T / \partial z + \Gamma)}{(\partial \bar{u} / \partial z)^2} \quad (2.7)$$

where  $g$  is the acceleration due to gravity,  $T$  is the absolute temperature, and  $\Gamma$  is the adiabatic lapse rate ( $\approx 1^\circ \text{C}/100 \text{ m}$ ). Following Monin and Obukhov (1954), Russian workers have used  $z/L$  as the basic parameter in

place of the Richardson number, where  $L$  is the scaling length defined on dimensional grounds as

$$L = - \frac{u_*^3}{k(g/T)(H/c_p \rho)} \quad (2.8)$$

where  $H$  is the heat flux in the vertical direction, and  $c_p$  the specific heat of air at constant pressure ( $= 0.24 \text{ cal/}^\circ \text{C} - \text{gram}$ ). When the atmosphere is unstable, both  $Ri$  and  $z/L$  are negative; and for stable atmosphere, both are positive (Lumley and Panofsky, 1964).

Of the purely empirical extension of the wind profile law to the diabatic atmospheric condition, the most applicable is that due independently to Laikhtman (1944, cited by Priestley, 1959) and Deacon (1949) who proposed the form

$$\frac{d\bar{u}}{dz} = \Lambda z^{-\beta} \quad (2.9)$$

where  $\Lambda$  is independent of  $z$ , and  $\beta$  is greater or less than unity in unstable or stable conditions respectively. Deacon's observations showed that the magnitude of  $\beta$  determined from mean profiles was related to the Richardson number. Rider (1954) found satisfactory agreement of this relationship in all but stable conditions. Deacon (1957) pointed out that  $\beta$  is not truly constant with height. Pasquill (1962a) observed that the determination of  $\beta$  implies a knowledge of  $d^2\bar{u}/dz^2$  which is difficult to achieve with sufficient accuracy.

Another empirical relation used to represent the wind profile is by the power law (Frost, 1947; as reported by Sutton, 1953)

$$\bar{u} = \bar{u}_1 \left( \frac{z}{z_1} \right)^p \quad (2.10)$$



where  $\bar{u}_1$  is the mean velocity at a fixed reference height  $z_1$ , and  $p$  is an index which depends on the stability of the atmosphere. Frost reported different values of  $p$  related to the temperature difference between 5 and 400 ft. Although the power law proposed by Deacon (Eq.(2.9)) is different from that given by Eq. (2.10) (Sutton, 1953), the difficulties in determining  $p$  are similar to those in determining  $\beta$ .

Most of the recent progress in the understanding of the wind profile has been brought about by the Monin - Obukhov (1954) 'similarity theory'. According to this theory, there exist, near the ground, a friction velocity  $u_*$  and a scaling length  $L$  that are essentially invariant with height, and the flow characteristics in the surface layer of the atmosphere can entirely be determined by them. On dimensional grounds, Monin and Obukhov (1954) proposed the generalized wind profile relationship as

$$\frac{d\bar{u}}{dz} = \frac{u_*^2}{K_M} = \frac{u_*}{k} \cdot \frac{1}{z} \phi(z/L) \quad (2.11)$$

where  $K_M$  is the eddy viscosity and  $\phi(z/L)$  is the universal function of the dimensionless ratio  $z/L$ , which, for small values of  $z/L$ , they gave as

$$\phi(z/L) \approx 1 + \alpha z/L \quad (2.12)$$

where  $\alpha$  is a universal constant. Thus, for adiabatic conditions,  $L$  tends to infinity and  $\phi(z/L)$  tends to unity, giving

$$\frac{d\bar{u}}{dz} = \frac{u_*}{k} \cdot \frac{1}{z} \quad (2.13)$$

which, on integration, gives Eq. (2.5). For diabatic conditions and

small values of  $z/L$ , Monin - Obukhov relation gives

$$\bar{u} = \frac{u_*}{k} \left( \ln \frac{z}{z_0} + \alpha \frac{z - z_0}{L} \right) \quad (2.14)$$

The constant  $\alpha$  was originally assigned the value of 0.6 by Monin and Obukhov (1954) on the basis of experimentally determined wind profiles, but there is a controversy regarding the numerical value of  $\alpha$ , and the question of the numerical value of the constant  $\alpha$  and its universality can not be considered to have been settled (Matveev, 1967). The value of  $\alpha$  depends on the stability conditions (Takeuchi, 1961). For unstable conditions, the values of  $\alpha$  suggested are 0.7 (Ellison, 1957), 4.5 (Panofsky et al., 1960), 3.0 (Taylor, 1960), 0.6 (O'Brien, 1965), etc.; whereas for stable conditions 6.0 (Taylor, 1960), 7.0 (McVehil, 1962; quoted by Lumley and Panofsky, 1964), 5.0 (O'Brien, 1965), 4.7 (Businger et al., 1971), etc.

Avoiding the evaluation of  $\alpha$ , Swinbank (1962; 1964) suggested an exponential wind profile as

$$\frac{d\bar{u}}{dz} = \frac{u_*}{kL} \frac{1}{(1 - \exp(-z/L))} \quad (2.13a)$$

and 
$$\bar{u} = \frac{u_*}{k} \ln \left( \frac{\exp z/L - 1}{\exp z_0/L - 1} \right) \quad (2.14a)$$

The wind profile for highly unstable stratification (free convection condition) has been given by Kazanskii and Monin (Kazanskii, 1965; Gurvich, 1965) as

$$\bar{u} = c(-z/L)^{-1/3} + \text{constant} \quad (2.15)$$

where  $c$  is a constant, which is evaluated as very near unity (Gifford, 1962). Gurvich (1965) recommends  $c = 1.3 - 1.4$ . Priestley (1959) reported

that the free convection begins at about  $Ri = -0.03$ . Gurvich (1965), and Kazanskii (1965) take free convection conditions at  $Ri = -0.03$  to  $-0.05$ , whereas Taylor (1960) takes at  $Ri = -0.08$ .

In general, according to Monin - Obukhov similarity theory,

$$\bar{u} = \frac{u_*}{k} f(z/L) - f(z_0/L) \quad (2.16)$$

where  $f(z/L)$  is a universal function of  $z/L$  and  $f(z_0/L)$  is the similar function of  $z_0/L$ .

The relation between the Richardson number  $Ri$  and the Monin-Obukhov stability parameter  $z/L$  can be theoretical established (for example, Kazanskii, 1965) as

$$z/L = (K_H/K_M) \cdot Ri \quad (z/L) \quad (2.17)$$

where  $K_H$  is the eddy conductivity,  $K_M$  the eddy viscosity, and  $(z/L)$  is same universal function defined in Eq. (2.11). For the unstable conditions of the atmosphere, Pandolfo (1966) has suggested the relation

$$K_M = K_H \cdot \phi(z/L) \quad (2.18)$$

Hence, from Eqs. (2.17) and (2.18), for unstable conditions, the stability parameters  $z/L$  and  $Ri$  are equal. This has also been tested experimentally by Businger et al. (1971).

#### 2.2.4. Turbulent Fluctuations

Lumley and Panofsky (1964) reported that turbulent fluctuations of velocity, which are responsible for the transfer processes in the surface layer of the atmosphere, are relatively stable when averaged

over a time of the order of 10 to 20 minutes.

According to Monin (1962), the joint probability distribution for the values of dimensionless fluctuations at a fixed point in space-time depends only upon the parameter  $z/L$ . He reports that the first moments of this distribution are equal to zero, and all the second moments can be expressed by means of standard deviations  $\sigma_u/u_*$ ,  $\sigma_v/u_*$  and  $\sigma_w/u_*$  considered as functions of  $z/L$ , where  $\sigma_u$ ,  $\sigma_v$ ,  $\sigma_w$  are the standard deviations of axial, lateral and vertical velocities respectively.

#### 2.2.4.1 Vertical Fluctuations

On the basis of the Monin-Obukhov similarity theory, the standard deviation of vertical velocity,  $\sigma_w$ , is given by an equation of the form (Monin, 1959b)

$$\sigma_w = b u_* h(z/L) \quad (2.19)$$

where  $b$  is a constant and  $h(z/L)$  is a universal function of the dimensionless parameter  $z/L$ . Monin (1959b) further showed from the equation of energy balance that the function  $h(z/L)$  was of the form

$$h(z/L) = \left[ 1 - \frac{z/L}{\phi(z/L)} \right]^{\frac{1}{4}} \quad (2.20)$$

where  $\phi(z/L)$  is as defined earlier in Eq. (2.11).

Panofsky and Mc Cormick (1960) suggest the relation

$$\sigma_w = b u_* [\phi(z/L) - 2.4 (z/L)]^{1/3} \quad (2.21)$$

on dimensional arguments.

Hanna (1968) reports that both the above formulae correspond to the experimental data for  $z/L \geq -5$ , but for  $z/L < -5$ , the agreement is poor, and hence he suggests the form

$$\sigma_w = b u_* (1 + 7 z/(-L))^{1/6} \quad (2.22)$$

for unstable atmospheric conditions.

For adiabatic conditions of the atmosphere,  $L$  tends to infinity and

$$\sigma_w = b u_* \quad (2.23)$$

thus giving that  $b$  is the ratio of the standard deviation of vertical velocity under adiabatic conditions to the friction velocity  $u_*$

(Lumley and Panofsky, 1964). The value of  $b$  is in dispute between Western and Russian workers. Panofsky and McCormick (1960) obtained  $b$  as 1.25, Pasquill (1962b) as 1.33, Pasquill (1966) as 1.25.

Monin (1962) reported  $b$  as 0.7, Gurvich as 0.7, Perepelkina as 0.87 (reported by Lumley and Panofsky, 1964). The estimate of Busch and Panofsky (1968) leads to more generally accepted value of  $b$  as 1.3.

#### 2.2.4.2 Lateral Fluctuations

Unlike  $\sigma_w$ , the standard deviation of lateral velocity,  $\sigma_v$ , is insensitive to changes in height (Lumley and Panofsky, 1964), and is given by

$$\sigma_v = \sigma_\theta \bar{u} \quad (2.24)$$

where  $\sigma_\theta$  is the standard deviation of azimuth, which is usually measured, and  $\sigma_\theta$  and  $\bar{u}$  are measured at the same height.

Panofsky and Prasad (1965) related  $\sigma_v/u_*$  with a non-dimensional stability ratio B which they define as

$$B = \frac{\beta}{T} \cdot \frac{z^2}{u} \cdot \left( \frac{\partial T}{\partial z} + \Gamma \right) \quad (2.25)$$

They have also shown a graphical relationship between B and  $z/L$ .

Monin (1965), in his theoretical analysis of turbulence, gives the following relations

$$\frac{\sigma_u^2}{\sigma_v^2} = 1 + \left( \frac{\sigma_{u_0}^2}{\sigma_{v_0}^2} - 1 \right) \left( \frac{\phi(z/L)}{\phi(z/L) - z/L} \right) \quad (2.26)$$

$$\text{and } \frac{\sigma_w^2}{\sigma_v^2} = \frac{\sigma_{w_0}^2}{\sigma_{v_0}^2} - \left( \frac{\sigma_{u_0}^2}{\sigma_{v_0}^2} - 1 \right) \left( \frac{z/L}{\phi(z/L) - z/L} \right) \quad (2.27)$$

where  $\sigma_u$  is the standard deviation of longitudinal velocity,  $(z/L)$  is as defined earlier in Eq. (2.11), and  $\sigma_{u_0}$ ,  $\sigma_{v_0}$ ,  $\sigma_{w_0}$  are the values of  $\sigma_u$ ,  $\sigma_v$ ,  $\sigma_w$  under neutral conditions of the atmosphere.

Lateral Standard Deviation,  $\sigma_v$  is insensitive to changes in height, but is very sensitive to changes in stability. Hence Cramer (1959) has used  $\sigma_\theta (= \sigma_v/\bar{u})$  as predictor for other characteristics of turbulence. Inoue (1959) has also shown a relation to relate with stability parameters, as

$$\sigma_\theta = \frac{\beta u_*}{\bar{u}} \quad (2.24a)$$

where  $\beta$  is a constant, and  $\sigma_\theta$  and  $\bar{u}$  are reckoned at same height.

From Eq. (2.16)

$$\sigma_{\theta} = \frac{\beta k}{f\left(\frac{z}{L}\right) - f\left(\frac{z_0}{L}\right)} \quad (2.24b)$$

### 2.3. Diffusion Theories

The problem of turbulent diffusion in the atmosphere has not yet been uniquely formulated in the sense that a single basic physical model capable of explaining all the significant aspects of the problem has not yet been proposed. There are three alternative approaches available, none of which can be categorically eliminated from consideration since each has areas of utility (Gifford, 1968).

The theoretical treatment of diffusion in a turbulent field has developed along the following main lines :

1. Gradient-transfer theory
2. Statistical theory
3. Lagrangian Similarity theory.

In the first, the eddy transfer of material across a plane is represented as a product of the gradient of material (normal to the plane) and an eddy diffusivity. This theory is Eulerian in nature in that it considers properties of the fluid motion relative to a spatially fixed coordinate system. The second and third theories involve statistical descriptions and laws for velocities and trajectories of typical particles in the fluid, and thus can be described as Lagrangian.

### 2.3.1. The Gradient - Transfer Theory

In his studies of molecular diffusion, Fick showed that (Goldstein, 1938) the diffusive flux of a substance is proportional to the gradient of its concentration. Thus, mass flux  $J_i$  of a material is given by

$$J_i = k_d \frac{\partial c}{\partial i} \quad (2.28)$$

where  $k_d$  is the coefficient of molecular diffusion,  $c$  the concentration of material, and  $i$  the coordinate direction parallel to flow and perpendicular to reference plane.

Analogous to the molecular diffusion given by Fick, Schmidt developed a theory in 1925 for the diffusion in turbulent flow (Sutton, 1953). He assumed that a fluid in turbulent motion has a kind of granular structure, in which 'lumps' or 'eddies' of fluid break away from the mean motion and lead an independent life for a short time, and absorb again into the mean flow at some different level. These eddies transfer the material or momentum in the body of fluid.

Schmidt showed that for a turbulent flow, the instantaneous flux of material through a unit area of  $x$ - $y$  plane can be given by

$$J_z = k_d \frac{\partial c}{\partial z} + \rho c w' \quad (2.29)$$

where the first term on the right hand side is the contribution arising from the molecular agitation, and the second term shows that due to turbulent fluctuations. Taking an instantaneous values



of  $c$  to be made up of mean component  $\bar{c}$  and fluctuation  $c'$ , i.e.

$c = \bar{c} + c'$ , he got the mean flux as

$$J_z(\text{mean}) = k_d \frac{\partial \bar{c}}{\partial z} + \overline{c' w'} \quad (2.30)$$

Using the exchange-coefficient hypothesis, the term  $\overline{c' w'}$  can be expressed as the product of a virtual coefficient of diffusion and the gradient of the mean entity  $\frac{\partial \bar{c}}{\partial z}$  (Schmidt, 1925; reported by Sutton, 1953). If  $K$  is this coefficient, on this hypothesis

$$J_z(\text{mean}) = (k_d + K) \frac{\partial \bar{c}}{\partial z} \quad (2.31)$$

Usually  $K \gg k_d$  (Sutton, 1953), hence

$$J_z(\text{mean}) \approx K \frac{\partial \bar{c}}{\partial z} \quad (2.32)$$

which is analogous to Eq. (2.28).

Richardson independently applied similar hypothesis to the atmospheric diffusion in 1926 (Gifford, 1968).

Using Eq. (2.32) with a continuity equation, Schmidt derived a general equation of diffusion in three dimensions, as

$$\frac{\partial \bar{c}}{\partial t} = \frac{\partial}{\partial x} (K_x \frac{\partial \bar{c}}{\partial x}) + \frac{\partial}{\partial y} (K_y \frac{\partial \bar{c}}{\partial y}) + \frac{\partial}{\partial z} (K_z \frac{\partial \bar{c}}{\partial z}) \quad (2.33)$$

where  $K_x$ ,  $K_y$  and  $K_z$  are the eddy diffusion coefficients in the  $x$ -,  $y$ -, and  $z$ -directions.

The problem of the atmospheric diffusion is reduced to that of solving Eq. (2.33) under appropriate boundary conditions. This is called the gradient - transfer theory or the  $K$ -theory. If  $K_x$ ,  $K_y$

and  $K_z$  are independent of spatial coordinates, the diffusion becomes Fickian (Pasquill, 1962a).

### 2.3.1.1. Limitations of Gradient-Transfer Theory

The entire gradient-transfer theory of diffusion hinges over the selection of the eddy coefficients of diffusion,  $K_x$ ,  $K_y$  and  $K_z$ . There are two main points to be noted regarding this.

The exchange-coefficient hypothesis, as stated earlier, is based on the postulate that the rate of transfer of a conservative entity is proportional to the gradient of the mean value of the entity; the exchange coefficient is simply the factor of proportionality. Provided that this be accepted as a definition, no objection can be raised to the gradient-transfer theory in a mathematical sense (Sutton, 1953). In the physical sense, however, there is no real justification of the exchange-coefficient hypothesis. There is no defensible ground for the use of Eq. (2.31) and its use, at the present stage, is considered as empirical only (Pasquill, 1970a). Priestley (1959) points out that there is no precise physical basis for the use of this assumption as the foundation for the description of turbulent diffusion in the atmosphere, and consequently the validity of the gradient-transfer theory "is normally judged from the degree of success achieved in ... predicting particular diffusion phenomena". Calder (quoted by Gifford, 1968) studied the applicability of the diffusion equation to the atmospheric case and concluded that the standard K-theory form, Eq. (2.33), can not be generally valid. Russian workers, e.g. Monin (1959a), refer to the gradient-transfer

theory as a semi-empirical theory of diffusion. Pasquill (1970a) noted that the fundamental validity of the gradient-transfer approach has always been regarded as a matter of debate. The basic nature of the gradient-transfer theory must be kept in mind as the chain of deductions from the original equation grows larger and more involved.

Over and above the theoretical difficulty mentioned above, the determination of actual values of the coefficients of diffusion has always remained problematic. Many expressions for evaluation of  $K$  in the atmosphere, both under adiabatic as well as thermally stratified conditions, have been suggested. There is abundant literature on this phase, and has been reviewed by Priestley (1959), Lumley and Panofsky (1964) and Matveev (1967). Also reference should be made to the recent profiles suggested by Hanna (1968), Pasquill (1970a), O'Brien (1970), and Cohen et al. (1972). The expressions for  $K$ -profiles within the surface layer of the atmosphere have been based on Monin-Obukhov (1964) similarity theory, but the expressions for entire boundary layer remain empirical.

Some plausible universal forms have been suggested (Hanna, 1968; Pasquill, 1970a) which can be used irrespective of height and stability in the atmosphere, but they have yet not been put to test for diffusion studies, mainly because the expressions require estimation of such quantities which require special turbulence measurements.

### 2.3.1.2. Solution of Eq. (2.33)

Once the selection of K-profile is properly done, the Eq. (2.33) is required to be solved to get mean concentration  $\bar{c}$  at any point (x,y,z). Depending upon the form of K-profile, many types of solutions of Eq. (2.33) have been attempted.

Sutton (1953) states the early attempts of Roberts to solve the Eq. (2.33), assuming that  $K_x$ ,  $K_y$  and  $K_z$  are constants (i.e. Fickian) and that the wind velocity  $\bar{u}$  is constant at all points. The failure of these exact solutions to conform to the observations produced unassailable evidence that eddy diffusion in the atmosphere can not be represented by the Fickian equation. Roberts also gives solutions assuming power-law forms of  $\bar{u}$  and  $K_z$  and a line source, but it considers neither varying conditions of ground roughness nor varying thermal stability. Thus it could be expected to apply only on aerodynamically smooth terrain, and at times of neutral conditions of atmosphere.

Using Deacon (1949)'s wind-and  $K_z$ -profiles for both adiabatic as well as diabatic conditions, Calder (1949) gave solutions for two-dimensional diffusion. Rounds (1955) extended the work and gave solutions of Eq. (2.33) for different types of sources. Limitations of Deacon's profiles in determining the value of  $\beta$  (Eq. (2.9)) reflect in both the above applications.

Smith (1957) treated the two-dimensional equation, for the case of an elevated line source, with the conjugate-power-laws for

wind and diffusivity. The index of the power-law form depends on the stability of the atmosphere, and has to be decided empirically.

While the two-dimensional case was being studied, some workers also attempted to solve the case of continuous point source. Davies (1950) gave a solution where  $K_z$  and  $\bar{u}$  have conjugate-power-law forms, and  $K_y \propto z^p$ , where  $p$  is the index, same as that for  $\bar{u}$ . Smith (1957) and Godson (1958) also gave solutions for different sources and stability conditions using power-law forms for  $K_y$  and  $K_z$ . All these works have the same limitation of empirical determination of power-law index.

For a continuous elevated source, Bosanquet and Pearson (1936) solved the diffusion equation making use of dimensional analysis. The average ground level concentration at any point  $(x,y,z)$  according to them, is given by

$$\bar{c}(x,y,z) = \frac{Q}{\sqrt{2\pi} p q \bar{u} x^2} \exp \left[ -\left( \frac{y^2}{2q^2 x^2} + \frac{H_e}{px} \right) \right] \quad (2.34)$$

where  $Q$  is the rate at which pollutant is released,  $H_e$  is the effective height of the stack,  $p$  is the index of vertical diffusion, and  $q$  is the index of horizontal diffusion. They gave values of  $p$  and  $q$  for three different turbulence fields. Empirical selection of  $p$  and  $q$ , and constantancy of  $p$  with height are the main limitations of this approach. Strictly speaking, this equation can be applied only in neutral conditions of stability (Pasquill, 1962a).

Monin-Obukhov (1954) similarity theory gave generalized wind and  $K_z$  profiles within the surface layer of the atmosphere. Using

these profiles, an exact solution of Eq. (2.33) is not available, but computer methods using finite-difference scheme have been used to solve it (Jaffe, 1967; Hino, 1968a; Shir, 1970). Their attempts show that this method is very promising. However, determination of  $K_z$ -profile beyond the surface layer has remained arbitrary (Cohen et al., 1972).

Walters (1962), Peters and Klinzing (1971), Heines and Peters (1973) gave solutions of Eq. (2.33) for different source positions, using the form of the eddy diffusion coefficient as

$$\begin{aligned} K_y &= A_y \cdot x^q \\ K_z &= A_z \cdot x^n \end{aligned} \tag{2.35}$$

where  $x$  is the downwind distance from the source,  $q$  and  $n$  are indices which depend upon stability conditions,  $A_y$  and  $A_z$  are coefficients. All the previous workers had used the forms of  $K_y$  and  $K_z$  which did not vary with the downwind distance. But it is always difficult to get the universal forms of  $K_y$  and  $K_z$  of the kind shown by Eq. (2.35).

In general, it can be noted that the basic theoretical limitation of the gradient-transfer theory is in the use of Eq. (2.31), whereas, on practical side, the determination of  $K$  profiles has been empirical at the present stage. When the diffusion in the vertical direction is to be estimated in the surface layer of the atmosphere, the mathematical analysis of the gradient-transfer theory becomes very complicated.

Despite its limitations, the gradient-transfer theory has great appeal to research workers in atmospheric turbulent diffusion. If the selection of K profile is properly done, this theory does provide many useful, practical results. An approach to the difficult problem of the deposition of polydisperse aerosols has been made via K theory (Gifford, 1968). This theory has been applied to diffusion problems involving non-linear chemical reactions and thus simulating the concentrations of chemically reactive pollutants (Lamb, 1973). For multiple-source urban diffusion problem, the gradient-transfer theory has been used and both the analytical solutions (Gifford, 1970; Gifford and Hanna, 1970) and computer-oriented numerical solutions (Randerson, 1970) have been offered.

### 2.3.2. The Statistical Theory

The statistical theory of turbulent diffusion, based on G. I. Taylor's pioneer work (Taylor, 1921), studies the histories of the motion of individual fluid particles and tries to determine from these the statistical properties necessary to represent diffusion.

In a turbulent field, the diffusive spread of tagged particles from a source is a random process. Taylor considered the displacement  $x$  of a single tagged particle as it is carried away from the origin by a turbulent wind  $\bar{u}$ . The mean-square of the displacement,  $\overline{x^2}$ , for a homogeneous and stationary field of turbulence is given by

$$\overline{x^2} = 2 \overline{u'^2} \int_0^t (t-\xi) R(\xi) d\xi \quad (2.36)$$

where  $\overline{u'^2}$  is the mean-square of eddy velocity and  $R(\xi)$  is the Lagrangian correlation coefficient between the velocity of the single particle at time  $t$  and that at time  $(t + \xi)$ . The latter is given by

$$R(\xi) = \frac{\overline{u'(t) u'(t+\xi)}}{\{\overline{u'^2(t)}\}^{1/2} \{\overline{u'^2(t+\xi)}\}^{1/2}} \quad (2.37)$$

The quantity  $(\overline{x^2})^{1/2}$  is the one-dimensional standard deviation,  $\sigma_x$ , of the probability distribution of the particle positions after some given time  $t$ . The analysis is extended to three-dimensions by introducing separate expression for  $(\overline{y^2})^{1/2}$  and  $(\overline{z^2})^{1/2}$ .

The basic assumption on which the statistical theory progresses is that the turbulence is homogeneous and stationary. This idea of turbulence homogeneity is a simplification introduced into the theory to avoid the mathematical complications (Rouse, 1959). The Lagrangian correlation coefficient,  $R(\xi)$  of Eq. (2.37), is based on this assumption. In the real atmosphere, this assumption of turbulence homogeneity is not valid. Turbulence in the upper portion of the planetary boundary layer may approximate the homogeneous type, but surface layer turbulence is decidedly inhomogeneous (Gifford, 1968). The use of this theory, therefore, within the surface layer of the atmosphere is always questionable (Randerson, 1970).

#### 2.3.2.1. Sutton's Approach

The form of  $R(\xi)$  must be established before the  $\overline{x^2}$  can be evaluated. Frenkiel (1953) has considered various possible functional



forms of  $R(\xi)$ . All these forms require prior evaluation of time-scale

$$t_L = \int_0^{\infty} R(\xi) d\xi \quad (2.38)$$

which is rarely available. An explicit formulation of  $R(\xi)$  is proposed by Sutton (1934), which later he generalizes to the case of aerodynamically rough surfaces (Sutton, 1953), as

$$R(\xi) = \left( \frac{N}{N + \overline{u'^2} \cdot \xi} \right)^n \quad (2.39)$$

where he defines  $N$  as macroviscosity ( $= u_* z_0$ ), and  $n$  depends upon stability conditions. Using this form of  $R(\xi)$ , Sutton derives expressions for  $\overline{x^2}$ ,  $\overline{y^2}$  and  $\overline{z^2}$ .

Sutton's approach was questioned on two main points. One, the study is applied to the surface layer of the atmosphere where the assumption of turbulent homogeneity is definitely not applicable. Second, the integral of the explicit form of  $R(\xi)$ , Eq. (2.39), is not convergent (Pasquill, 1962a). Moreover, Sutton uses the index  $n$  as the stability factor in describing  $R(\xi)$  (and hence  $\overline{x^2}$ , etc). It was originally assumed that  $n$  could be determined from the power relation

$$\frac{\overline{u_1}}{\overline{u_2}} = \left( \frac{z_1}{z_2} \right)^{n/(2-n)} \quad (2.40)$$

where the subscripts refer to the different elevations. But  $R(\xi)$  assumes a homogeneous turbulent field that is true for Eq. (2.40) only if  $n = 0$  (Gifford, 1968).

Sutton's model has been widely used inspite of the theoretical difficulties mentioned above. It should certainly be regarded as a model which is theoretically oriented and physically motivated. But it should not be accorded the unequivocal status of a law of nature. Pasquill (1961) observes that these formulae are reliable for specifying the average distribution, over a few hundred metres downwind of a source operating for a few minutes on level unobstructed terrain, with a steady wind direction and neutral conditions of atmospheric stability; but extension to other circumstances has depended on empirical and often speculative adjustments of the diffusion parameters.

Sutton's scheme has been applied empirically to greater distances by introducing the separate stability parameters,  $n_y$  and  $n_z$ , for each direction (Leonard, 1959; Barad and Haugen, 1959).

#### 2.3.2.2. Pasquill's Method

Alternative approach in evaluating  $\overline{x^2}$ ,  $\overline{y^2}$  and  $\overline{z^2}$  (or,  $\sigma_x$ ,  $\sigma_y$  and  $\sigma_z$ ), avoiding the determination of the form of  $R(\xi)$ , has been suggested. Hay and Pasquill (1957) have presented experimental evidence that the vertical distribution of spreading particles from an elevated point is related to the standard deviation of the wind elevation angle,  $\sigma_\phi$ , at the point of release. Cramer (1959) used spectral considerations to link  $\sigma_y$  and  $\sigma_z$  to the standard deviations of wind vane fluctuations in azimuth and elevation ( $\sigma_\theta$  and  $\sigma_\phi$ ), respectively, by

$$\sigma_y = \sigma_\theta x^f \text{ and } \sigma_z = \sigma_\phi x^g \quad (2.41)$$

where  $x$  is the distance downwind and  $f$  and  $g$  depend on stability conditions. Hay and Pasquill (1959) showed that

$$\sigma_y = x [\sigma_\theta]_{\tau, T/\beta} \quad (2.42)$$

where  $[\sigma_\theta]_{\tau, T/\beta}$  is the standard deviation of azimuth, averaged on moving intervals; it is the maximum angle of lateral wind fluctuations averaged over period  $s = T/\beta$ , where  $T$  is the travel time and  $\tau$  is sampling time of pollutant. Hino (1968b) has shown a method of evaluating the value of  $[\sigma_\theta]_{\tau, T/\beta}$ . He has given a relationship between the ratio of  $[\sigma_\theta]_{\tau, T/\beta}/\sigma_\theta$ , sampling time  $\tau$  and the averaging time  $s(=T/\beta)$ .

On the basis of available data and guided by theoretical expectations, Pasquill (1961) proposed a method for estimating diffusion when detailed wind data are not available. The standard deviations of the lateral and vertical distributions are expressed in terms of an angular lateral spread  $\theta$  and a vertical spread  $h$ , defined by concentrations one-tenth of the axial or ground-level values respectively. Pasquill tabulated a weather classification and gave families of curves of  $h$  and  $\theta$  as a function of distance downwind  $x$ , for six stability categories. Gifford (1961) converted Pasquill's values of angular spread and vertical spread into standard deviations of plume concentration distribution,  $\sigma_y$  and  $\sigma_z$ . Gifford's work was based primarily on diffusion data cited by, Pasquill (1961).

Turner (1964) has modified the Pasquill's stability categories, so also has been done by Meteorological Agency of Japan (Hino, 1968b).

Pasquill's stability categories are qualitative, and hence they can not directly be related to unique values of stability length  $L$  (Panofsky and Prasad, 1965). Hino (1968b) has shown the ranges of stability length  $L$  for different Pasquill's stability categories.

Pasquill-Gifford-Turner method of estimating  $\sigma_y(x)$  and  $\sigma_z(x)$  has been very widely used in the last decade (Clarke, 1964; Miller and Holzworth, 1967; Koolger et al. 1967; Bowne, 1969; Roberts et al., 1970; Fortak, 1970; Hanna, 1971; Martin, 1971). The estimates of  $\sigma_y(x)$  and  $\sigma_z(x)$  were given from diffusion studies carried out at Porton, England. These studies were conducted in the open country with the average surface roughness of 3 cm (Pasquill, 1966). These graphs, therefore, are applicable to diffusion in open countries only. In the original paper, Pasquill (1961) observes that the treatment has only been verified for grassland, but implication is that increases in roughness of a moderate order (for example, due to crops, small bushes and hedges) are unlikely to make a vast difference to the vertical diffusion; however, for large disturbances such as those caused by woods, buildings or sharp changes in contour, this method can not be representative. Despite this, urban pollution models derived in the past decade (Turner, 1964; Bowne 1969; Roberts et al. 1970, etc.) have been derived from Pasquill's original estimates of spread, without any serious attempts to modify his estimate for the

effects of increased urban roughness. This made Pasquill (1970b) to observe :

"Some models appear to generalize about the standard deviation of particle spread in vertical and horizontal directions,  $\sigma_y$  and  $\sigma_z$ , by using practical observations of the distribution of urban air pollutants. Although not unreasonable, it should be emphasised that such a procedure cannot be accepted automatically as justification for applying the model to flow and terrain conditions other than those obtaining in the pollutant survey. For the most useful generalization we must seek independent specifications of  $\sigma_y$  and  $\sigma_z$  in terms of meteorological parameters that can either be measured at the time in question or estimated from routine meteorological data."

The studies carried out at St. Louis is perhaps very indicative Mc Elroy and Pooler (1968) report their analysis of diffusion experiments carried out at the urban area of St. Louis. Their Fig. 16 (a and b) (reproduced here as Fig. 2.1) compares their results according to Pasquill-Gifford stability classes with those given by Pasquill-Gifford (1961) for the open country. The effective surface roughness for the St. Louis city is reported to be between 1 and 3 m (Pasquill, 1970a), which is of the same order of roughness observed in other cities. It is observed that in the range of 700 - 10000 m distance from the source, the vertical spreads in the St. Louis city were 3-4 times more than those in the open country, except in the case of B category of stability where also the vertical spread was about 2 times that for open country at 500 m distance.

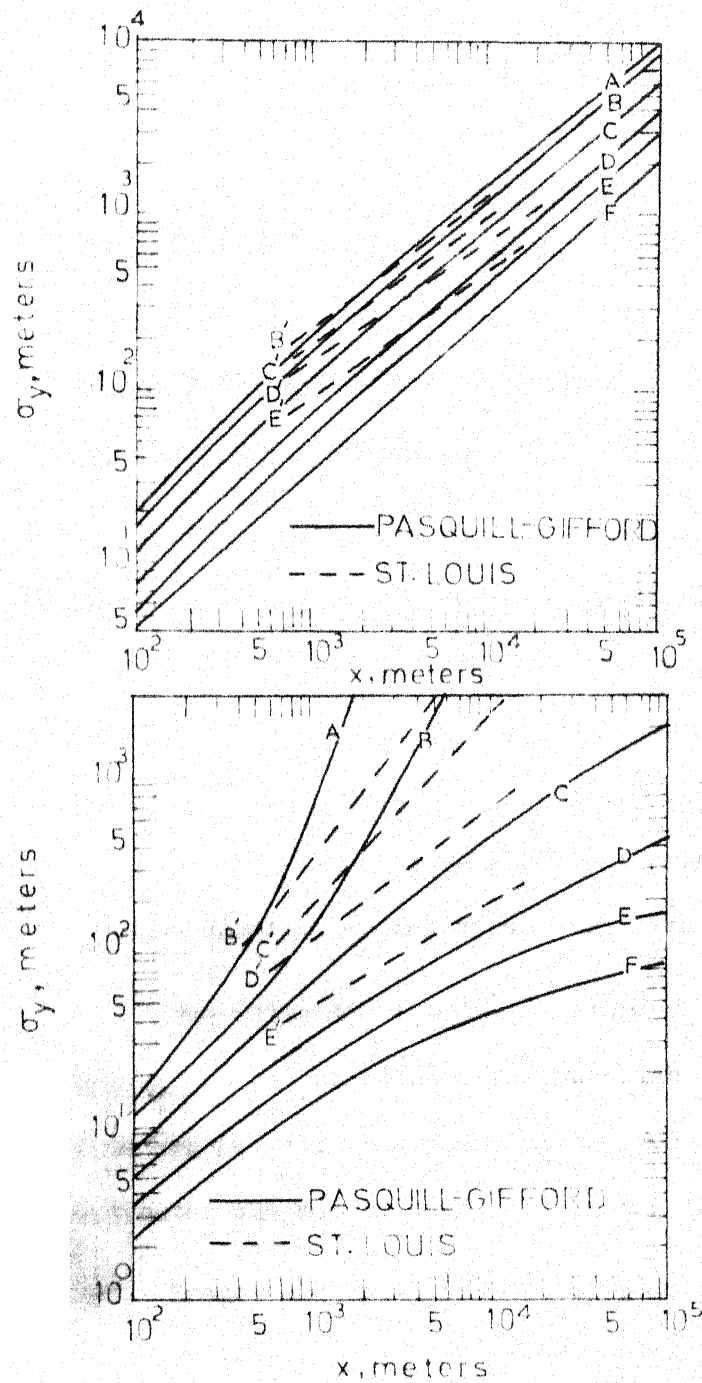


FIG. 2.1 COMPARISON OF THE RESULTS OF THE ST. LOUIS (McELROY AND POOLER 1968 b) EXPERIMENTS WITH THOSE SUMMARIZED BY PASQUILL AND GIFFORD (1961)

The lateral spreads,  $\sigma_y$ , also showed the effect of increased urban roughness. However, in this case, the effect of increase in surface roughness was not as pronounced as in the case of vertical spread. Around 700 m distance the spread was about 2 times which reduced to about 1.2 times around 5000 m.

Although the concept that the enhanced roughness in an urban area would cause an increase in vertical spread, as compared with open and relatively smooth country, seems to have been accepted (Pasquill, 1966), very little theoretical estimate of the magnitude of the effect has yet been offered. This point is referred to again in the following section, but point in order here is that the estimates of  $\sigma_y$  and  $\sigma_z$  do vary with the surface roughness.

The estimate of lateral spread  $\sigma_y$  is based on Eq. (2.42), but  $\sigma_\theta$  is not constant with the height, hence  $\sigma_y$  should vary with the height. Because of these reasons, Pasquill-Gifford estimates can not be used indiscriminately.

Singer and Smith (1966), Singer, Frizzola and Smith (1966) gave the power law relation for  $\sigma_y$  and  $\sigma_z$  in the form of

$$\sigma = b x^q \quad (2.43)$$

where the coefficient  $b$  and power  $q$  vary according to the meteorological conditions and the scale of the problem.

### 2.3.2.3. Concentration Distribution

Once the standard deviations of concentration distribution  $((\overline{y^2})^{\frac{1}{2}}, (\overline{z^2})^{\frac{1}{2}} \text{ or } \sigma_y, \sigma_z)$  are determined, the average concentration of

pollutant at any distance from the centre of the cloud or axis of the plume may be assumed to be given by an exponential function (Pasquill, 1962a). The Gaussian distribution has been assumed for a continuous-source diffusion model by Sutton (1934), Frenkiel (1953), A.S.M.E. (1968), Turner (1970) and many other workers. Thus, for a continuous point source, the average concentration  $\bar{c}$  at any point  $(x, y, z)$  from the source is given by

$$\bar{c}(x, y, z) = \frac{Q}{2\pi \bar{u} \sigma_y \sigma_z} \exp \left[ -\frac{1}{2} \left( \frac{y^2}{\sigma_y^2} + \frac{z^2}{\sigma_z^2} \right) \right] \quad (2.44)$$

where  $Q$  is the quantity of material released per unit time, and  $\bar{u}$  is the effective mean wind speed invariant with the height.

Strictly speaking, the Gaussian diffusion model applied only in the limit of large diffusion time and for homogeneous, stationary conditions (Gifford, 1968). The empirical support for the Gaussian shape comes only from lateral distributions from continuous sources, or, of vertical distributions from effectively elevated sources (Pasquill, 1970a). On the other hand, Pasquill (1970b) observes, there is no real basis for assuming vertical Gaussian distribution from a ground-level source. The theoretical and empirical indications point to a shape between Gaussian and simple exponential, and the experimentally determined values of the exponent  $s$  in the exponential form,  $\exp(-bz^s)$ , lie in the range of 1.1 to 1.5 (Pasquill, 1962a). The workers like Bosanquet-Pearson (1936), Calder (quoted by Pasquill, 1962), etc. have used  $s = 1$ .



In general, within the limitations cited above, both Sutton's as well as Pasquill's methods are very useful in the diffusion studies, but their use beyond the specified circumstances becomes more of empirical nature.

### 2.3.3. The Lagrangian Similarity Theory

In the last few years, attempts have been made to apply the so-called Lagrangian similarity principles to the problem of diffusion from a source of passive material on the ground.

Ellison (1959), prompted by a remark by Batchelor (1959) on Monin's (1959b) paper, applied a dimensional method to the determination of the diffusion downwind from a continuous point source in an adiabatic surface layer. He uses Monin's (1959b) (i) similarity hypothesis that the average vertical velocity of a particle released from a source is proportional to  $u_*$ , times some universal dimensionless function of Monin-Obukhov stability length  $L$  given by Eq. (2.19); (ii) similarity assumption that the average horizontal velocity of a particle is given by Eq. (2.16). Ellison, applying the Lagrangian similarity principles, shows that the probability  $\psi$  that a particle diffusing in the surface layer will reach a distance  $r = (x^2 + y^2 + z^2)^{1/2}$  from its average position characterized by coordinates  $\bar{x}$ ,  $\bar{y}$ ,  $\bar{z}$  must be a universal function of  $(x-\bar{x})/\bar{z}$ ,  $(y-\bar{y})/\bar{z}$  and  $(z-\bar{z})/\bar{z}$ . On dimensional reasoning he shows that for a continuous point source located in a neutral atmosphere, the average axial ground-level concentration  $\bar{c}$  is given by

$$\bar{c} = Q \int_{-\infty}^{\infty} \frac{\psi\left(\frac{\bar{x}-\bar{x}}{\bar{z}}, 0, 0\right) d\left(\frac{\bar{x}-\bar{x}}{\bar{z}}\right)}{b u_* \bar{z}^2 \left(\frac{\bar{x}-\bar{x}}{\bar{z}} + \frac{d\bar{x}}{d\bar{z}}\right)} \quad (2.45)$$

where  $b$  is a universal constant, and  $Q$  is the rate of emission. On simplification, he shows that

$$\frac{\bar{c}}{Q} \cdot b u_* \propto \frac{1}{\bar{z}^2 \left[\frac{\bar{x}}{\bar{z}} + \frac{1}{kb}\right]} \quad (2.46)$$

where from Eqs. (2.16) and (2.19),

$$\bar{x} = \frac{1}{kb} \left[ \bar{z} \left( \ln \frac{\bar{z}}{\bar{z}_0} - 1 \right) \right] \quad (2.47)$$

By evaluating Eq. (2.46), Ellison (1959) showed that in the adiabatic surface layer the downwind concentration from a continuous point source varies as  $\bar{x}^p$ , where  $p$  varies approximately in the range -1.8 to -1.9. For a continuous, infinite crosswind line source, the downwind concentration was found to vary as  $\bar{x}^{-1}$ . These results are in excellent agreement with data, and hence provide an alternative to Sutton's solution that leads to essentially the same results.

For the diabatic case, Gifford (1962) proposes

$$\frac{\bar{c}}{Q} \propto \frac{1}{\bar{z}^2 \bar{u}(\bar{z})} \quad (2.48)$$

which is the counterpart of Eq. (2.46). For a relation between axial ground-level concentration and mean downwind distance  $\bar{x}$  to be obtained, a relation between  $\bar{x}$  and  $\bar{z}$  must be established, which, according to Monin (1959b), is given from Eqs. (2.16) and (2.19) as

$$\frac{bk}{L} \bar{x} = \int_{z_0/L}^{z/L} \frac{[f(z/L) - f(z_0/L)]}{h(z/L)} d(z/L) \quad (2.49)$$

The results obtained by Gifford are in reasonably close agreement with detailed experimental atmospheric concentration measurements. Wind-tunnel diffusion studies by Cermak (1963) have provided additional verification.

The most important feature of the Lagrangian similarity theory is that it treats surface layer diffusion without postulating a diffusivity. Thus it takes into account the inhomogeneity of turbulence in the surface layer of the atmosphere (unlike the statistical theory), but does not assume a diffusivity coefficient (as done in the gradient-transfer theory).

On the basis of the good agreement between the theoretical and observed axial concentration values, the hypothesis of Lagrangian similarity in both the adiabatic and diabatic surface layer conditions seems to be strongly supported. However, it has been tested only for axial ground-level concentrations. Moreover, in the application of this theory to a point source, the rate of increase of the lateral spread of the particles about their mean position is not explicitly stated. Calder (reported by Pasquill, 1966) observes that the lateral spread is implicitly proportional to the vertical spread. The physical acceptability of this implication of the similarity theory is questioned by Pasquill (1966).

## 2.4. Use of Lagrangian Similarity Theory to Estimate the Vertical Spread

Although the Lagrangian similarity theory was put forward to predict the variation of a continuous point-source concentration with distance downwind, it can also be used to estimate the vertical spread.

In fact, the similarity theory approach to problem of diffusion, started by Ellison (1959) and Batchelor (1959), was stimulated by Monin's (1959b) paper on smoke propagation in the surface layer of the atmosphere, in which he gave equation of the shape of the boundary of the smoke plume, which took into account the variation of wind velocity with altitude. He shows that the height  $z$  and distance  $x$  reached by a particle released from a source are given by

$$\frac{dz}{dt} = bu_* h(z/L) \quad (2.50)$$

$$\frac{dx}{dt} = \frac{u_*}{k} [f(z/L) - f(z_0/L)] \quad (2.51)$$

from which

$$\frac{dx}{dz} = \frac{1}{bk} \frac{[f(z/L) - f(z_0/L)]}{h(z/L)} \quad (2.52)$$

Integrating,

$$\frac{bk}{L} \bar{x} = \int_{z_0/L}^{z/L} \frac{[f(z/L) - f(z_0/L)]}{h(z/L)} d(z/L) \quad (2.53)$$

Monin integrates Eq. (2.53) numerically and the results are expressed in a series of curves of  $z/L$  (upto  $z/L = 5$ ) against  $bk x/L$  for three values of  $z_0/L$ . Gifford (1962) re-evaluated the curves for the

stable conditions. Monin gives  $b$  to be close to or a little exceeding unity. Gifford does not give any value of  $b$ .

The main point to be noted with Monin's approach is that he takes the Eq. (2.54) to represent the boundaries of the plume. Unlike infinite Gaussian spread assumed by all Western researchers, he takes the spread to be finite and assumes that the Eq. (2.53) represents the boundary of the spread.

A slightly modified approach suggested by Panofsky and Prasad (1965) makes use of the root-mean-square vertical component of eddy velocity,  $\sigma_w$ , and thus they take Eq. (2.52) as  $\bar{u}/\sigma_w$  which is proportional to  $1/\sigma_\phi$ , where  $\sigma_\phi$  is the standard deviation of wind elevation angle, hence

$$\bar{x} \propto \int_0^z \frac{1}{\sigma_\phi} dz$$

Empirical data on  $\sigma_\phi$  as a function of  $z$ ,  $z_0$  and  $L'$  ( $= \frac{K_H}{K_M} \cdot L$ , where  $K_H$  is eddy conductivity and  $K_M$  eddy viscosity) have been summarized by them, and numerical integration gives  $x - z$  curves.

Pasquill (1966), trying to examine the extent to which a satisfactory representation of vertical spread was provided by similarity theory, emphasized that  $z$  in Eqs. (2.50), (2.52) and (2.53) is the mean height of an ensemble of particles. Hence, these equations become

$$\frac{d\bar{z}}{dt} = bu_* h(\bar{z}/L) \quad (2.50a)$$

$$\frac{d\bar{x}}{dt} = \frac{u_*}{k} [f(\bar{z}/L) - f(z_0/L)] \quad (2.51a)$$

$$\frac{d\bar{x}}{d\bar{z}} = \frac{1}{bk} \frac{[f(\frac{\bar{z}}{L}) - f(\frac{z_0}{L})]}{h(\bar{z}/L)} \quad (2.52a)$$

and

$$bk \frac{\bar{x}}{L} = \int_{z_0/L}^{\bar{z}/L} \frac{[f(\frac{\bar{z}}{L}) - f(\frac{z_0}{L})]}{h(\bar{z}/L)} \quad (2.53a)$$

He further showed that

$$\frac{d\bar{z}}{dt} = \int_0^{\infty} c \frac{dK_M}{dz} dz / \int_0^{\infty} c dz \quad (2.54)$$

where  $c$  is the concentration of pollutant at any height  $z$ ,  $K_M$  is the eddy diffusivity. He proved, on this basis,  $b$  to be equal to  $k$  ( $= 0.4$ ) and got good agreement at 100 m distance with observed vertical spread in adiabatic conditions. However, using  $z$  as the mean height of an ensemble of particles and  $b = k$  for the thermally stratified conditions, he observed theoretical as well as practical inadequacies. For such cases, he demonstrated that vertical spread at a distance of 100 m from a source for  $z_0 = 0.08$  cm, was in much better agreement of observed values if vertical spread was represented by the height of cloud  $z_{max}$  (concentration at  $z_{max}$  is 10% of axial concentration) and  $b = 1.2$ , substantially similar to the treatment of Monin.

Pasquill (1970a) gave additional verification for neutral conditions of the atmosphere, and showed that the similarity theory could predict the vertical spread, in the neutral conditions, to a considerable range of distance upto 5 Km.

This method of predicting vertical spread of pollutants with the help of the Lagrangian similarity theory has a great potential. It makes use of both the important points of the similarity theory, viz., taking the atmospheric turbulence as inhomogeneous and at the same time avoiding use of diffusivity concept, and steers clear of the controversy of the use of implicit crosswind spread of the similarity theory in predicting the concentration downwind. But it should be noted that although the treatment has a fairly convincing theoretical background, it has so far been tested in a very limited way.

Thus, the present-day status of mathematical modelling of atmospheric diffusion is such that even when both the gradient-transfer theory and statistical theory are in use, the Pasquill-Gifford method has become more popular in the last few years, and is used even for urban diffusion studies, despite its limited applicability to open, unobstructed terrain only. It is interesting to investigate whether the Lagrangian similarity theory can be used on field conditions to predict vertical spreads and hence concentration distribution. Such investigations have been done in a very limited way. The effects of varying aerodynamic roughness of underlying surfaces and different stability conditions of atmosphere can also be examined, which have been reported in the following chapters.

## Chapter Three

### DEVELOPMENT OF A MATHEMATICAL MODEL FOR PREDICTION OF POLLUTANT CONCENTRATIONS

#### 3.1 Importance of Mathematical Models

To safeguard against air pollution hazards to health and property, air pollution control programmes have to be undertaken. The concentration of a pollutant at the points of significance from community point of view depends on source strength and the dispersal capacity of the intervening atmosphere. Hence, for any air-quality-management programme to be rational, simulation models of diffusion of air pollutants have to be developed. Such diffusion models are the yardsticks for furnishing quantitative evaluation of concentrations of pollutants in the ambient air.

Mathematical diffusion models can be used as an aid to decision making in air pollution control, and city and regional planning. These models can be used in long-range air-resource-management programmes for the evaluation of future air quality with regard to increased industrialization or increased population. They can be used to evaluate the effectiveness of individual control or abatement procedures for a given source or combination of sources. Models may also be useful for determining most suitable locations for pollution-causing industrial units as also of sampling stations used to monitor air pollution levels. It may be possible to use



short-range predictions of meteorological variables with appropriate source information to produce, in a few minutes with the help of a digital computer, maps of expected air pollution concentrations. These would be an aid in initiating immediate measures necessary to achieve desired air quality levels (Turner, 1964; Middleton, 1970).

Major elements of the mathematical diffusion model for urban air pollution problem can best be shown through a flow-diagram as shown in Fig. 3.1 (Fortak, 1970). It shows that the mathematical model to describe the dispersion of pollutants in the real atmosphere plays a very important role in diffusion modelling.

### 3.2 Earlier Models

To estimate concentrations of pollutants downwind of a source in the surface layer of the atmosphere, as discussed earlier, three diffusion theories are in use. The gradient-transfer theory and Lagrangian similarity theory of diffusion have the merit of incorporating the turbulence inhomogeneity. However, the similarity theory has a doubtful implication about crosswind spread and its use requires evaluating the function  $\psi$ , Eq. (2.45), which is not always available.

#### 3.2.1 Bosanquet-Pearson Model.

The gradient-transfer theory can give good results if proper form of K-profile is available, but it involves complicated mathematical analysis. Bosanquet and Pearson's equation, Eq. (2.3.4), based on classical diffusion equation, have been popular in diffusion

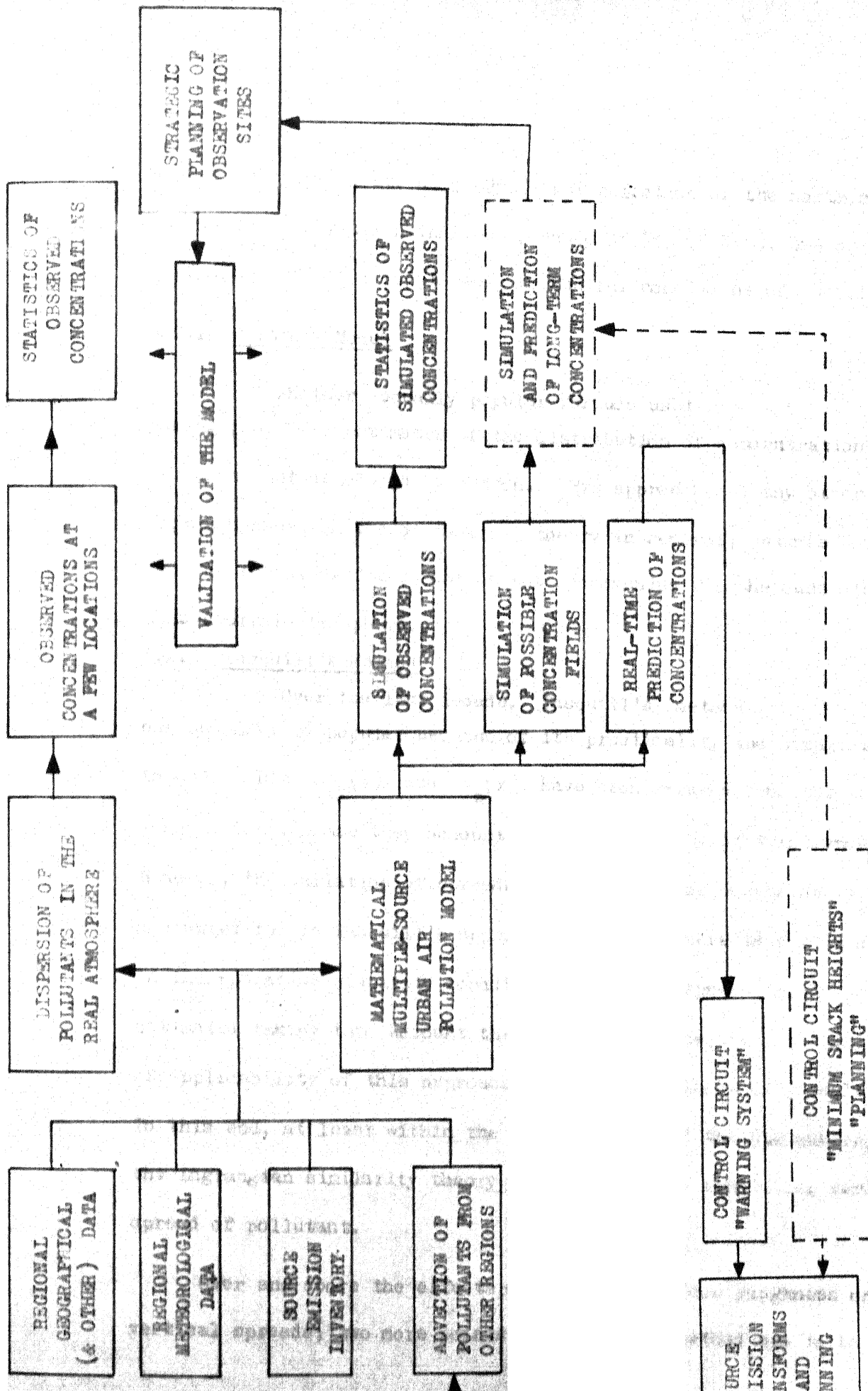


FIGURE 3.1 MAJOR ELEMENTS OF THE URBAN AIR POLLUTION PROBLEM CONNECTED WITH MATHEMATICAL MODELLING (FORTAK, 1970)

modelling (Magill, et. al., 1956) but selection of the horizontal and vertical diffusion indices,  $p$  and  $q$  of Eq. (2.3.4), has been empirical, and it is applicable to neutral conditions of stability only.

### 3.2.2 Sutton's Model

Another equally popular formula used in making practical estimates of the distribution of concentration has been that developed by Sutton. His approach, as any other approach based on the statistical theory in general, assumes homogeneous turbulent field, and is not recommended for the case other than neutral atmosphere.

### 3.2.3 Pasquill's Method

Over the last decade, Pasquill's method has become very popular because of its practicality and simplicity in use. His  $\sigma_y(x)$  and  $\sigma_z(x)$  have been derived from the actual observations, hence they account for inhomogeneity of turbulence. However, the variation of spreads with the surface roughness is not accounted for in Pasquill's approach. Again, there is a discontinuity in incorporating stability conditions. If the spreads could be estimated taking into account these two variations also, the field of applicability of this approach would become almost universal. To this end, at least within the surface layer of the atmosphere, the Lagrangian similarity theory may be useful in predicting vertical spread of pollutant.

Over and above the effects of enhanced surface roughness on vertical spreads, two more points of Pasquill's method are to be noted.

In estimating  $\sigma_y(x)$  by Eq. (2.42), the standard deviation of azimuth is taken as invariant with height, and hence  $\sigma_y(x)$  is taken as same at all heights, which is not true. Further, in the estimation of concentration distribution by Eq. (2.44),  $\bar{u}$  is also assumed invariant with height, which is consistent with the assumption of homogeneous turbulence, but unjustified in the actual atmospheric conditions.

### 3.2.4 Model based on Lagrangian Similarity

Eqs. (2.53) & (2.53a), based on similarity theory, relate the vertical spread of pollutant with the downwind distance  $\bar{x}$ , roughness length  $z_0$ , and stability length  $L$ . In the use of these equations in predicting vertical spread downwind, there is a controversy in as much as Monin maintains that Eq. (2.53) reckons the spread upto the plume boundary and there is no concentration beyond this boundary, whereas Pasquill argues that the  $z$  in Eq. (2.53) is the ensemble mean  $\bar{z}$ , and Eq. (2.53) becomes Eq. (2.53a).

The best-developed simulation model of this category to-date is by Monin (1959b) briefly described in Section 2.4. As referred to in the section quoted gives equations to compute the upper boundary of the plume and also developed curves to directly read off  $z/L$  if values of  $bk\bar{x}/L$  are known. The curves given by Monin only cover a range of  $\frac{z}{L}$  upto 5 for the unstable and stable conditions of the atmosphere. Since Monin's approach appears to be one of the most promising for application on field, the approach has been

extended to cover a larger range of  $\frac{z}{L}$  and neutral conditions of atmospheric stability in the later sections.

Neither of the above approaches have been adequately tested on field data for stratified field.

### 3.3 Extension of Monin's Approach to Cover Practical Ranges of $z/L$ for All Conditions.

Monin (1959b), in his work as briefly referred to in Section 2.4, assumed that the integral (Eq. (2.53))

$$bk\bar{x} = \int_{z_0/L}^{z/L} \frac{[f(z/L) - f(z_0/L)]}{h(z/L)} dz/L \quad (3.1)$$

showed the relationship between the vertical spread and downwind distance travelled by pollutant particles. He further assumed that Eq. (3.1) represented the equation of motion of particles at the upper boundary of plume which was of a finite width. To differentiate Monin's reference to plume boundary from mean vertical spreads,  $z$  in Eq. (3.1) for Monin's approach is denoted here as

$z_{\max}$ .

Monin has given a set of graphs of  $bk\bar{x}/L$  versus  $z/L$  (in present case,  $z_{\max}/L$ ) for stable as well as unstable stratification, in his Fig. 3. The set of  $z_0/L$  values consists of  $z_0/L =$   
(i) 0.0010, (ii) 0.010 and (iii) 0.10. For the comparison with

the approach presented later in this chapter with mean vertical spread, these graphs given by Monin need extension to values of  $z_{\max}/L$  beyond 5 for the unstable atmospheric conditions. For both the unstable as well as stable conditions, graphs at  $z_0/L=0.0001$  are required for the comparison purpose. For neutral conditions of the atmosphere, Monin has not given any graph.

In the following three paragraphs, the equations and graphs are developed using Monin's approach, for unstable, stable and neutral atmospheric conditions.

**3.3.1 Unstable Atmosphere.** For the unstable atmosphere, as shown in Section 2.2.3.3 and later sections, free convection occurs at  $z/(-L) = 0.08$ , and the wind velocity profile can be given as

Forced convection, i.e.,  $-\frac{z_0}{L} \leq -z/L \leq 0.08$ ,

$$\bar{u} = \frac{u_*}{k} \ln \frac{z}{z_0}$$

Free convection, i.e.,  $0.08 < -z/L$

$$\bar{u} = \frac{u_*}{k} [0.48 - 2.3 \log (z_0/(-L)) - 1.3(-z/L)^{-1/3}]$$

From eq. (2.16)

$$f(z/L) - f(z_0/L) = \ln z/z_0 \text{ for } -\frac{z_0}{L} \leq -z/L \leq 0.08 \quad (3.2)$$

$$\& \quad f(z/L) - f(z_0/L) = 0.48 - 2.3 \log \left( \frac{z_0}{-L} \right) - 1.3(-z/L)^{-1/3} \text{ for } 0.08 < -z/L$$

The standard deviation of vertical wind velocity fluctuations can be given by

$$\sigma_w = bu_* \quad \text{for } -z_o/L \leq -z/L \leq 0.08$$

$$\sigma_w = bu_* h(z/L) \quad \text{for } 0.08 < -z/L$$

For free convection layer, as shown in Sec. 2.2.4.1 many expressions for  $h(z/L)$  (and hence for  $\sigma_w$ ) are available. For  $z/(-L) > 5$ , the only expression available is by Hanna (1968) (Eq. (2.22)).

Adopting his relationship

$$\sigma_w = bu_* (1 + 7 z/(-L))^{1/6}$$

$$h(z/L) = (1 + 7 z/(-L))^{1/6} \quad (3.3)$$

Substituting the expressions of Eqs. (3.2) and (3.3) in the Eq. (3.1)

$$\begin{aligned} \frac{bkx}{(-L)} = & \frac{0.08}{z_o(-L)} \frac{\ln z/z_o}{1} d(z/L) + \\ & \int_{0.08}^{z_{\max}/(-L)} \frac{0.48 - 2.3 \log z_o/(-L) - 1.3(z/(-L))^{-1/3}}{(1 + 7 z/(-L))^{1/6}} d z/(-L) \end{aligned} \quad (3.4)$$

The integral of Eq. (3.4) was evaluated numerically by using Gauss-Legendre Quadrature method, for which number of points used were four, in an interval of  $z/L = 1$ . The computer programme for the evaluation of this equation is shown in the appendix A-1. Three

cases of different values of  $z_0/(-L)$  were studied.

In the above derivations, it is assumed that free convection occurs at  $z/(-L) = 0.08$ . When  $z_0/(-L) \geq 0.08$ , free convection conditions can be assumed from  $z_0/(-L)$  itself, In that case

$$\bar{u} = \frac{u_*}{k} [1.3 (z_0/(-L))^{-1/3} - 1.3 (z/(-L))^{-1/3}]$$

$$\therefore f(z/L) = 1.3 (z_0/(-L))^{-1/3} - 1.3 (z/(-L))^{-1/3} \quad (3.5)$$

Then Eq. (3.4) becomes

$$\frac{bk\bar{x}}{(-L)} = \int_{z_0/(-L)}^{z_{\max}/(-L)} \frac{1.3(z_0/(-L))^{-1/3} - 1.3(z/(-L))^{-1/3}}{(1+7 z/(-L))^{1/6}} dz/(-L) \quad (3.6)$$

Eq. (3.6) was also evaluated numerically as was Eq. (3.4).

From Eqs. (3.4) and (3.6), the following Table 3.1 is prepared, where  $bk\bar{x}/(-L)$  values for different values of  $z_{\max}/(-L)$  are tabulated, for the cases of  $z_0/(-L) =$  (i) 0.0001, (ii) 0.001, (iii) 0.01 and (iv) 0.1. Figure 3.2 graphically presents these values. Thus for unstable atmospheric conditions, a relationship has been obtained between the  $z_{\max}$  and the mean downwind distance  $\bar{x}$  from the source, if  $z_0$  and  $L$  are known.



TABLE 3.1

THE VALUES OF  $z_{\max}/(-L)$  AND CORRESPONDING VALUES OF  $\overline{bkx}/(-L)$ , FOR DIFFERENT  $z_0/(-L)$ , BY USING EQS. (3.4) AND (3.6), FOR UNSTABLE ATMOSPHERIC CONDITIONS

A33099

$z_0/(-L)$	0.00010	0.0010	0.010	0.10
$z_{\max}/(-L)$	$\overline{bkx}/L$			
0.03	0.141	0.075	0.013	-
0.10	0.531	0.306	0.131	-
0.20	1.181	0.244	0.315	-
0.50	3.144	2.134	1.133	0.204
0.70	4.417	3.053	1.698	0.390
1.00	6.333	4.497	2.544	0.706
2.00	12.157	8.785	5.308	1.789
5.00	27.983	20.566	13.098	5.178
7.00	37.771	27.894	18.018	7.418
10.00	51.762	38.399	25.088	10.706
20.00	94.839	70.866	47.128	21.228
50.00	208.993	157.281	106.428	50.383
70.00	278.729	210.198	142.818	68.558
100.00	377.921	285.487	194.578	94.573

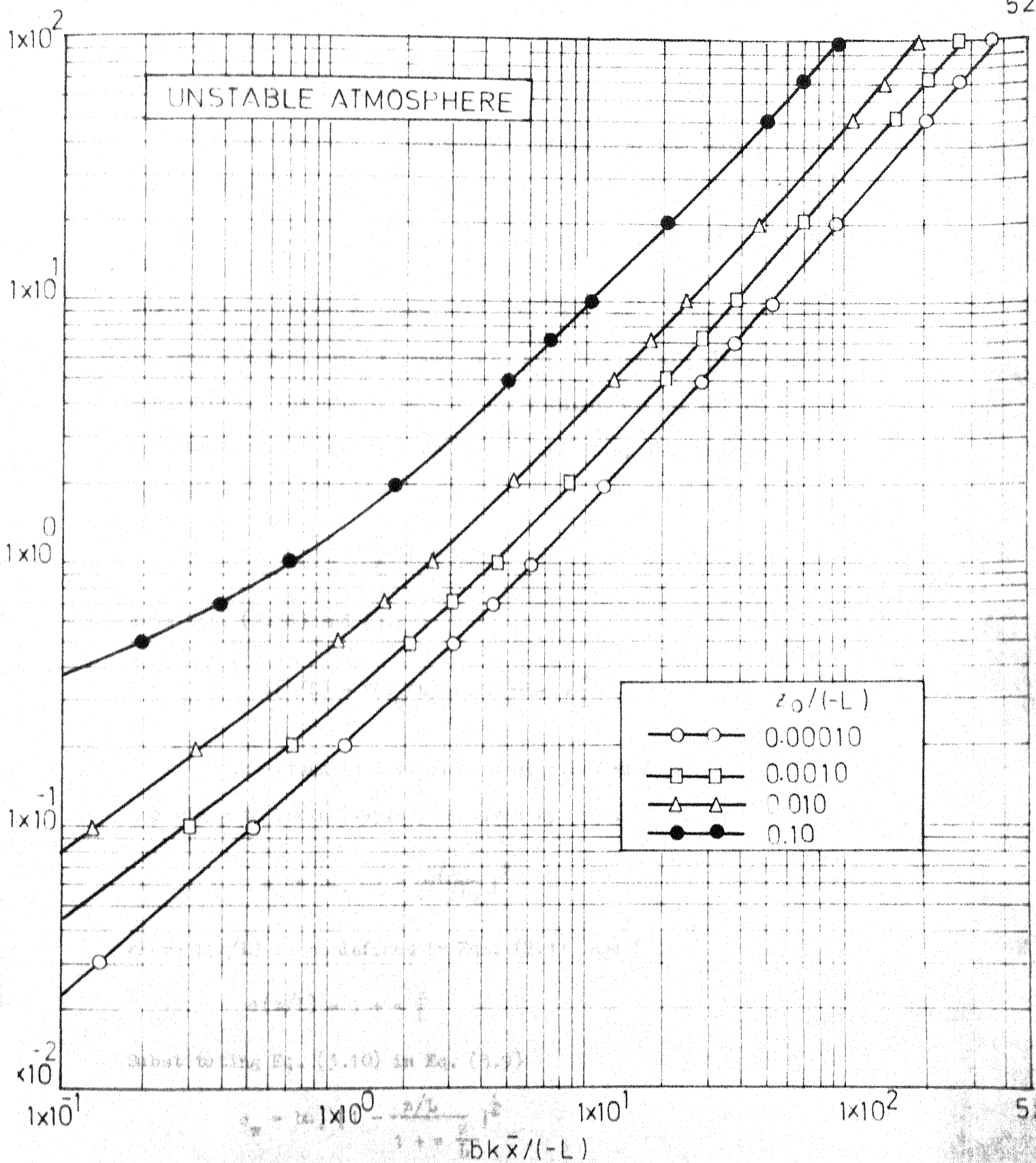


FIG. 3.2 PLOT OF  $z_{\max}/(-L)$  VS  $bk\bar{x}/(-L)$  FOR DIFFERENT VALUES OF  $z_0/(-L)$  AS GIVEN BY EQS.(3.4) and (3.6) FOR UNSTABLE ATMOSPHERIC CONDITIONS

### 3.3.2. Stable Atmosphere

For the stable atmospheric conditions, the wind profile can be given by

$$\bar{u} = \frac{u_*}{k} \left[ \ln \frac{z}{z_0} + \alpha \frac{(z-z_0)}{L} \right] \quad (3.7)$$

where  $\alpha$  is a universal constant. The value of  $\alpha$ , as discussed in sec. 2.2.3.3, can be taken as 6.0 for the stable atmospheric conditions. The second term on the right-hand side can be taken as  $\alpha z/L$  for all practical purposes, and thus, the equation can be written as

$$\bar{u} = \frac{u_*}{k} \left[ \ln \frac{z}{z_0} + \alpha \frac{z}{L} \right] \quad (3.7a)$$

From Eqs. (2.16) and (3.7a)

$$f(z/L) - f(z_0/L) = \ln \frac{z}{z_0} + \alpha \frac{z}{L} \quad (3.8)$$

The standard deviation of vertical wind velocity fluctuations, according to Monin (1959b), is given by (Eqs. (2.19) and (2.20))

$$\sigma_w = bu_* \left[ 1 - \frac{z/L}{\phi(z/L)} \right]^{\frac{1}{4}} \quad (3.9)$$

where  $\phi(z/L)$  is as defined by Eqs. (2.11) and (2.12). Accordingly

$$\phi(z/L) = 1 + \alpha \frac{z}{L} \quad (3.10)$$

Substituting Eq. (3.10) in Eq. (3.9)

$$\begin{aligned} \sigma_w &= bu_* \left[ 1 - \frac{z/L}{1 + \alpha \frac{z}{L}} \right]^{\frac{1}{4}} \\ \therefore \sigma_w &= bu_* \left[ \frac{1 + (\alpha - 1) \frac{z}{L}}{1 + \alpha \frac{z}{L}} \right]^{\frac{1}{4}} \end{aligned} \quad (3.11)$$

From Eqs. (3.11) and (2.20)

$$h(z/L) = \left[ \frac{1 + \frac{1}{2} \frac{z/L}{1 + \frac{1}{2} \frac{z/L}{L}}}{1 + \frac{1}{2} \frac{z/L}{L}} \right]^{\frac{1}{2}} \quad (3.12)$$

Using Eqs. (3.8) and (3.12) in Eq. (3.1)

$$\begin{aligned} bk \frac{\bar{x}}{L} &= \int_{z_0/L}^{z_{\max}/L} \frac{f(z/L) - f(z_0/L)}{h(z/L)} d(z/L) \\ bk \frac{\bar{x}}{L} &= \int_{z_0/L}^{z_{\max}/L} \frac{\ln \frac{1 + \frac{1}{2} \frac{z/L}{L}}{1 + \frac{1}{2} \frac{z_0/L}{L}} + \alpha \frac{z/L}{L}}{\left[ \frac{1 + \frac{1}{2} \frac{z/L}{L}}{1 + \frac{1}{2} \frac{z/L}{L}} \right]^{\frac{1}{2}}} d(z/L) \end{aligned} \quad (3.13)$$

Eq. (3.13) can be integrated numerically. For  $z_0/L$  values = (i) 0.0001, (ii) 0.001, (iii) 0.01 and (iv) 0.1, the equation was evaluated numerically using Gauss-Legendre Quadrature method (Carnahan et al., 1969). Some of the important values of  $bk \bar{x}/L$  corresponding to  $z_{\max}/L$  have been tabulated in Table 3.2 and Fig. 3.3 shows the relations graphically.

TABLE 3.2

THE VALUES OF  $z_{\max}/L$  AND CORRESPONDING VALUE OF  $zk \bar{x}/L$ , FROM DIFFERENT  $z_0/L$ , BY USING EQ. (3.13), FOR STABLE ATMOSPHERIC CONDITIONS

$z_0/L$	0.0001	0.001	0.01	0.1
$z_{\max}/L$	$bk \bar{x}/L$			
0.01	0.046	0.013	-	-
0.02	0.085	0.040	0.004	-
0.05	0.261	0.145	0.038	-
0.07	0.390	0.228	0.078	-
0.10	0.625	0.393	0.161	-
0.20	1.452	0.993	0.525	0.069
0.50	4.590	3.410	2.240	0.900
0.70	7.100	5.450	3.810	1.875
1.00	11.400	9.100	6.650	3.911
2.00	30.387	25.710	21.000	15.210
5.00	127.100	115.120	105.310	88.598

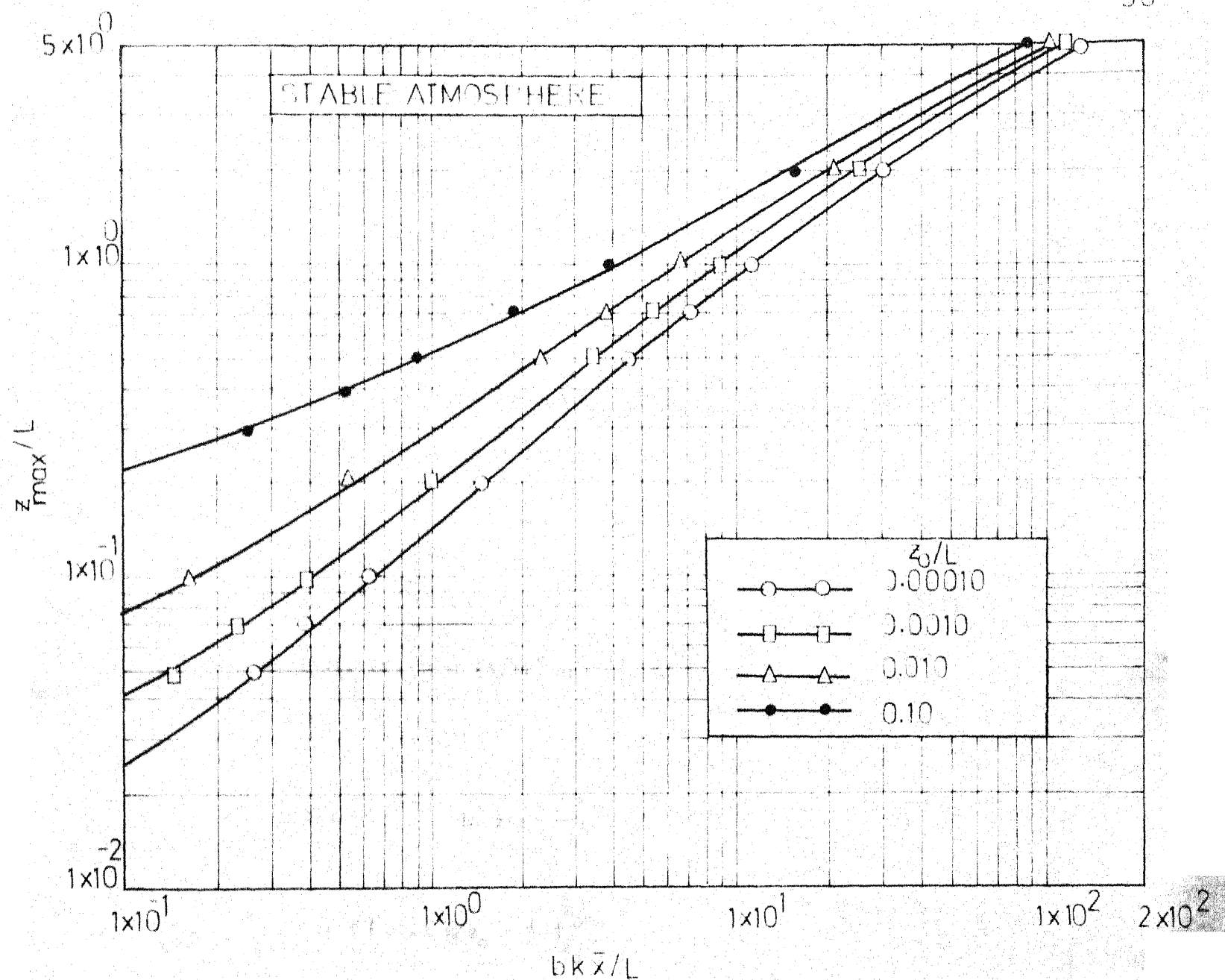


FIG 3.3 PLOT OF  $z_{\max}/L$  VS  $bk\bar{x}/L$  FOR DIFFERENT VALUES OF  $z_0/L$  AS GIVEN BY EQ. (3.13), FOR STABLE ATMOSPHERIC CONDITIONS

Eq. (3.16) gives the relationship between the  $z_{\max}$  and the mean downwind distance  $\bar{x}$  from the source, if the roughness length  $z_0$  is known, for the neutrally stable conditions of the atmosphere.

Table 3.3 and Fig. 3.4 show the  $z_{\max}/z_0$  and corresponding  $\bar{x}/z_0$  values evaluated from Eq. (3.1.6), taking  $b = 1.2$ .

TABLE 3.3

THE VALUES OF  $z_{\max}/z_0$  AND CORRESPONDING VALUES OF  $\bar{x}/z_0$ , FROM Eq. (3.16), FOR NEUTRAL ATMOSPHERIC CONDITIONS, TAKING  $b = 1.2$ .

$z_{\max}/z_0$	$\bar{x}/z_0$
10	29.2
20	85.5
30	152.0
50	304.0
70	475.0
100	752.0
150	1250.0
200	1795.0
500	5410.0
700	8080.0
1000	12300.0
2000	27500.0
3000	43750.0
4000	60900.0
5000	78100.0

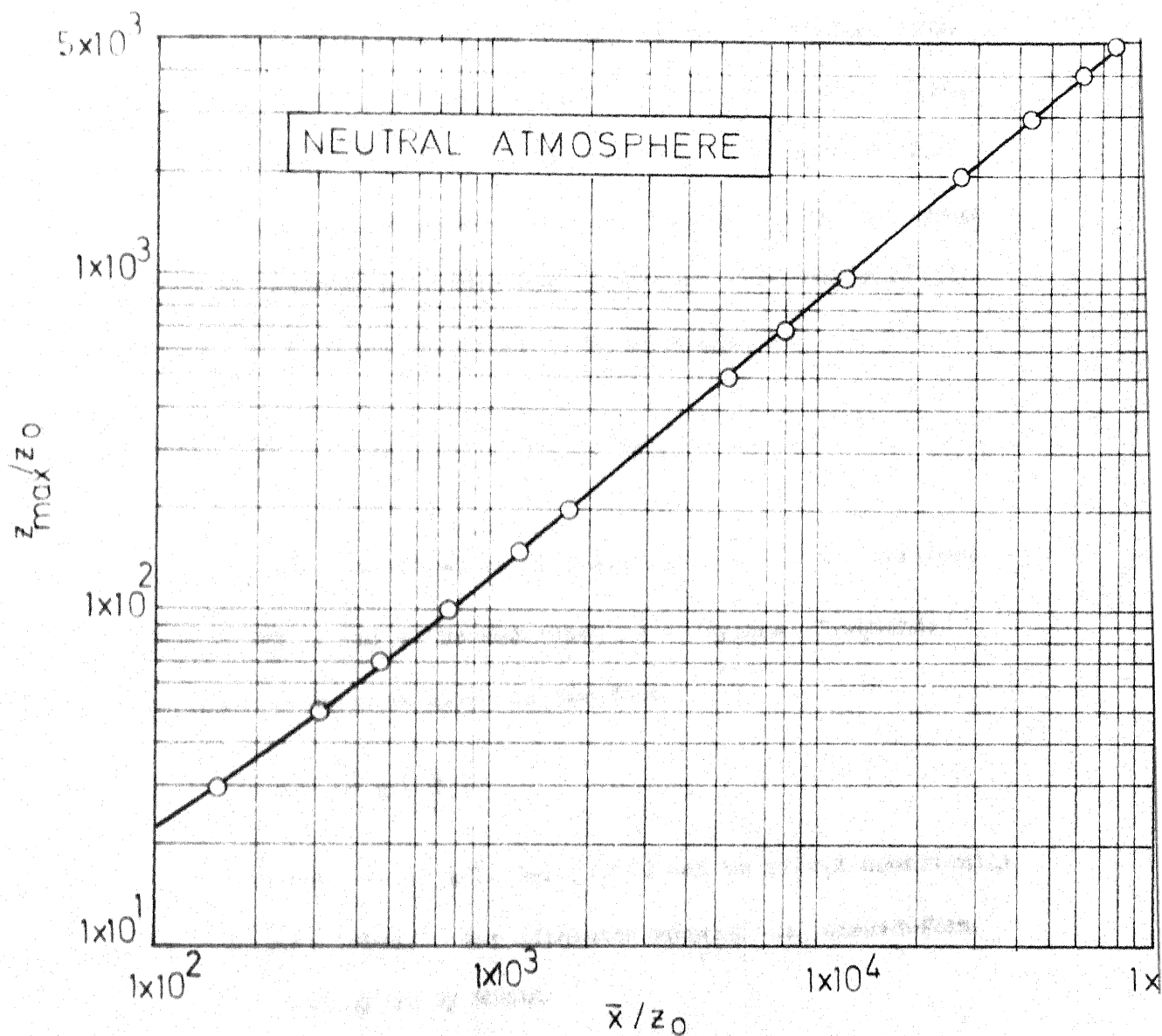


FIG. 3.4 PLOT OF  $z_{max}/z_0$  Vs  $\bar{x}/z_0$ , as given by Eq. (3.16) for neutral atmospheric conditions, taking  $b=1.2$



### 3.3.4 Concentration Distribution by Monin's Approach

For determination of the distribution of pollutant with height, Monin (1959b) proposed the use of a hyperbolic equation, in place of common use of parabolic equation. He assumed that the plume had a finite spread, and accordingly use of "telegraph equation" of hyperbolic nature was consistent with the principle of limited propagation velocity. The equations are

$$\frac{\partial C}{\partial t} + \frac{\partial F}{\partial z} = 0, \quad \frac{\partial F}{\partial t} + 2 a F = - w^* \frac{\partial w^* C}{\partial z} \quad (3.17)$$

where  $c$  is the concentration of pollutant,  $F$  is the vertical flux,  $w^* = \frac{\partial z}{\partial t}$ , and  $a$  is described as a 'typical frequency' of turbulence, which is given in the form

$$a = \frac{u_*}{z} \psi \left( \frac{z}{L} \right)$$

For some function  $\psi$  of  $z/L$ . Eq. (3.17) can be solved numerically for any stratification. For adiabatic conditions, closed-form solution has been given by Monin.

Pasquill (1962a) gave a comparison between the concentration profile given by Monin's hyperbolic equation and parabolic equation commonly used for diffusion studies, and showed almost identical results, except near the top of the spread, where Monin's profile, in accordance with the concept of finite propagation velocity, suddenly falls to zero concentration.

### 3.3.5 Critical Appraisal of Monin's Approach

Monin assumed that Eq. (3.1) represented the equation of motion of particles at the upper boundary of plume. But looking to the Eqs. (2.50) and (2.51) by which  $h(z/L)$  and  $[f(z/L) - f(z_0/L)]$  are determined, it can be seen that  $z$  in Eq. (3.1) should represent mean height of ensemble of particles (Pasquill, 1966). Although the assumption of finite diffusion is more realistic physically, Eq. (3.1) should mean to represent mean height. The determination of concentration distribution consistent with finite-width plume becomes complicated and estimated concentrations are not very much different from those given by simple exponential distributions, usually adopted in the diffusion studies. Thus, it can not be denied that finite diffusion is physically more realistic although the practical difference is probably not great.

If exponential distribution of concentration is adopted for simplicity in use,  $z$  in Eq. (3.1) should represent some near-extreme spread of particles. Pasquill (1966) arbitrarily assumed that  $z$  in Eq. (3.1) was representing the height at which concentration falls down to 10% of the axial concentration.

Monin's approach was first put forth in 1959; Pasquill (1966) used it to predict vertical spread. However, very little verification has been done on field data, especially for thermally stratified field and with large surface roughness.

### 3.4 Objectives of this Study.

There is a need of developing a comprehensive model of atmospheric diffusion, which can take into account the effects of both the inhomogeneous turbulence field of different stability conditions of the atmosphere as well as of different aerodynamic roughnesses of the underlying surface; and would lend itself to simple and reliable predictions of pollutant concentration at various points.

The present study was taken up to investigate the applicability of the Lagrangian similarity theory in predicting the vertical spread of pollutants for different stability conditions and different aerodynamic roughnesses. Equations, using similarity theory, have been developed to predict mean vertical spread, unlike near-extreme spreads given by Monin. Both these approaches are tested on field data.

Consistent with the actual atmospheric observations, the variation of  $\bar{u}$  and  $\sigma_y(x)$  with the height were also incorporated in the formulation of concentration distribution in the downwind direction from a source.

Based on the above, a procedure was evolved to compute pollutant spread taking into account surface roughness of the area as also the atmospheric turbulence and stability as indicated by various micro-meteorological parameters. Besides mathematical

models, tables and charts have been developed through numerical solution of the equation with the help of a digital computer for ready use on field.

### 3.5 Evolution of a Comprehensive Diffusion Model

#### 3.5.1 Estimation of Vertical Spread

In the derivations that follow, the following assumptions are made:

- (i) as soon as the particles are released from a source, they instantaneously attain the velocity field of the surrounding environment, and
- (ii) the distance  $x$  travelled by the particles in the downwind direction in time  $t$  is the mean distance,  $\bar{x}$  of ensemble of particles, each of which has travelled a specific time.

It is further assumed that the vertical displacement of the particles  $z$  in time  $t$  is the mean displacement given by  $\bar{z}$  (following Pasquill, 1966 ). Under the above assumptions, Pasquill's approach is applicable and the rate of the mean vertical displacement is given by Eq. (2.50a) as

$$\frac{d\bar{z}}{dt} = bu_* h (\bar{z}/L) \quad (3.18)$$

Also, as shown by Pasquill,

$$\frac{d\bar{z}}{dt} = \int_0^{\infty} c \cdot \frac{dK_M}{dz} dz / \int_0^{\infty} c dz \quad (3.19)$$

Unlike the approach of Pasquill (1966) where he assumes  $b = k = 0.40$  for all the conditions of stability, it is proposed by the author that parameters of Eq. (3.18) be obtained from Eq. (3.19) separately for each case of stability, and employing these forms of  $d\bar{z}/dt$ , relationships between mean downwind distance  $\bar{x}$  and mean vertical displacement  $\bar{z}$  be established.

In Eq. (3.19),  $c$  is the mean concentration of pollutant at any height  $z$  in the vertical plane at a distance  $\bar{x}$  from the source. To get  $c$ , one requires the shape of the distribution of pollutant in the vertical direction. As discussed earlier in Section 2.3.2.3, the shape is assumed as an exponential form, given by an equation  $\exp(-bz^s)$  where  $s$  varies from 1 to 1.5. Assuming  $s = 1$ , following Bosanquet and Pearson (1936), the form becomes simply  $\exp(-bz)$ . Writing the equation in terms of  $\sigma_z$ , for an exponential distribution, by definition of  $\sigma_z$ ,

$$c = c_0 \exp\left(-1.414 \frac{z}{\sigma_z}\right) \quad (3.20)$$

where  $c_0$  is the axial or the ground-level concentration, and  $\sigma_z$  is standard deviation of vertical spread.

To establish the relation between the standard deviation of  $\sigma_z$  and mean displacement  $\bar{z}$  of vertical spread, the first moment is taken (Kapur and Saxena, 1972) as

$$\begin{aligned}
\bar{z} &= \frac{\int_0^{\infty} c \cdot z \, dz}{\int_0^{\infty} c \, dz} \\
&= \frac{\int_0^{\infty} c_0 \exp(-1.414 \frac{z}{\sigma_z}) z \, dz}{\int_0^{\infty} c_0 \exp(-1.414 \frac{z}{\sigma_z}) \, dz} \\
&= \frac{1}{(1.414/\sigma_z)^2} / \frac{1}{(1.414/\sigma_z)} \\
&= \frac{\sigma_z}{1.414} \\
\bar{z} &= \frac{\sigma_z}{1.414} \tag{3.21}
\end{aligned}$$

$$\text{and} \quad c = c_0 \exp\left(-\frac{z}{\sigma_z}\right) \tag{3.22}$$

In the Eq. (3.19),  $K_M$  is the eddy viscosity and within the surface layer of the atmosphere, it is given by Monin-Obukhov (1954) similarity theory as (Eq. (2.11))

$$K_M = \frac{u_*^2}{d\bar{u}/dz} \tag{3.23}$$

For each case of stability condition  $d\bar{u}/dz$  is known and  $K_M$  can be derived and used in the Eq. (3.19).

While  $d\bar{z}/dt$  gives the mean vertical velocity of the ensemble of particles, the mean horizontal velocity of the ensemble of particles

has to be established. As it is assumed that the pollutant particles have the same velocity field as that of air around, the mean horizontal velocity at any height for any stability conditions can be derived from Eqs. (2.4a), (2.14) and (2.15). To get the mean horizontal velocity for the ensemble of particles in any plane, one can write

$$\frac{d\bar{x}}{dt} = \frac{\int_0^{\infty} c \cdot \bar{u} dz}{\int_0^{\infty} c dz} \quad (3.24)$$

Once  $d\bar{z}/dt$  and  $d\bar{x}/dt$  are established, the relation between  $\bar{x}$  and  $\bar{z}$  can be easily achieved by

$$\frac{d\bar{x}}{d\bar{z}} = \frac{d\bar{x}/dt}{d\bar{z}/dt} \quad (3.25)$$

$$\text{and} \quad \bar{x} = \int \frac{d\bar{x}/dt}{d\bar{z}/dt} d\bar{z} \quad (3.26)$$

within the appropriate boundary conditions.

The cases of thermally neutral, unstable and stable atmospheres are studied separately in the following paragraphs.

#### 3.5.1.1 Neutral Atmosphere

For the neutral atmosphere, the wind velocity profile is given by Eq. (2.4a) as

$$\bar{u} = \frac{u_*}{k} \ln (z/z_0)$$

$$\frac{d\bar{u}}{dz} = \frac{u_*}{k} \cdot \frac{1}{z} \quad (3.27)$$

Substituting Eq. (3.27) in the Eq. (3.23)

$$K_M = \frac{u_*^2}{(u_*/kz)}$$

$$K_M = ku_* z \quad (3.28)$$

Hence  $\frac{dK_M}{dz} = ku_* \quad (3.29)$

Using Eqs. (3.22) and (3.29) in the Eq. (3.19)

$$\frac{d\bar{z}}{dt} = \frac{\int_0^{\infty} c_0 \exp(-\frac{z}{Z}) \times (ku_*) dz}{\int_0^{\infty} c_0 \exp(-\frac{z}{Z}) dz}$$

Simplifying

$$\frac{d\bar{z}}{dt} = ku_* \quad (3.30)$$

To get the mean horizontal velocity of ensemble of particles,

$$\frac{d\bar{x}}{dt} = \frac{\int_0^{\infty} c_0 \exp(-\frac{z}{Z}) \times (\frac{u_*}{k} \ln z/z_0) dz}{\int_0^{\infty} c_0 \exp(-\frac{z}{Z}) dz}$$



$$\begin{aligned}
&= \frac{u_*}{k} \frac{\int_0^{\infty} \exp(-\frac{z}{\bar{z}}) (\ln z - \ln z_0) dz}{\int_0^{\infty} \exp(-\frac{z}{\bar{z}}) dz} \\
&= \frac{u_*}{k} \frac{[-\bar{z} (\ln \gamma / \bar{z}) - \bar{z} \ln z_0]}{\bar{z}}
\end{aligned}$$

using Laplace Transforms (Erdelyi et al., 1954),  $\gamma$  being Euler-Mascheroni constant ( $= e^c$ , where  $c = 0.5772$ ) numerically equal to 1.781.

$$\begin{aligned}
\frac{d\bar{x}}{dt} &= \frac{u_*}{k} [-\ln \gamma + \ln \bar{z}/z_0] = \frac{u_*}{k} [-0.5772 + \ln \bar{z}/z_0] \\
&= \frac{u_*}{k} [\ln 0.56 + \ln \bar{z}/z_0] \\
\frac{d\bar{x}}{d\bar{z}} &= \frac{u_*}{k} [\ln (0.56 \bar{z}/z_0)] \quad (3.31)
\end{aligned}$$

From Eqs. (3.30) and (3.31),

$$\begin{aligned}
\frac{d\bar{x}}{d\bar{z}} &= \frac{u_*}{k} [\ln(0.56 \bar{z}/z_0)] / ku_* \\
&= \frac{1}{k^2} \ln(0.56 \bar{z}/z_0) \\
\therefore \bar{x} &= \int_{z_0}^{\bar{z}} \frac{1}{k^2} \ln(0.56 \bar{z}/z_0) d\bar{z} \\
&= \frac{1}{k^2} [\bar{z} \ln(0.56 \bar{z}/z_0) - \bar{z}]_{z_0}^{\bar{z}}
\end{aligned}$$

$$= \frac{1}{k^2} [\bar{z} \ln (0.56 \bar{z}/z_0) - \bar{z} - z_0 \ln 0.56 + z_0]$$

$$= \frac{1}{k^2} [\bar{z} (\ln 0.56 \bar{z}/z_0 - 1) + 1.58 z_0]$$

$$k^2 x = \bar{z} [\ln(0.56 \bar{z}/z_0) - 1] + 1.58 z_0$$

$$\text{or} \quad \frac{k^2 \bar{x}}{z_0} = \frac{\bar{z}}{z_0} [2.3 \log (0.56 \bar{z}/z_0) - 1] + 1.58 \quad (3.32)$$

For the neutrally stable conditions of the atmosphere, the Eq. (3.32) gives the relation between the mean vertical spread  $\bar{z}$  and the mean downwind distance  $\bar{x}$  from the source, if the roughness length  $z_0$  is known.

Table 3.4 and Fig. 3.5 show the  $\bar{z}/z_0$  and corresponding  $\bar{x}/z_0$  values evaluated from Eq. (3.32).

TABLE 3.4

THE VALUES OF  $\bar{z}/z_0$  AND CORRESPONDING VALUES OF  $\bar{x}/z_0$ , FROM EQ. (3.32), FOR NEUTRAL ATMOSPHERIC CONDITIONS

$\bar{z}/z_0$	$\bar{x}/z_0$	$\bar{z}/z_0$	$\bar{x}/z_0$	$\bar{z}/z_0$	$\bar{x}/z_0$
10	55	70	1180	400	11100
15	114	80	1405	500	14500
20	187	90	1650	600	18000
30	350	100	1890	700	21800
40	536	150	3220	800	25550
50	740	200	4650	900	29400
60	950	300	7825	1000	33300

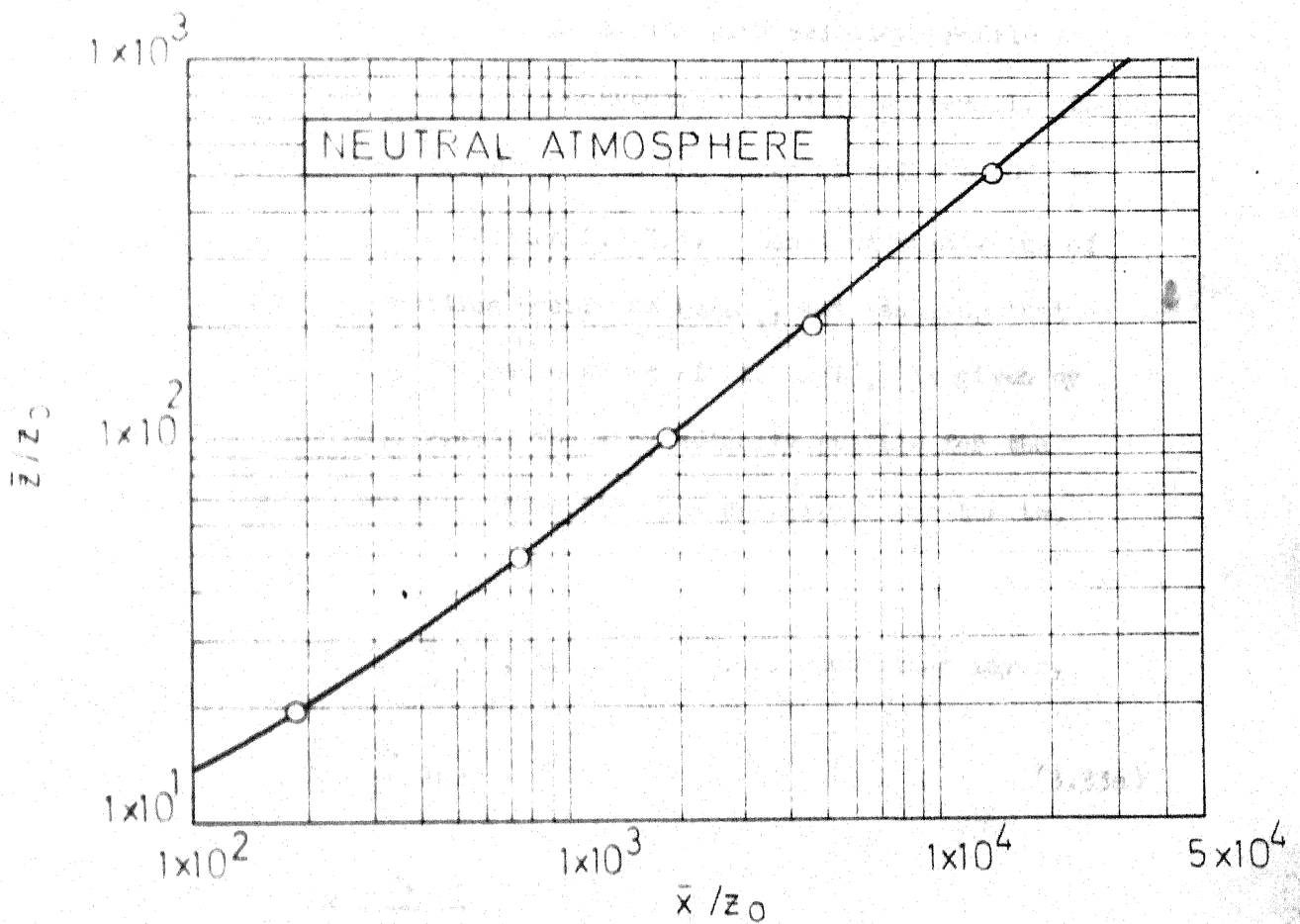


FIGURE 3.5 PLOT OF  $\bar{z}/z_0$  Vs  $\bar{x}/z_0$ , as given by Eq. (3.32) for neutral atmospheric condition.

### 3.5.1.2 Unstable Atmosphere

For the unstable atmosphere, the wind velocity profile is given by Eq. (2.15) when free convection conditions prevail. Such free convection conditions occur in the range of  $z/L = -0.03$  to  $-0.08$ , as discussed in Section 2.2.3.3. Denoting this value of  $z/L$  where free convection occurs as  $(z/L)_*$ , and assuming that wind velocity within the range of  $z_0/L$  to  $(z/L)_*$  is given by logarithmic law (Eq. 2.4a), the wind velocity profile for the entire range of unstable atmosphere can be written for the two layers as follows.

For  $-\frac{z_0}{L} \leq -\frac{z}{L} \leq (-\frac{z}{L})_*$ , i.e., the forced convection layer,

$$\bar{u} = \frac{u_*}{k} \ln \frac{z}{z_0} \quad (3.33a)$$

$$\therefore \frac{d\bar{u}}{dz} = \frac{u_*}{k} \frac{1}{z}$$

From Eq. (3.6)  $\left\{ \begin{aligned} K_M &= \frac{u_*^2}{(u_*/k\bar{z})} \\ &= ku_*z \end{aligned} \right.$

$$\therefore \frac{dK_M}{dz} = ku_* \quad (3.34a)$$

For  $(-\frac{z}{L})_* < -\frac{z}{L}$ , i.e., the free convection layer,

$$\bar{u} = \frac{u_*}{k} [-1.3(-z/L)^{-1/3} + \text{constant}] \quad (3.33b)$$

$$\frac{d\bar{u}}{dz} = \frac{u_*}{k} \times \frac{1.3}{3} \left(-\frac{z}{L}\right)^{-4/3} (-L)^{-1}$$

From Eq. (3.23)

$$K_M = \frac{u_*^2}{\frac{u_*}{k} \times \frac{1.3}{3} (-z/L)^{-4/3} (-L)^{-1}}$$

$$= 2.31 ku_* (-z/L)^{4/3} (-L)$$

$$\frac{dK_M}{dz} = 2.31 \left[ \frac{4}{3} ku_* (-z/L)^{1/3} \right]$$

$$= 3.08 ku_* (-z/L)^{1/3} \quad (3.34b)$$

Using Eqs. (3.22), (3.34a) and (3.34b) in the Eq. (3.19) and writing  $z_* = (-z/L)_* (-L)$ ,

$$\frac{dz}{dt} = \frac{\int_0^\infty c_0 \exp\left(-\frac{z}{z}\right) \cdot \left(\frac{dK_M}{dz}\right)_1 dz + \int_{z_*}^\infty c_0 \exp\left(-\frac{z}{z}\right) \left(\frac{dK_M}{dz}\right)_2 dz}{\int_0^\infty c_0 \exp(-z/\bar{z}) dz}$$

where  $\left(\frac{dK_M}{dz}\right)_1$  is the rate of change of  $K_M$  in the range of  $-z_0/L \leq -z/L \leq (-z/L)_*$  and

$\left(\frac{dK_M}{dz}\right)_2$  is for  $(-z/L)_* < -z/L$ .

$$\frac{dz}{dt} = \frac{\int_0^{z_*} c_0 \exp(-\frac{z}{z}) (ku_*) dz + \int_{z_*}^{\infty} c_0 \exp(-\frac{z}{z}) \times (3.08 ku_* (-\frac{z}{L}))^{1/3} dz}{\int_0^{\infty} c_0 \exp(-\frac{z}{z}) dz}$$

$$= \frac{ku_* [-z \exp(-\frac{z}{z})]_0^{z_*} + 3.08 \frac{ku_*}{(-L)^{1/3}} [\int_{z_*}^{\infty} z^{1/3} \exp(-\frac{z}{z}) dz]}{[-z \exp(-\frac{z}{z})]_0^{\infty}}$$

$$\frac{dz}{dt} = ku_* [1 - \exp(-\frac{z_*}{z})] + 3.08 \frac{ku_*}{z(-L)^{1/3}} \int_{z_*}^{\infty} z^{1/3} \exp(-\frac{z}{z}) dz \quad (3.35)$$

Using Laplace Transforms (Erdelyi et. al., 1954), the integral on the right-hand side can be evaluated as

$$\int_{z_*}^{\infty} z^{1/3} \exp(-\frac{z}{z}) dz = [z]^{4/3} \Gamma(4/3, z_*/z) \quad (3.36a)$$

where  $\Gamma(4/3, z_*/z)$  is the incomplete Gamma function, which is given by (Erdelyi, et. al., 1954)

$$\begin{aligned} \Gamma(4/3, z_*/z) &= \int_{z_*/z}^{\infty} \exp(-z) z^{1/3} dz \\ &= \Gamma(4/3) - \int_0^{z_*/z} \exp(-z) z^{1/3} dz \\ &= [1 - \frac{1}{\Gamma(4/3)} \int_0^{z_*/z} \exp(-z) z^{1/3} dz] \Gamma(4/3) \\ &= [1 - P(4/3, z_*/z)] \Gamma(4/3) \end{aligned} \quad (3.36b)$$

where  $\Gamma(4/3)$  is the complete Gamma function, and  $P(4/3, z_*/\bar{z})$  is the incomplete Gamma function ratio, as tabulated by Khamis (1965). Substituting Eqs. (3.36a) and (3.36b) in the Eq. (3.35)

$$\begin{aligned}\frac{d\bar{z}}{dt} &= ku_* \left[ 1 - \exp\left(-\frac{z_*}{\bar{z}}\right) \right] + 3.08 \frac{ku_*}{\bar{z}(-L)^{1/3}} (\bar{z})^{4/3} \Gamma(4/3) [1 - P(4/3, \frac{z_*}{\bar{z}})] \\ &= ku_* \left[ 1 - \exp\left(-\frac{z_*}{\bar{z}}\right) + 3.08 \times 0.8934 (-\bar{z}/L)^{1/3} (1 - P(4/3, z_*/\bar{z})) \right]\end{aligned}$$

since value of  $\Gamma(4/3) = 0.8934$

$$\frac{d\bar{z}}{dt} = ku_* \left[ 1 - \exp\left(-\frac{z_*}{\bar{z}}\right) + 2.75 (-\bar{z}/L)^{1/3} (1 - P(4/3, z_*/\bar{z})) \right] \quad (3.37)$$

Eq. (3.37) shows the mean vertical velocity of the ensemble of particles in the unstable atmosphere. It can be seen that  $z_*/\bar{z} = (-z/L)_* \times (-L)/\bar{z} = (z/L)_*/(\bar{z}/L)$ , and for small values (e.g. 0.1 or less) of  $(z/L)_*/(\bar{z}/L)$ ,  $[1 - \exp(-\frac{z_*}{\bar{z}})]$  and  $P(\frac{4}{3}, \frac{z_*}{\bar{z}})$  tend to become very small, and hence the Eq. (3.37) can approximately be written as

$$\begin{aligned}\frac{d\bar{z}}{dt} &= ku_* [2.75 (-\bar{z}/L)^{1/3}] \\ \text{or } \frac{d\bar{z}}{dt} &= 2.75 ku_* (-\bar{z}/L)^{1/3} \text{ for } (-\bar{z}/L) \gg (-z/L)_* \quad (3.37a)\end{aligned}$$

To get the mean horizontal velocity of ensemble of particles in the unstable atmospheric conditions, the wind velocity profile

Eqs. (3.32a) and (3.32b) has to be fully established. At  $(-z/L)_*$ , both  $\bar{u}$  and  $K_M$  profiles have to be continuous. For  $K_M$ -profile to be continuous at  $z = (-z/L)_* \times (-L) = z_*$

$$K_M = k u_* z_* \quad \text{for the lower layer}$$

$$= 2.31 \times k u_* \left(-\frac{z_*}{L}\right)^{4/3} (-L)^{-1} \quad \text{for the upper layer}$$

$$\therefore z_* = 2.31 \left(-\frac{z_*}{L}\right)^{4/3} (-L)^{-1}$$

$$\text{or, } \left(-\frac{z_*}{L}\right)^{1/3} = \frac{1}{2.31}$$

$$\text{or } \left(-\frac{z_*}{L}\right) = 0.08 \quad (3.38)$$

$$\text{i.e. } (-z/L)_* = 0.08$$

This shows that upto the height  $= 0.08 \times (-L)$  from the surface, the logarithmic wind profile will be applicable and beyond the  $1/3$ -profile will dominate. At  $z = 0.08 \times (-L)$ , the wind velocity given by each of the formulae must be the same, i.e.,

$$\begin{aligned} \bar{u} &= \frac{u_*}{k} \ln \frac{0.08 \times (-L)}{z_0} \\ &= \frac{u_*}{k} \left[ -1.3 \left( \frac{0.08 \times (-L)}{-L} \right)^{-1/3} + \text{constant} \right] \end{aligned}$$

$$\therefore \ln \frac{0.08 \times (-L)}{z_0} = -1.3(0.08)^{-1/3} + \text{constant}$$

$$\begin{aligned} \text{or } \quad \text{constant} &= 1.3(0.08)^{-1/3} + 2.3 \log \frac{0.08}{(z_0/-L)} \\ &= 3.08 + 2.3 \log 0.08 - 2.3 \log (z_0/-L) \end{aligned}$$



$$= 3.00 - 2.52 - 2.3 \log (z_0/-L)$$

$$= 0.48 - 2.3 \log (z_0/-L)$$

Substituting the value of the constant,  $\bar{u}$ , beyond  $z = 0.08 \times (-L)$ , becomes

$$\bar{u} = \frac{u_*}{k} [0.48 - 2.3 \log (z_0/-L) - 1.3(-z/L)^{-1/3}]$$

Thus, the overall wind profile becomes

$$\begin{aligned} \bar{u} &= \frac{u_*}{k} \ln z/z_0 \quad \text{for } -\frac{z_0}{L} \leq -\frac{z}{L} \leq (-\frac{z}{L})_* \\ &= \frac{u_*}{k} [0.48 - 2.3 \log (z_0/-L) - 1.3(-z/L)^{-1/3}] \text{ for } \quad (3.39) \\ &\quad -z/L > (-z/L)_* \end{aligned}$$

Using Eq. (3.39), the mean horizontal wind velocity of ensemble of particles can be now established

$$\frac{dx}{dt} = \frac{\int_0^{z_*} c \cdot \frac{u_*}{k} \ln \frac{z}{z_0} dz + \int_{z_*}^{\infty} c \cdot \frac{u_*}{k} [0.48 - 2.3 \log (z_0/-L) - 1.3(-\frac{z}{L})^{-1/3}] dz}{\int_0^{\infty} c dz}$$

$$= \frac{u_*}{k} \left[ \int_0^{z_*} \exp(-\frac{z}{L}) \cdot \ln \frac{z}{z_0} dz + \int_{z_*}^{\infty} \exp(-\frac{z}{L}) \right.$$

$$\left. (0.48 - 2.3 \log (z_0/-L) - 1.3(z/-L)^{-1/3}) dz \right]$$

$$/ \int_0^{\infty} \exp(-\frac{z}{L}) dz$$

$$\begin{aligned}
&= \frac{u_*}{k} \cdot \frac{1}{z} \left[ \int_0^{z_*} \exp\left(-\frac{z}{z}\right) \ln z \, dz - \int_0^{z_*} \exp\left(-\frac{z}{z}\right) \ln z_0 \, dz \right. \\
&\quad + \int_{z_*}^{\infty} (0.48 - 2.3 \log(z_0/L)) \exp(-z/\bar{z}) \, dz \\
&\quad \left. - \int_{z_*}^{\infty} (1.3(z/L)^{-1/3}) \exp(-z/\bar{z}) \, dz \right] \\
&= \frac{u_*}{k} \cdot \frac{1}{z} \left[ \int_0^{\infty} \exp\left(-\frac{z}{z}\right) \ln z \, dz - \int_{z_*}^{\infty} \exp\left(-\frac{z}{z}\right) \ln z \, dz \right. \\
&\quad - \ln z_0 \left(-\bar{z} \exp\left(-\frac{z}{z}\right)\right) \Big|_0^{z_*} + (0.48 - 2.3 \log(-\frac{z_0}{L})) \left(-\bar{z} \exp\left(-\frac{z}{z}\right)\right) \Big|_{z_*}^{\infty} \\
&\quad \left. - \frac{1.3}{(-L)^{-1/3}} \int_{z_*}^{\infty} z^{-1/3} \exp(-z/\bar{z}) \, dz \right]
\end{aligned}$$

Using Laplace Transforms (Erdelyi, et. al., 1954) to evaluate the three integrals in above,

$$(i) \int_0^{\infty} \exp\left(-\frac{z}{z}\right) \ln z \, dz = -\bar{z} \ln(\gamma/\bar{z}), \text{ where } \gamma \text{ is}$$

Euler-Mascheroni constant ( $= e^c$ , where  $c = 0.5772$ ),

$$(ii) \int_{z_*}^{\infty} \exp\left(-\frac{z}{z}\right) \ln z \, dz = \bar{z} \left[ \exp\left(-\frac{z_*}{z}\right) \ln z_* - E_1\left(-z_*/\bar{z}\right) \right]$$

$$\text{where } -E_1\left(-z_*/\bar{z}\right) = \int_{z_*/\bar{z}}^{\infty} \exp(-z) z^{-1} \, dz$$

which is the exponential integral, tabulated values being given by Pagurova (1961).

$$(iii) \int_{z_*}^{\infty} z^{-1/3} \exp(-z/\bar{z}) dz = (\bar{z})^{2/3} \Gamma(2/3, z_*/\bar{z})$$

where again  $\Gamma(2/3, z_*/\bar{z})$  is the incomplete Gamma function, and is given by

$$\begin{aligned} \Gamma(2/3, z_*/\bar{z}) &= \int_{z_*/\bar{z}}^{\infty} \exp(-z) z^{-1/3} dz \\ &= \Gamma(2/3) - \int_0^{z_*/\bar{z}} \exp(-z) z^{-1/3} dz \\ &= \Gamma(2/3) \left[ 1 - \frac{1}{\Gamma(2/3)} \int_0^{z_*/\bar{z}} \exp(-z) z^{-1/3} dz \right] \\ &= \Gamma(2/3) [1 - I(2/3, z_*/\bar{z})] \end{aligned}$$

where  $P(2/3, z_*/\bar{z})$  is the incomplete Gamma function ratio, as tabulated by Khamis (1965). Substituting these three integrals,

$$\begin{aligned} \frac{d\bar{x}}{dt} &= \frac{u_*}{k \cdot \bar{z}} \left[ -\bar{z} \ln(\gamma/\bar{z}) - \bar{z} (\exp(-z_*/\bar{z}) \ln z_* \right. \\ &\quad \left. - E_1(-z_*/\bar{z})) - \ln z_0 (\bar{z} - \bar{z} \exp(-\frac{z_*}{\bar{z}})) \right. \\ &\quad \left. + (0.48 - 2.3 \log(\frac{z_0}{-L})) (0 + \bar{z} \exp(-\frac{z_*}{\bar{z}})) \right. \\ &\quad \left. - \frac{1.3}{(-L)^{-1/3}} (\bar{z})^{2/3} \Gamma(2/3) (1 - P(2/3, z_*/\bar{z})) \right] \end{aligned}$$

Simplifying the equation, it becomes

$$\begin{aligned}
\frac{d\bar{x}}{dt} = & \frac{u_*}{k} \left[ -0.5772 - \ln \frac{z_*}{z_0} \exp \left( -\frac{z_*}{\bar{z}} \right) + \ln \bar{z}/z_0 \right. \\
& + E_1(-z_*/\bar{z}) + (0.48 - 2.3 \log(-\frac{z_0}{L})) \exp(-z_*/\bar{z}) \\
& \left. - 1.76 (\bar{z}/-L)^{-1/3} (1 - I(2/3, z_*/\bar{z})) \right] \quad (3.40)
\end{aligned}$$

The Eq. (3.40) gives the mean horizontal velocity of the ensemble of particles. On the evaluation of  $d\bar{x}/dt$ , it was observed that for small values of  $z_*/\bar{z}$  (i.e.  $(-z/L)_*/(\bar{z}/L)$ ), the summation of first four terms on the right-hand side becomes almost negligible for different values of  $z_0$ . Similarly  $\exp(-z_*/\bar{z}) \rightarrow 1$  and  $I(2/3, z_*/\bar{z}) \rightarrow 0$  for this condition, hence

$$\begin{aligned}
\frac{d\bar{x}}{dt} = & \frac{u_*}{k} \left[ 0.48 - 2.3 \log \left( -\frac{z_0}{L} \right) - 1.76 \left( -\frac{\bar{z}}{L} \right)^{-1/3} \right] \\
& \text{for } \left( -\frac{\bar{z}}{L} \right) \gg \left( -\frac{z_*}{L} \right) \quad (3.40a)
\end{aligned}$$

Once the mean vertical and horizontal velocities have been arrived at, the relation between the downwind distance  $\bar{x}$  and the vertical spread  $\bar{z}$  can be established. From Eqs. (3.37) and (3.40),

$$\frac{d\bar{x}}{d\bar{z}} = \frac{d\bar{x}}{dt} / \frac{d\bar{z}}{dt}$$

$$\begin{aligned}
\frac{d\bar{x}}{d\bar{z}} = & \frac{1}{k^2} \left[ -0.5772 - \ln \frac{z_*}{z_0} \exp \left( -\frac{z_*}{\bar{z}} \right) + \ln \bar{z}/z_0 \right. \\
& + E_1(-z_*/\bar{z}) + (0.48 - 2.3 \log(-\frac{z_0}{L})) \exp(-z_*/\bar{z})
\end{aligned}$$

$$\begin{aligned}
& - 1.76 (\bar{z}/-L)^{-1/3} (1 - P(2/3, z_*/\bar{z})) / [1 - \exp(-\frac{z_*}{\bar{z}})] \\
& + 2.75 (\bar{z}/-L)^{1/3} (1 - P(4/3, z_*/\bar{z}))] \quad (3.41)
\end{aligned}$$

Here

$$z_* = (z/-L)_* \times (-L) = 0.08 \times (-L), \text{ hence}$$

$$\begin{aligned}
\frac{k^2 d\bar{x}}{d\bar{z}} &= [-0.5772 - 2.3 \log \frac{0.08}{(z_0/-L)} \exp(-\frac{0.08}{(z/-L)}) + \\
& 2.3 \log(\frac{\bar{z}/-L}{z_0/-L}) - (-E_1(-0.08/(\bar{z}/-L))) + \\
& (0.48 - 2.3 \log(-z_0/L)) \exp(-0.08/(\bar{z}/-L)) - \\
& 1.76 (\bar{z}/-L)^{-1/3} (1 - P(2/3, 0.08/(\bar{z}/-L))) ] / \\
& [1 - \exp(-\frac{0.08}{(\bar{z}/-L)}) + 2.75 (\bar{z}/-L)^{1/3} (1 - P(4/3, \frac{0.08}{(\bar{z}/-L)}))]
\end{aligned}$$

Integrating,

$$\begin{aligned}
\frac{k^2 \bar{x}}{(-L)} &= \int_{z_0/(-L)}^{\bar{z}/(-L)} [k^2 \frac{d\bar{x}}{d\bar{z}}] d(\bar{z}/-L) \\
&= \int_{z_0/(-L)}^{\bar{z}/(-L)} [-0.5772 - 2.3 \log \frac{0.08}{(z_0/-L)} \exp(-\frac{0.08}{(z/-L)}) + \\
& 2.3 \log(\frac{\bar{z}/-L}{z_0/-L}) - (-E_1(-0.08/(\bar{z}/-L))) + (0.48 - 2.3 \log(\frac{z_0}{-L})) \\
& \exp(-0.08/(\bar{z}/-L)) - 1.76 (\bar{z}/-L)^{-1/3} (1 - P(2/3, 0.08/(\bar{z}/-L))) ] / \\
& [1 - \exp(-\frac{0.08}{(\bar{z}/-L)}) + 2.75 (\bar{z}/-L)^{1/3} (1 - P(4/3, \frac{0.08}{(\bar{z}/-L)}))] d(z/-L) \quad (3.42)
\end{aligned}$$

The integral of Eq. (3.42) was evaluated numerically by using Gauss-Legendre Quadrature method (Carnahan et. al., 1969), for which number of points used was four, in an interval of  $\bar{z}/(-L) = 0.01$ . The computer programme for the evaluation of this equation numerically is shown in the Appendix A-1. Three cases of different values of  $z_0/(-L)$  were studied. It was observed that for  $\bar{z}/(-L) \geq 1.0$ , the integral of Eq. (3.42) could be simplified, as many terms in the numerator as well as the denominator become negligible. Using Eqs. (3.37a) and (3.40a), a relation can be established as

$$\frac{d\bar{x}}{d\bar{z}} = \frac{1}{k^2} [0.48 - 2.3 \log(-z_0/L) - 1.76 (-\bar{z}/L)^{-1/3}] / [2.75 (\bar{z}/-L)^{1/3}]$$

$$= \frac{1}{2.75k^2} [(0.48 - 2.3 \log(\frac{z_0}{-L})) (\frac{\bar{z}}{-L})^{-1/3} - 1.76 (\frac{\bar{z}}{-L})^{-2/3}]$$

$$\therefore k^2 \bar{x}/(-L) = \frac{1}{2.75} \int_1^{\bar{z}/(-L)} [(0.48 - 2.3 \log(\frac{z_0}{-L})) (\frac{\bar{z}}{-L})^{-1/3} - 1.76 (\frac{\bar{z}}{-L})^{-2/3}] d(\bar{z}/(-L)) + (\frac{k^2 \bar{x}}{-L})_1$$

where  $(\frac{k^2 \bar{x}}{-L})_1$  is the value of  $\frac{k^2 \bar{x}}{-L}$  upto  $(\bar{z}/-L) = 1$ ,

arrived at by numerical integration

$$\therefore \frac{k^2 \bar{x}}{(-L)} = \frac{1}{2.75} [(0.48 - 2.3 \log(\frac{z_0}{-L})) (\frac{\bar{z}}{-L})^{2/3} \times \frac{3}{2} - 1.76 (\frac{\bar{z}}{-L})^{1/3} \times 3]_1^{\bar{z}/-L} + (\frac{k^2 \bar{x}}{-L})_1$$

$$\text{or, } \frac{k^2 \bar{x}}{(-L)} = 0.545 \left[ (0.48 - 2.3 \log(\frac{z_0}{-L})) (\frac{\bar{z}}{-L})^{2/3} - 3.52 (\frac{\bar{z}}{-L})^{1/3} \right. \\ \left. + 3.04 + 2.3 \log(\frac{z_0}{-L}) \right] + (\frac{k^2 x}{-L})_1 \quad (3.43)$$

Eq. (3.43) gives the relationship between the mean downwind distance  $\bar{x}$  and the mean vertical spread  $\bar{z}$  when  $\bar{z}/(-L) \geq 1$ . Thus solving Eq. (3.42) numerically the values of  $k^2 \bar{x}/(-L)$  can be derived for  $\bar{z}/(-L) \leq 1$ . For  $\bar{z}/(-L) \geq 1$ , the Eq. (3.43) can be used.

In the above derivations, it is assumed that free convection occurs at  $\bar{z}/(-L) = 0.08$ . When the ratio of roughness length to stability length,  $z_0/(-L)$ , is equal to or greater than 0.08, the free convection conditions can be assumed from  $z_0/(-L)$  value of  $\bar{z}/(-L)$  itself. In such circumstances, Eq. (3.39) giving  $\bar{u}$  has to be revised. In the free convection conditions,

$$\bar{u} = \frac{u_*}{k} [-1.3 (z/(-L))^{-1/3} + \text{constant}]$$

When  $z/(-L) = z_0/(-L)$ ,  $\bar{u} = 0$

$$\therefore 0 = \frac{u_*}{k} [-1.3 (z_0/(-L))^{-1/3} + \text{constant}]$$

$$\text{or, constant} = 1.3 (z_0/(-L))^{-1/3}$$

$$\text{Hence, } \bar{u} = \frac{u_*}{k} [1.3 (z_0/(-L))^{-1/3} - 1.3 (z/(-L))^{-1/3}] \quad (3.44)$$

$$\text{And, } K_M = \frac{u_*^2}{d\bar{u}/dz}$$

$$= \frac{u_*^2}{\frac{u_*}{k} \left[ \frac{1.3}{3} \left( \frac{z}{-L} \right)^{-4/3} (-L) \right]}$$

$$= 2.31 k u_* \left( \frac{z}{-L} \right)^{4/3} (-L)^{-1}$$

$$\begin{aligned} \therefore \frac{d\bar{z}}{dt} &= \frac{\int_0^\infty c \frac{dK_M}{dz} dz}{\int_0^\infty c dz} \\ &= \frac{\int_0^\infty c_0 \exp\left(-\frac{z}{\bar{z}}\right) \times \left(3.08 k u_* \times \left(\frac{z}{-L}\right)^{1/3}\right) dz}{\int_0^\infty c_0 \exp\left(-\frac{z}{\bar{z}}\right) dz} \end{aligned}$$

$$= \frac{3.08 k u_*}{(-L)^{1/3}} \frac{\int_0^\infty z^{1/3} \exp\left(-\frac{z}{\bar{z}}\right) dz}{\int_0^\infty \exp\left(-\frac{z}{\bar{z}}\right) dz}$$

$$= \frac{3.08 k u_*}{\bar{z}(-L)^{1/3}} \left[ \Gamma(4/3) \cdot \bar{z}^{4/3} \right]$$

$$= 3.08 \left[ 0.8934 k u_* \left( \frac{\bar{z}}{-L} \right)^{1/3} \right]$$

$$\frac{d\bar{z}}{dt} = 2.75 k u_* \left( \frac{\bar{z}}{-L} \right)^{1/3} \quad (3.45)$$

And also,

$$\frac{d\bar{x}}{dt} = \frac{\int_0^\infty c \bar{u} dz}{\int_0^\infty c dz}$$



$$= \frac{\int_0^{\infty} c_0 \exp\left(-\frac{z}{\bar{z}}\right) \frac{u_*}{k} \left[1.3 \left(\frac{z_0}{-L}\right)^{-1/3} - 1.3 \left(\frac{z}{-L}\right)^{-1/3}\right] dz}{\int_0^{\infty} c_0 \exp\left(-\frac{z}{\bar{z}}\right) dz}$$

$$= 1.3 \frac{u_*}{k} \frac{1}{\bar{z}} \left[ \int_0^{\infty} \left(\frac{z_0}{-L}\right)^{-1/3} \exp\left(-\frac{z}{\bar{z}}\right) dz - \int_0^{\infty} \left(\frac{z}{-L}\right)^{-1/3} \exp\left(-\frac{z}{\bar{z}}\right) dz \right]$$

$$= \frac{1.3 u_*}{k \bar{z}} \left[ \left(\frac{z_0}{-L}\right)^{-1/3} \bar{z} - \frac{(\bar{z})^{2/3}}{(-L)^{-1/3}} \Gamma(2/3) \right]$$

$$\frac{d\bar{x}}{dt} = 1.3 \frac{u_*}{k} \left[ \left(\frac{z_0}{-L}\right)^{-1/3} - 1.35 \left(\frac{\bar{z}}{-L}\right)^{-1/3} \right] \quad (3.46)$$

From Eqs. (3.45) and (3.46), the relation between  $\bar{x}$  and  $\bar{z}$  can be achieved, as

$$\frac{d\bar{x}}{d\bar{z}} = \frac{d\bar{x}/dt}{d\bar{z}/dt}$$

$$= \frac{1.3}{2.75 k^2} \left[ \left(\frac{z_0}{-L}\right)^{-1/3} \left(\frac{\bar{z}}{-L}\right)^{-1/3} - 1.35 \left(\frac{\bar{z}}{-L}\right)^{-2/3} \right]$$

$$\therefore \frac{k^2 \bar{x}}{(-L)} = \frac{1.3}{2.75} \int_{z_0/(-L)}^{\bar{z}/(-L)} \left[ \left(\frac{z_0}{-L}\right)^{-1/3} \left(\frac{\bar{z}}{-L}\right)^{-1/3} - 1.35 \left(\frac{\bar{z}}{-L}\right)^{-2/3} \right] d(\bar{z}/-L)$$

$$= 0.473 \left[ \left(\frac{z_0}{-L}\right)^{-1/3} \left(\frac{\bar{z}}{-L}\right)^{2/3} \times \frac{3}{2} - 1.35 \times 3 \left(\frac{\bar{z}}{-L}\right)^{1/3} \right] \frac{\bar{z}/(-L)}{z_0/(-L)}$$

$$\frac{k^2 \bar{x}}{(-L)} = 0.71 \left[ \left(\frac{z_0}{-L}\right)^{-1/3} \left(\frac{\bar{z}}{-L}\right)^{2/3} - 2.7 \left(\frac{\bar{z}}{-L}\right)^{1/3} + 1.7 \left(\frac{z_0}{-L}\right)^{1/3} \right]$$

$$(3.47)$$

Eq. (3.47) relates  $\bar{x}$  and  $\bar{z}$  for the case  $(z_0/-L) \geq 0.08$ .

Using Eqs. (3.42) - (3.43) and (3.47) the following Table 3.5 is prepared, where  $k^2 \bar{x}/(-L)$  values for different values of  $\bar{z}/-L$  are tabulated for the cases of  $z_0/(-L) =$  (i) 0.0001, (ii) 0.001, (iii) 0.01 and (iv) 0.1. Figure 3.6 graphically presents these values.

The equations (3.42), (3.43) and (3.47) or the Table 3.5 and Fig. 3.6 can be used to predict the vertical spread for different condition of unstable atmosphere.

### 3.5.1.3 Stable Atmosphere

As discussed in Section 2.2.3.3, the wind velocity profile under stable atmospheric conditions can be given by Eq. (2.14), viz.,

$$\bar{u} = \frac{u_*}{k} \left[ \ln \frac{z}{z_0} + \alpha \frac{(z - z_0)}{L} \right] \quad (3.48)$$

where  $\alpha$  is the universal constant, the numerical value of which can be taken as 6.0. For all practical purposes, the last term of the equation (3.48) can be approximated as  $\alpha z/L$ , and the whole equation becomes

$$\bar{u} = \frac{u_*}{k} \left[ \ln \frac{z}{z_0} + \alpha \frac{z}{L} \right] \quad (3.48a)$$

The first derivative w.r.t.  $z$  will be

TABLE 3.5

THE VALUES OF  $\bar{z}/(-L)$  AND CORRESPONDING VALUES OF  $k^2 \bar{x}/(-L)$ ,  
 FOR DIFFERENT  $z_o/(-L)$ , BY USING Eqs. (3.42) - (3.43) AND  
 (3.47), FOR UNSTABLE ATMOSPHERIC CONDITIONS

$z_o/(-L)$	0.00010	0.0010	0.010	0.10
$\bar{z}/(-L)$	$k^2 \bar{x}/(-L)$			
0.01	0.0200	0.0050	-	-
0.02	0.0602	0.0222	-	-
0.03	0.0978	0.0397	-	-
0.04	0.1334	0.0571	-	-
0.05	0.1674	0.0742	0.0002	-
0.06	0.2010	0.0914	0.0010	-
0.07	0.2349	0.1094	0.0031	-
0.08	0.2693	0.1281	0.0062	-
0.09	0.3038	0.1475	0.0103	-
0.10	0.3382	0.1770	0.0151	-
0.20	0.6862	0.3690	0.0714	-
0.30	1.0402	0.5960	0.1669	-
0.40	1.3822	0.8230	0.2779	-
0.50	1.7142	1.0470	0.3949	0.0040
0.60	2.0342	1.2660	0.5129	0.0420
0.70	2.3442	1.4800	0.6319	0.0650
0.80	2.6442	1.6900	0.7504	0.1080
0.90	2.9392	1.8970	0.8689	0.1380
1.00	3.2267	2.1000	0.9866	0.1710
2.00	5.8570	3.9800	2.1400	0.5760
5.00	12.0570	8.5100	5.000	1.7530
10.00	20.3570	14.6000	8.9400	3.5300
20.00	33.8570	24.5000	15.4600	6.6600
50.00	64.8570	47.6000	30.8800	14.2100
100.00	105.6570	78.0000	51.1500	24.6600

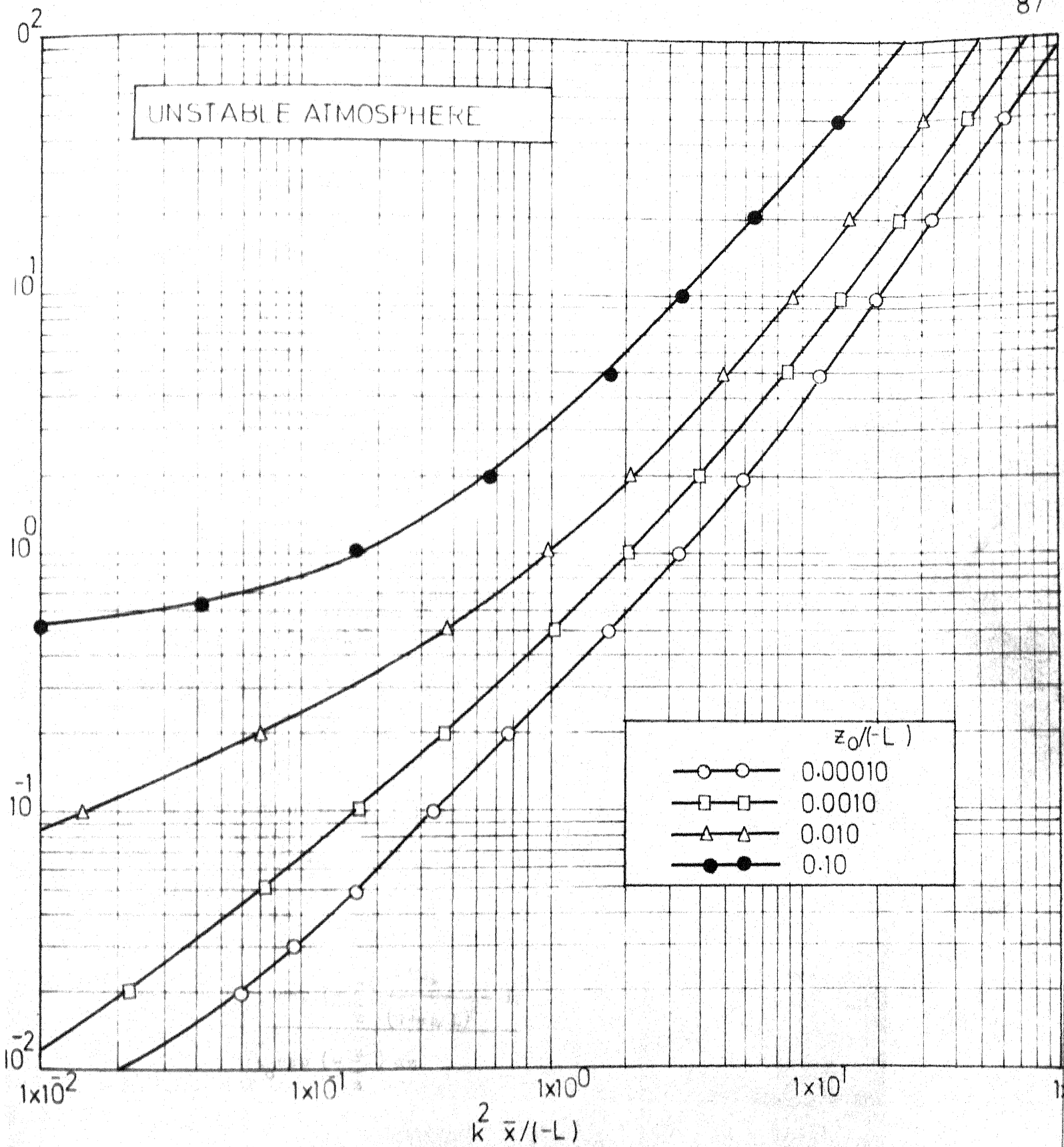


FIG. 3.6 PLOT OF  $\bar{z}/(-L)$  VS  $k^2 \bar{x}/(-L)$  FOR DIFFERENT VALUES OF  $z_0/(-L)$  AS GIVEN BY EQS. (3.42)-(3.43) AND (3.47) FOR UNSTABLE ATMOSPHERIC CONDITIONS

$$\begin{aligned}\frac{d\bar{u}}{dz} &= \frac{u_*}{k} \left[ \frac{1}{z} + \frac{\alpha}{L} \right] \\ &= \frac{u_*}{kz} \left[ 1 + \alpha \frac{z}{L} \right]\end{aligned}\quad (3.49)$$

The eddy viscosity  $K_M$  is given by

$$\begin{aligned}K_M &= \frac{u_*^2}{\frac{d\bar{u}}{dz}} \\ &= \frac{u_*^2}{\frac{u_*}{kz} (1 + \alpha z/L)} \\ K_M &= \frac{ku_* z}{(1 + \alpha z/L)}\end{aligned}\quad (3.50)$$

and 
$$\frac{dK_M}{dz} = \frac{ku_* (1 + \alpha z/L) - ku_* z (\alpha/L)}{(1 + \alpha z/L)^2}$$

$$\frac{dK_M}{dz} = \frac{ku_*}{(1 + \alpha z/L)^2} \quad (3.51)$$

Using this equation in Eq. (3.19)

$$\begin{aligned}\frac{d\bar{z}}{dt} &= \frac{\int_0^{\infty} c \frac{dK_M}{dz} dz}{\int_0^{\infty} c dz} \\ &= \frac{\int_0^{\infty} c_0 \exp\left(-\frac{z}{L}\right) \frac{ku_*}{(1 + \alpha z/L)^2} dz}{\int_0^{\infty} c_0 \exp\left(-\frac{z}{L}\right) dz}\end{aligned}$$

$$\begin{aligned}
&= ku_* \frac{\int_0^{\infty} \exp\left(-\frac{z}{\bar{z}}\right) \frac{1}{z (1+\alpha z/L)^2} dz}{\int_0^{\infty} \exp\left(-\frac{z}{\bar{z}}\right) dz} \\
&= ku_* \frac{\int_0^{\infty} \exp\left(-\frac{z}{\bar{z}}\right) \frac{1}{z (1+\alpha z/L)^2} dz}{\left[-\bar{z} \exp\left(-\frac{z}{\bar{z}}\right)\right]_0^{\infty}} \\
&= ku_* \bar{z} \int_0^{\infty} \exp\left(-\frac{z}{\bar{z}}\right) \frac{1}{z (1+\alpha z/L)^2} dz \quad (3.52)
\end{aligned}$$

Substituting  $\frac{\alpha z}{L} = T$ ,  $dz = \frac{L}{\alpha} dT$  in Eq. (3.52)

$$\frac{d\bar{z}}{dt} = \frac{ku_*}{\bar{z}} \int_0^{\infty} \exp\left(-\frac{LT}{\alpha \bar{z}}\right) \frac{1}{(1+T)^2} \times \frac{L}{\alpha} dT$$

Letting  $\frac{L}{\alpha \bar{z}} = p$ ,

$$\frac{d\bar{z}}{dt} = ku_* p \int_0^{\infty} \exp(-pT) \frac{1}{(1+T)^2} dT$$

Using Laplace Transforms (Erdelyi et. al., 1954)

$$\frac{d\bar{z}}{dt} = ku_* p [1 - p \exp(p) (-E_1(-p))]$$

where  $[(-E_1(-p))] = \int_p^{\infty} \exp(-T) T^{-1} dT$ , which is the exponential integral. The values of this integral have been tabulated by Lagurova (1961).

$$\frac{d\bar{z}}{dt} = \frac{ku_* L}{\alpha \bar{z}} \left[1 - \frac{L}{\alpha \bar{z}} \exp\left(\frac{L}{\alpha \bar{z}}\right) (-E_1(-\frac{L}{\alpha \bar{z}}))\right] \quad (3.53)$$

Eq. (3.53) gives the mean vertical velocity of the ensemble of particles in the stable atmospheric conditions. To get the mean horizontal velocity, Eq. (3.24) gives

$$\begin{aligned}\frac{d\bar{x}}{dt} &= \frac{\int_0^{\infty} c \bar{u} dz}{\int_0^{\infty} c dz} \\ &= \frac{\int_0^{\infty} [c_0 \exp(-\frac{z}{L}) \frac{u_*}{k} (\ln \frac{z}{z_0} + \frac{\alpha z}{L})] dz}{\int_0^{\infty} c_0 \exp(-\frac{z}{L}) dz} \\ &= \frac{u_*}{k} \frac{[\int_0^{\infty} \exp(-\frac{z}{L}) \ln \frac{z}{z_0} dz + \int_0^{\infty} \exp(-\frac{z}{L}) \frac{\alpha z}{L} dz]}{\int_0^{\infty} \exp(-\frac{z}{L}) dz}\end{aligned}$$

$$\begin{aligned}\therefore \frac{d\bar{x}}{dt} &= \frac{u_*}{kz} \left[ \int_0^{\infty} \exp(-\frac{z}{L}) \ln z dz - \ln z_0 \int_0^{\infty} \exp(-\frac{z}{L}) dz \right. \\ &\quad \left. + \frac{\alpha}{L} \int_0^{\infty} z \exp(-\frac{z}{L}) dz \right] \quad (3.54)\end{aligned}$$

Using Laplace Transforms (Erdelyi et. al., 1954)

$$\int_0^{\infty} \exp(-\frac{z}{L}) \ln z dz = -L \ln (\gamma/L) \quad (3.55)$$

where  $\gamma$  is Euler-Mascheroni constant, numerically equal to 1.781

$$\int_0^{\infty} z \exp(-\frac{z}{L}) dz = L^2 \quad (3.56)$$

Substituting Eqs. (3.55) and (3.56) in Eq. (3.54),

$$\begin{aligned}
 \frac{d\bar{x}}{dt} &= \frac{u_*}{k\bar{z}} \left[ -\bar{z} \ln(v/\bar{z}) - \ln z_0 \times \bar{z} + \frac{\alpha}{L} \bar{z}^2 \right] \\
 &= \frac{u_*}{k} \left[ -\ln v + \ln \bar{z} - \ln z_0 + \frac{\alpha}{L} \bar{z} \right] \\
 &= \frac{u_*}{k} \left[ \ln(0.56) + \ln \bar{z} - \ln z_0 + \frac{\alpha}{L} \bar{z} \right] \\
 \frac{d\bar{x}}{d\bar{z}} &= \frac{u_*}{k} \left[ \ln\left(\frac{0.56 \bar{z}}{z_0}\right) + \alpha \frac{\bar{z}}{L} \right] \quad (3.57)
 \end{aligned}$$

From Eqs. (3.53) and 3.57), the relation between  $\bar{x}$  and  $\bar{z}$  is derived as

$$\begin{aligned}
 \frac{d\bar{x}}{d\bar{z}} &= \frac{d\bar{x}/dt}{d\bar{z}/dt} \\
 &= \frac{1}{k^2} \frac{\left[ 2.3 \log\left(\frac{0.56 \bar{z}}{z_0}\right) + \alpha \frac{\bar{z}}{L} \right]}{\frac{L}{\alpha \bar{z}} \left[ 1 - \frac{L}{\alpha \bar{z}} \exp\left(\frac{L}{\alpha \bar{z}}\right) (-E_1(-\frac{L}{\alpha \bar{z}})) \right]} \\
 \frac{k^2 \bar{x}}{L} &= \int_{z_0/L}^{\bar{z}/L} \frac{\left[ 2.3 \log\left(\frac{0.56 \bar{z}}{z_0}\right) + \alpha \frac{\bar{z}}{L} \right]}{\frac{L}{\alpha \bar{z}} \left[ 1 - \frac{L}{\alpha \bar{z}} \exp\left(\frac{L}{\alpha \bar{z}}\right) (-E_1(-\frac{L}{\alpha \bar{z}})) \right]} d\bar{z} \quad (3.58)
 \end{aligned}$$

Again Eq. (3.58) was solved numerically, taking  $\alpha = 6$ , and different values of  $z_0/L$ . The integral was evaluated by Gauss-Legendre Quadrature method (Carnahan et.al., 1969). For



$z_0/L = (i) 0.0001, (ii) 0.001, (iii) 0.01$  and  $(iv) 0.1$ , Eq. (3.58) was evaluated and values were tabulated (Table 3.6) and plotted (Fig. 3.7).

The equation (3.58) or the Table 3.6 and Fig. 3.7 can be used to estimate the vertical spread different conditions of stable atmosphere.

The vertical spread of pollutants can be predicted by these equations (Eqs. (3.32), (3.42) - (3.43) - (3.47) and (3.58)) or Tables 3.4 through 3.6 and Figures 3.5 through 3.7. for neutral, unstable or stable atmospheric conditions. The validity of the prediction by this approach is tested in the following chapter for different aerodynamic roughnesses of surface and different stability conditions of atmosphere.

It should be emphasized that in the above approach (Eqs. (3.32), (3.42) - (3.43) - (3.47) and (3.58)) the vertical spread estimated is the mean of the ensemble of particles.

### 3.5.2. Estimation of Lateral Spread

As stated in Section 2.3.2.2, in the Pasquill-Gifford method of estimating concentration distribution, a set of curves is used in which  $\sigma_y$  and  $\sigma_z$  are given for downwind distance from a source. To estimate  $\sigma_y$ , Pasquill (1961), in his original paper, gave (reported earlier as Eq. (2.42)),

$$\sigma_y = x [\sigma_\theta]_{\tau,s} \quad (3.59)$$

TABLE 3.6

THE VALUES OF  $\bar{z}/L$  AND CORRESPONDING VALUES OF  $k^2 \bar{x}/L$ , FOR DIFFERENT  $z_o/L$ , USING Eq. (3.58), FOR STABLE ATMOSPHERIC CONDITIONS

$z_o/L$	0.0001	0.001	0.01	0.1
$\bar{z}/L$	$k^2 \bar{x}/L$			
0.01	0.006	0.001	-	-
0.02	0.050	0.020	-	-
0.03	0.108	0.051	0.003	-
0.04	0.178	0.090	0.012	-
0.05	0.262	0.138	0.027	-
0.06	0.351	0.192	0.047	-
0.07	0.450	0.254	0.072	-
0.08	0.557	0.322	0.102	-
0.09	0.674	0.398	0.138	-
0.10	0.800	0.481	0.178	-
0.20	2.231	1.371	0.726	0.040
0.30	4.381	2.991	1.716	0.500
0.40	7.571	5.380	3.207	1.202
0.50	11.211	7.562	5.457	2.511
0.60	17.151	12.861	8.606	4.512
0.70	22.561	16.010	12.496	7.141
0.80	31.181	24.213	17.297	10.543
0.90	40.881	32.262	23.635	15.200
1.00	51.382	41.010	30.687	20.505

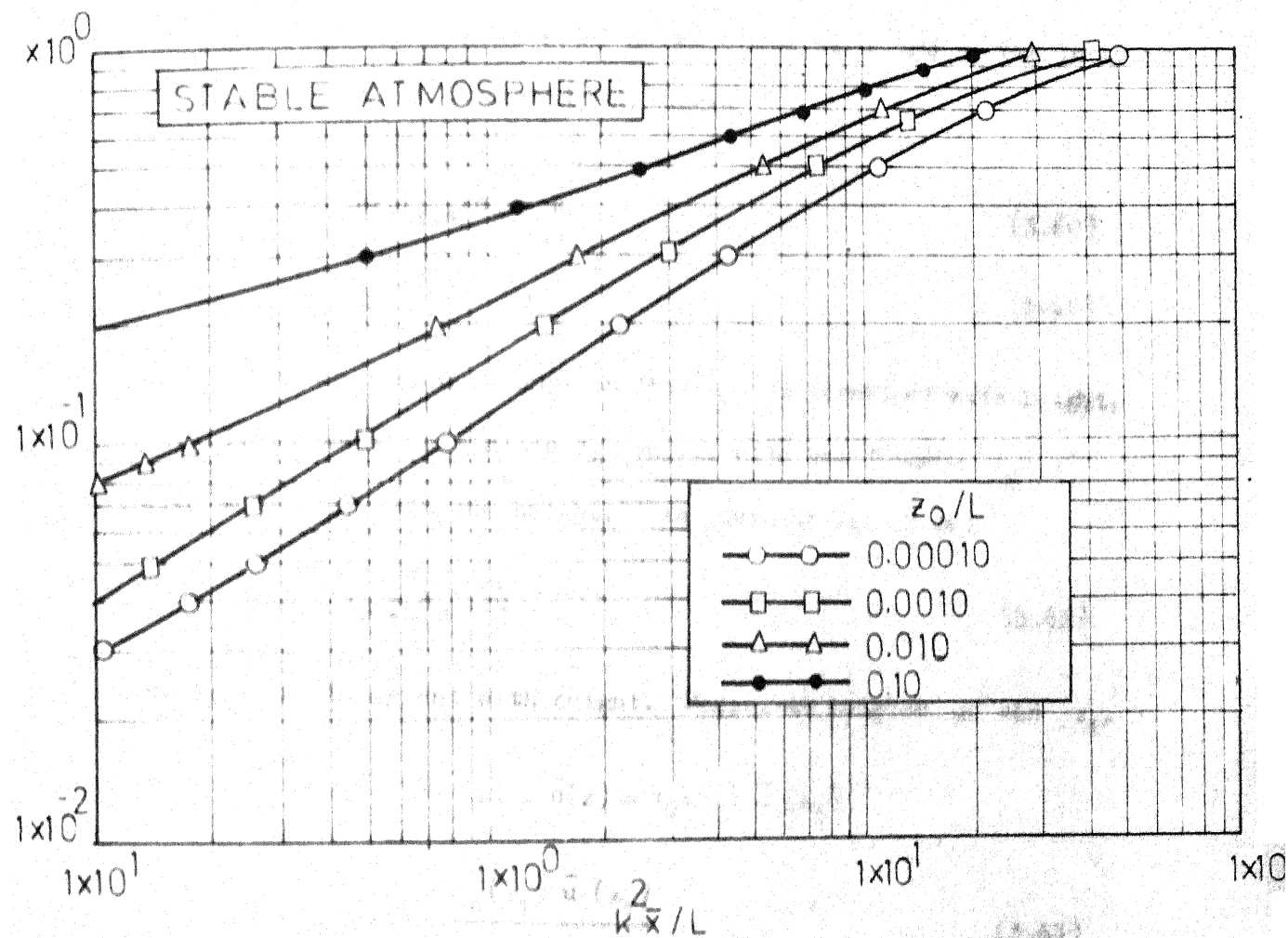


FIG. 3.7 PLOT OF  $z/L$  VS  $k^2 x/L$  FOR DIFFERENT VALUES OF  $z_0/L$  AS GIVEN BY EQ. (3.58), FOR STABLE ATMOSPHERIC CONDITIONS

$$\text{or } \sigma_y(z) = \bar{x} R \frac{\sigma_v}{\bar{u}(z)} \quad (3.64b)$$

In Eq. (3.64a),  $\sigma_\theta(z_1)$  and  $\bar{u}(z_1)$  are usually measured at any height  $z_1$ . If  $\sigma_\theta$  is not available, but temperatures at two heights and wind velocity at one of these heights are available, using Pansfsky and Prasada (1965) s' method, Sec. 2.2.4.2,  $\sigma_v$  can be estimated, which can be used in Eq. (3.64b).

The effects of roughness length  $z_0$  and stability (given by L) are taken care of in determination of  $\sigma_\theta$  (or  $\sigma_v$ ), and hence Eq. (3.64a) or (3.64b) can be used to predict standard deviation of lateral spread of pollutant at any distance  $\bar{x}$  from a source.

### 3.5.3 Estimation of Concentration Distribution

Once  $\sigma_y(x)$  and  $\sigma_z(x)$  (or  $\bar{z}(x)$ ) are determined, the concentration distribution of pollutant can be estimated. Unlike earlier efforts, it should be noted that in the present development of estimation of  $\sigma_y(x)$  and  $\sigma_z(x)$ , the concept of inhomogeneous field of turbulence is not sacrificed.

Also unlike Pasquill-Gifford method of estimating concentration distribution using  $\sigma_y(x)$  and  $\sigma_z(x)$ , where they assume  $\bar{u}$  to be invariant with height, Sec. 2.3.2.3, above formulation allows for variations of  $\bar{u}$  with height. As discussed in that section, concentration distribution follows Gaussian shape in the lateral direction. Assuming simple exponential variation of concentration in the vertical direction, as done in development of  $\sigma_z(x)$ ,

the mean concentration of pollutant at any point  $(x, z)$  in the vertical plane passing through axis can be given by (see Sec. 3.4.1, Eq. (3.4))

$$\bar{c}(x, z) = \bar{c}(x, 0) \exp\left(-1.414 \frac{z}{\sigma_z}\right) \quad (3.65)$$

Similarly, mean concentration at any point  $(x, y)$  in any horizontal plane can be given by Gaussian distribution as

$$\bar{c}(x, y) = \bar{c}(x, 0) \exp\left(-\frac{1}{2} \frac{y^2}{\sigma_y^2}\right) \quad (3.66)$$

Combining Eqs. (3.65) and (3.66), the mean concentration of pollutant at any point  $(x, y, z)$  can be given by

$$\bar{c}(x, y, z) = \bar{c}(x, 0, 0) \exp\left(-\frac{1}{2} \frac{y^2}{\sigma_y^2}\right) \exp\left(-1.414 \frac{z}{\sigma_z}\right)$$

or

$$\bar{c}(x, y, z) = \bar{c}(x, 0, 0) \exp\left[-\frac{1}{2} \frac{y^2}{\sigma_y^2} - 1.414 \frac{z}{\sigma_z}\right] \quad (3.67)$$

For a continuous point source at ground level, the continuity equation gives the  $Q$ , quantity of pollutant released per unit time, by

$$Q = \int_0^\infty \int_{-\infty}^\infty \bar{u} \bar{c}(x, y, z) dy dz \quad (3.68)$$

From Eq. (3.67)

$$\begin{aligned} Q &= \int_0^\infty \int_{-\infty}^\infty \bar{u} \bar{c}(x, 0, 0) \exp\left[-\frac{1}{2} \frac{y^2}{\sigma_y^2} - 1.414 \frac{z}{\sigma_z}\right] dy dz \\ &= \bar{c}(x, 0, 0) \int_0^\infty \bar{u} \exp\left(-1.414 \frac{z}{\sigma_z}\right) \left[\int_{-\infty}^\infty \exp\left(-\frac{1}{2} \frac{y^2}{\sigma_y^2}\right) dy\right] dz \\ &= \bar{c}(x, 0, 0) \int_0^\infty \bar{u} \exp\left(-1.414 \frac{z}{\sigma_z}\right) [\sqrt{2\pi} \sigma_y] dz \end{aligned}$$

$$= \bar{c}(x,0,0) \sqrt{2\pi} \int_0^{\infty} \bar{u} \sigma_y \exp \left( -1.414 \frac{z}{\sigma_z} \right) dz$$

From Eq. (3.64b),  $\sigma_y = xR \sigma_v \sqrt{\bar{u}}$

$$Q = \bar{c}(x,0,0) \sqrt{2\pi} \int_0^{\infty} \bar{u} \left( \frac{xR \sigma_v}{\bar{u}} \right) \exp \left( -1.414 \frac{z}{\sigma_z} \right) dz$$

As  $\sigma_v$  is invariant with height,

$$Q = \bar{c}(x,0,0) \sqrt{2\pi} xR \sigma_v \int_0^{\infty} \exp \left( -1.414 \frac{z}{\sigma_z} \right) dz$$

$$= \bar{c}(x,0,0) \sqrt{2\pi} xR \sigma_v \left[ \frac{\sigma_z}{1.414} \right]$$

$$Q = 0.707 \sqrt{2\pi} \bar{c}(x,0,0) xR \sigma_v \sigma_z$$

$$\text{or } \bar{c}(x,0,0) = \frac{Q}{0.707 \sqrt{2\pi} xR \sigma_v \sigma_z} \quad (3.69)$$

Substituting Eq. (3.69) in Eq. (3.67)

$$\bar{c}(x,y,z) = \frac{Q}{0.707 \sqrt{2\pi} xR \sigma_v \sigma_z} \exp \left[ -\frac{1}{2} \frac{y^2}{\sigma_y^2} - 1.414 \frac{z}{\sigma_z} \right]$$

Knowing that  $0.707 \sigma_z = \frac{\sigma_z}{1.414} = \bar{z}$  (Eq. 3.4), and  $xR \sigma_v = \sigma_y \bar{u}$ ,

$$\bar{c}(x,y,z) = \frac{Q}{\sqrt{2\pi} \bar{u} \sigma_y \bar{z}} \exp \left[ -\frac{1}{2} \frac{y^2}{\sigma_y^2} - \frac{z}{\bar{z}} \right] \quad (3.70)$$

In Eq. (3.70),  $\sigma_y$  and  $\bar{u}$  are to be taken at the same height.

### 3.6. Closure

Thus, consistent with the real atmospheric inhomogeneous turbulence field, the spreads of pollutant and hence its concentration at any point downwind can be estimated from the formulation offered in the preceding paragraphs. For any diffusion study, the surface roughness length  $z_0$  of the site should be determined first. The stability length  $L$  at the time of diffusion experiment should be estimated. Once  $z_0$  and  $L$  are known, the spreads can be decided and then concentrations can be calculated.

This formulation and the extension of Monin's approach have to be verified on the field data. Such a verification on the available field data for two widely different surface roughness lengths is reported in the following chapter.

## Chapter Four

### VERIFICATION OF THE MATHEMATICAL MODEL ON AVAILABLE FIELD DATA

The mathematical model developed in Chapter Three would be meaningful only after it has been validated by testing on field data. The estimation of vertical spreads, and hence concentration distribution at any downwind distance from the theoretical considerations discussed earlier has to be verified with actually observed spreads and concentrations. This verification must be done under different conditions of surface roughness and atmospheric stability. Collection of such comprehensive data would be very expensive and time consuming job. Fortunately there is a significant amount of data collected by various research workers that can be used for validating the model developed. The diffusion programme conducted at the open, unobstructed terrain of O'Neill, Nebraska, U.S.A., was one of the most relevant studies of this type. For urban areas, the dispersion study conducted at St. Louis, Missouri, U.S.A. is similarly a comprehensive study and has been selected for use to verify the proposed mathematical model for areas with large surface roughness.

#### 4.1. Dispersion Study at Project Prairie Grass

During the summer of 1956, in United States, the Geophysics Research Directorate of the Air Force Cambridge Research Center sponsored and directed an experimental programme in micrometeorology. The field site was carefully selected to provide level terrain,



uniform vegetation cover (maintained at an average height of about 6 cm by mowing), and practically complete freedom from large roughness elements. The site selected was flat, prairie country near the town of O'Neill in north central Nebraska, U.S.A. The programme was given the name, Project Prairie Grass (or, in short, PFG).

The primary objective of the programme was to determine the rate of diffusion of a gas, emitted continuously at a point, as a function of meteorological parameters. The experiments were conducted in a wide variety of weather conditions, viz, wind speed, cloud cover, thermal stratification, etc.

#### 4.1.1. Experimental Techniques

The tracer used in Project Prairie Grass was sulphur-dioxide. The diffusion experiments involved determinations of average concentration at selected points downwind from a point source of sulphur-dioxide gas operated continuously for periods of 10 min. The tracer gas was released horizontally at a height of 46 cm above the ground during 64 experiments and at a height of 1.5 m for six experiments.

Midget impingers were used to sample the gas. The impingers were mounted at a height of 1.5 m along 5 concentric semicircular arcs located at travel distances of 50, 100, 200, 400 and 800 m from the source. An angular separation of  $2^\circ$  was used between impingers at the 4 inner arcs and a separation of  $1^\circ$  was used at 800 m.

Wind speed and temperature measurements were made at heights of 25, 50, 100, 200, 400, 800 and 1600 cm. Wind speeds were measured with modified Rikoken anemometers which had been calibrated and matched. The air temperature measurements were made with radiation-shielded copper-constantan thermocouples.

Of the 70 gas releases during July '56 and August '56, there were 34 during lapse or unstable conditions and 36 during inversions or stable conditions.

#### 4.1.2. Surface Roughness of PPG Site

Analysing the vertical wind profiles at the PPG site during near-neutral atmospheric conditions, the roughness length  $z_0$  for the site have been suggested in the range of 0.6 to 1.0 cm. (Haugen et al., 1961; Cermak, 1963; Lumley and Panofsky, 1964), and an average of 0.8 cm is adopted here.

#### 4.1.3. Stability Lengths for PPG Experiments

The stability lengths  $L$  for the PPG diffusion experiments have been suggested by two different workers. Takeuchi (1961) analysed the wind data and reported  $L$  values for all the 70 experimental runs. Haugen et al. (1961, reported by Pasquill, 1966) calculated Richardson number  $Ri$  (Eq. (2.7)) and thence suggested  $L'$  values, where  $L' = L \frac{K_H}{K_M}$ .  $K_H$  is the eddy conductivity and  $K_M$  the eddy viscosity. The ratio of  $K_H/K_M$  varies with stability (Lumley and Panofsky, 1964), and is not uniquely determined. Hence, instead of using  $L'$  and  $K_H/K_M$  to derive  $L$ , the values of  $L$

calculated directly from wind-temperature data by Takeuchi have been adopted and reported in Table 4.1.

#### 4.1.4. Vertical Spreads at 100 m from Source

Analysing the diffusion data, Haugen et al. (1961) have deduced the values of the standard deviations of vertical spreads at 100 m from the source for all the useful runs of the programme. Gaussian distribution of concentration in the vertical was assumed in deriving the standard deviations  $\sigma_z$ . These  $\sigma_z$  values are reported in Table 4.1. Out of the total 70 runs, 48 runs were found to give statistically reliable results (Haugen et al., 1961). Hence  $\sigma_z$  values of those 48 useful runs only have been reported in the Table 4.1.

Out of 48 useful runs 19 were during unstable atmospheric conditions, 11 during near-neutral and 18 during stable atmospheric conditions. Data of  $\sigma_z$  and corresponding L are reported for these three classes of atmospheric stability. As already discussed in Chapter 2 the stability length L is negative in the unstable atmosphere, infinite at neutral atmosphere and positive in the stable atmosphere. In part A of Table 4.1, entries are made for unstable atmospheric conditions in the sequence of decreasing instability. Part B records near-neutral cases, followed by Part C in which entries are in order of increasing stability.

TABLE 4.1

STANDARD DEVIATIONS OF VERTICAL SPREAD AT 100 m AND  
STABILITY LENGTHS L FOR PPG EXPERIMENTS

## (A) UNSTABLE ATMOSPHERIC CONDITIONS

SR No.	Run No.	$\sigma_z$ , m	L, m	$\frac{1}{L}$ , $m^{-1} \times 10^{-2}$	SR No.	Run No.	$\sigma_z$ , m	L, m	$\frac{1}{L}$ , $m^{-1} \times 10^{-2}$
1	16	10.1	-5.9	-16.95	11	49	4.5	-35.0	-2.86
2	15	7.7	-7.8	-12.82	12	50	5.9	-35.0	-2.86
3	52	10.0	-10.0	-10.00	13	61	4.8	-42.0	-2.38
4	25	9.0	-11.0	-9.09	14	62	6.9	-44.0	-2.27
5	43	7.0	-21.0	-4.76	15	30	5.6	-51.0	-1.96
6	19	6.0	-27.0	-3.70	16	20	5.8	-65.0	-1.54
7	51	4.8	-30.0	-3.33	17	31	6.5	-74.0	-1.35
8	27	5.8	-31.0	-3.23	18	33	5.1	-89.0	-1.12
9	44	6.3	-31.0	-3.23	19	48	5.8	-89.0	-1.12
10	26	5.7	-33.0	-3.03					

## (B) NEAR-NEUTRAL ATMOSPHERIC CONDITIONS

20	34	5.3	-100.0	-1.00	26	55	4.4	200.0	0.50
21	45	4.5	-104.0	-0.96	27	42	4.4	160.0	0.63
22	57	4.9	-230.0	-0.44	28	56	4.4	130.0	0.77
23	24	4.6	380.0	0.26	29	46	3.3	116.0	0.86
24	21	4.2	250.0	0.40	30	38	3.8	114.0	0.88
25	22	4.6	240.0	0.42					

TABLE 4.1 (CONTD.)

SR No.	Run No.	$\sigma_z$ , m	L, m	$\frac{1}{L}$ , $m^{-1} \times 10^{-2}$	SR No.	Run No.	$\sigma_z$ , m	L, m	$\frac{1}{L}$ , $m^{-1} \times 10^{-2}$
31	67	3.3	88.0	1.14	41	68	1.9	27.0	3.70
32	17	3.7	88.0	1.14	42	66	2.1	21.0	4.76
33	35-S	4.0	85.0	1.18	43	59	2.0	16.0	6.25
34	37	4.5	83.0	1.20	44	58	1.5	12.0	8.33
35	41	4.0	80.0	1.25	45	36	1.9	12.0	8.33
36	65	3.4	60.0	1.67	46	32	1.6	12.0	8.33
37	54	3.9	58.0	1.72	47	14	1.4	11.0	9.09
38	60	3.9	55.0	1.82	48	40	3.4	5.2	19.23
39	29	3.4	29.0	3.45					
40	18	2.7	29.0	3.45					

#### 4.1.5. Vertical Spread from Proposed Formulation

Knowing  $z_0$  and  $L$  for the runs, the vertical spreads at 100 m from the source were estimated from the proposed mathematical formulation given in Chapter Three.

For the unstable atmospheric conditions, firstly values of  $z_0/(-L)$  were calculated, followed by computation for the value of  $k^2 \bar{x}/(-L)$  where  $k$  is the Von Karman's constant and is equal to 0.4, and  $\bar{x} = 100$  m. From Fig. 3.6,  $\bar{z}/(-L)$  values were read for each pair of  $z_0/(-L)$  and  $k^2 \bar{x}/(-L)$ . These values are given in Table 4.2. Multiplying  $\bar{z}/(-L)$  values with corresponding  $(-L)$  values, the mean vertical spreads  $\bar{z}$  at 100 m were evaluated. To compare these  $\bar{z}$  values with the standard deviations of vertical spread observed,  $\bar{z}$  should be converted to  $\sigma_z$ . As the standard deviations of vertical spread  $\sigma_z$  given in Table 4.1 are based on the Gaussian distribution, the standard relation between  $\bar{z}$  and  $\sigma_z$  of Gaussian distribution can be used as (Kapur and Saxena, 1972)

$$\frac{\bar{z}}{\sigma_z} = 0.80 \quad (4.1)$$

Thus, for each run,  $\sigma_z$  values were computed. These computed values of  $\sigma_z$  should compare with the observed values of  $\sigma_z$  as reported in Table 4.1. The ratio of computed  $\sigma_z$  to observed  $\sigma_z$  for each run has been shown in the last column of Table 4.2.

The case of near-neutral atmospheric conditions was taken as comparable to neutral conditions given in Sec. 3.5.1.1. For

$\bar{x} = 100$  m, and  $z_0 = 0.008$  m,  $\bar{x}/z_0$  was calculated and from Fig. 3.5, corresponding value of  $\bar{z}/z_0$  was read. From  $\bar{z}/z_0$ ,  $\bar{z}$  and then  $\sigma_z$  using Eq. (4.1) were calculated. The ratio of computed  $\sigma_z$  to observed  $\sigma_z$  was calculated for each run. Part B of Table 4.2 reports the results.

The case of stable atmospheric conditions was handled similarly and reported as Part C of Table 4.2. From calculated values  $z_0/L$  and  $k^2 \bar{x}/L$  for each run, corresponding  $\bar{z}/L$  values were established using Fig. 3.7. Multiplying  $\bar{z}/L$  with  $L$  and using Eq. (4.1) the standard deviations  $\sigma_z$  of vertical spread under stable atmospheric conditions were computed. Here again, the last column of Table 4.2 gives the ratio of computed  $\sigma_z$  and observed  $\sigma_z$ .

Besides comparing the agreement between observed data with the approach proposed by the author, the validity of the extended Monin's approach to estimate the vertical spread as given in Chapter Three has also been checked. For this the standard deviations of vertical spread were computed using that approach, and compared with observed values of  $\sigma_z$ . In this case, for unstable atmospheric conditions values of  $z_{\max}/(-L)$  for each pair of  $z_0/(-L)$  and  $b k \bar{x}/(-L)$  were read from Fig. 3.2. The numerical value of  $b$  was taken as 1.2 (as suggested by Pasquill, 1966). Here again,  $k$  is Von Karman's constant and is equal to 0.4. From  $z_{\max}/(-L)$ ,  $z_{\max}$  were evaluated. The  $z_{\max}$  value corresponds to the height at which concentration is 10% of axial (or ground-level, for ground-level sources) concentration. For

Gaussian distribution, the  $z_{\max}$  value relates to  $\sigma_z$  by (Pasquill, 1962a)

$$z_{\max}/\sigma_z = 2.15 \quad (4.2)$$

Thus, for each value of  $z_{\max}$ , corresponding values of  $\sigma_z$  were evaluated and compared with observed values of  $\sigma_z$ . Table 4.3, part A, reports these results.

The near-neutral atmospheric conditions were treated separately in Part B of Table 4.3. For known value of  $\bar{x}/z_o$ ,  $z_{\max}/z_o$  was read off from Fig. 3.4. The ratio  $z_{\max}/z_o$  was used to evaluate  $z_{\max}$  and hence  $\sigma_z$ . Comparison of computed  $\sigma_z$  and observed  $\sigma_z$  is again made in the last column.

Part C, Table 4.3, reports results for stable atmospheric conditions. For this case again,  $z_{\max}/L$  were read off for each pair of  $z_o/L$  and  $b\bar{x}/L$  from Fig. 3.3, and values  $\sigma_z$  were computed and compared with observed values of  $\sigma_z$ .



TABLE 4.2

COMPARISON OF STANDARD DEVIATIONS OF VERTICAL SPREAD AS CALCULATED  
FROM PROPOSED FORMULATION

(A) UNSTABLE ATMOSPHERIC CONDITIONS

SR No.	Run No.	$\frac{z_0}{(-L)}$	$\frac{k^2 \bar{x}}{(-L)}$	$\frac{\bar{z}}{(-L)}$	Computed $\sigma_z$ , m	computed $\sigma_z$ observed $\sigma_z$
1	16	0.00149	2.710	1.35	9.95	0.985
2	15	0.00103	2.050	1.00	9.75	1.266
3	52	0.00080	1.600	0.70	8.75	0.875
4	25	0.00073	1.455	0.62	8.52	0.947
5	43	0.00038	0.763	0.28	7.35	1.050
6	19	0.00030	0.593	0.22	7.43	1.076
7	51	0.00027	0.533	0.19	7.12	1.485
8	27	0.00026	0.516	0.185	7.16	1.238
9	44	0.00026	0.516	0.185	7.16	1.138
10	26	0.00024	0.485	0.17	7.02	1.230
11	49	0.00023	0.457	0.16	7.00	1.558
12	50	0.00023	0.457	0.16	7.00	1.188
13	61	0.00019	0.381	0.121	6.35	1.327
14	62	0.00018	0.364	0.12	6.60	0.955
15	30	0.00016	0.314	0.098	6.25	1.110
16	20	0.00012	0.246	0.076	6.17	1.067
17	31	0.00011	0.216	0.065	6.00	0.924
18	33	0.00009	0.180	0.054	6.00	1.178
19	48	0.00009	0.180	0.054	6.00	1.033

TABLE 4.2 (CONTD.)

## (B) NEAR-NEUTRAL ATMOSPHERIC CONDITIONS

SR No.	Run No.	$\frac{\bar{x}}{z_0}$	$\frac{\bar{z}}{z_0}$	computed $\sigma_z$ m	$\frac{\text{Computed } \sigma_z}{\text{Observed } \sigma_z}$
20	34	12500	440	4.4	0.830
21	45	12500	440	4.4	0.978
22	57	12500	440	4.4	0.898
23	24	12500	440	4.4	0.956
24	21	12500	440	4.4	1.048
25	22	12500	440	4.4	0.956
26	55	12500	440	4.4	1.000
27	42	12500	440	4.4	1.000
28	56	12500	440	4.4	1.000
29	46	12500	440	4.4	1.333
30	38	12500	440	4.4	1.158

TABLE 4.2 (CONTD.)

(C) STABLE ATMOSPHERIC CONDITIONS

SR No.	Run No.	$\frac{z}{L}$	$\frac{k^2 x}{L}$	$\frac{z}{L}$	Computed $\sigma_z, m$	$\frac{\text{Computed } \sigma_z}{\text{Observed } \sigma_z}$
31	67	0.00009	0.182	0.040	4.40	1.333
32	17	0.00009	0.182	0.040	4.40	1.190
33	35-S	0.00009	0.188	0.041	4.36	1.082
34	37	0.00010	0.193	0.042	4.36	0.970
35	41	0.00010	0.200	0.043	4.30	1.067
36	65	0.00013	0.267	0.050	3.75	1.100
37	54	0.00014	0.276	0.052	3.77	0.968
38	60	0.00015	0.291	0.056	3.86	0.990
39	29	0.00028	0.553	0.085	3.08	0.906
40	18	0.00028	0.553	0.085	3.08	1.140
41	68	0.00030	0.593	0.094	3.18	1.760
42	66	0.00038	0.763	0.120	3.14	1.500
43	59	0.00050	1.000	0.140	2.80	1.400
44	58	0.00067	1.333	0.0175	2.62	1.750
45	36	0.00067	1.333	0.175	2.62	1.380
46	32	0.00067	1.333	0.175	2.62	1.640
47	14	0.00073	1.455	0.180	2.48	1.770
48	40	0.00154	3.08	0.320	2.04	0.612

TABLE 4.3

COMPARISON OF STANDARD DEVIATIONS OF VERTICAL SPREAD AS CALCULATED  
FROM EXTENSION OF MONIN'S APPROACH

(A) UNSTABLE ATMOSPHERIC CONDITIONS

SR No.	Run No.	$\frac{z_o}{(-L)}$	$\frac{bkx}{(-L)}$	$\frac{z_{max}}{(-L)}$	Computed $\sigma_z$ , m	$\frac{\text{Computed } \sigma_z}{\text{Observed } \sigma_z}$
1	16	0.00149	8.140	1.900	5.21	0.516
2	15	0.00103	6.150	1.350	4.90	0.635
3	52	0.00080	4.800	1.000	4.65	0.465
4	25	0.00073	4.360	0.920	4.71	0.525
5	43	0.00038	2.290	0.440	4.30	0.615
6	19	0.00030	1.780	0.350	4.40	0.638
7	51	0.00027	1.600	0.310	4.32	0.900
8	27	0.00026	1.550	0.300	4.47	0.771
9	44	0.00026	1.550	0.300	4.47	0.710
10	26	0.00024	1.455	0.290	4.45	0.780
11	49	0.00023	1.371	0.260	4.24	0.940
12	50	0.00023	1.371	0.260	4.24	0.719
13	61	0.00019	1.142	0.200	3.91	0.815
14	62	0.00018	1.090	0.195	4.00	0.580
15	30	0.00016	0.941	0.170	4.03	0.720
16	20	0.00012	0.740	0.135	4.08	0.704
17	31	0.00011	0.650	0.120	4.12	0.635
18	33	0.00009	0.540	0.100	4.14	0.810
19	48	0.00009	0.540	0.100	4.14	0.714

TABLE 4.3 (CONTD.)

(B) NEAR-NEUTRAL ATMOSPHERIC CONDITIONS

SR No.	Run No.	$\frac{\bar{x}}{z_0}$	$\frac{z_{max}}{z_0}$	Computed $\sigma_z, m$	$\frac{\text{Computed } \sigma_z}{\text{Observed } \sigma_z}$
20	34	12500	1000	3.82	0.72
21	45	12500	1000	3.82	0.85
22	57	12500	1000	3.82	0.78
23	24	12500	1000	3.82	0.83
24	21	12500	1000	3.82	0.91
25	22	12500	1000	3.82	0.83
26	55	12500	1000	3.82	0.87
27	42	12500	1000	3.82	0.87
28	56	12500	1000	3.82	0.87
29	46	12500	1000	3.82	1.158
30	38	12500	1000	3.82	1.007

TABLE 4.3 (CONTD.)

(C) STABLE ATMOSPHERIC CONDITIONS

SR No.	Run No.	$\frac{z_o}{L}$	$\frac{bk\bar{x}}{L}$	$\frac{\bar{z}_{max}}{L}$	Computed $\sigma_z, m$	$\frac{\text{Computed } \sigma_z}{\text{Observed } \sigma_z}$
31	67	0.00009	0.545	0.090	3.68	1.117
32	17	0.00009	0.545	0.090	3.68	0.995
33	35-S	0.00009	0.565	0.091	3.60	0.900
34	37	0.00010	0.580	0.092	3.55	0.790
35	41	0.00010	0.600	0.095	3.53	0.883
36	65	0.00013	0.800	0.123	3.43	1.010
37	54	0.00014	0.827	0.131	3.54	0.905
38	60	0.00015	0.875	0.140	3.58	0.919
39	29	0.00028	1.653	0.230	3.10	0.912
40	18	0.00028	1.653	0.230	3.10	1.15
41	68	0.00030	1.780	0.250	3.14	1.655
42	66	0.00038	2.280	0.310	3.03	1.442
43	59	0.00050	3.000	0.380	2.83	1.415
44	58	0.00067	4.000	0.520	2.90	1.932
45	36	0.00067	4.000	0.520	2.90	1.526
46	32	0.00067	4.000	0.520	2.90	1.812
47	14	0.00073	4.360	0.560	2.86	2.040
48	40	0.00154	9.240	1.02	2.46	0.725

Besides comparing the computed and observed values of  $\sigma_z$  in the individual cases, the observed values of  $\sigma_z$  can be compared graphically with  $\sigma_z$  values computed by the formulation given earlier. Fig. 4.1 shows  $\sigma_z$  values versus  $1/L$  values. The vertical spread depends on the stability conditions of the atmosphere, measured in terms of stability length  $L$ . The numerical value of stability length  $L$  approaches very large value as the atmospheric conditions approach neutral stability, and becomes infinite at the neutral conditions of atmospheric stability. Hence instead of plotting  $L$  graphically, the inverse values, i.e.  $1/L$  values, are used in Fig. 4.1. The observed values of  $\sigma_z$  are shown by simple dots in that figure. For the sake of comparison, the  $\sigma_z$  values are calculated from the proposed formulation for different values of stability length  $L$ .

Table 4.4 shows the values of standard deviation of vertical spread at 100 m from the source as calculated from the proposed formulation. Calculations were done for three different cases of Table 4.2. For six different values of stability length  $L$ , in the case of unstable atmospheric conditions,  $\sigma_z$  values were calculated from Fig. 3.6. Calculations were carried out exactly in the same way as were done for Table 4.2. Similar calculations were carried out for neutral atmosphere (using Fig. 3.5) and six cases of stable atmosphere (using Fig. 3.7). The computed  $\sigma_z$  values are shown by encircled points in Fig. 4.1.

Similarly, values of standard deviation  $\sigma_z$  of vertical spread at 100 m from the source were also computed using extension of Monin's approach shown in the previous chapter. Table 4.5 shows the  $\sigma_z$  values for six cases of unstable atmosphere (calculated using Fig. 3.2), a case of neutral stability (calculated using Fig. 3.4) and six cases of stable atmospheric conditions (derived from Fig. 3.3). The computed  $\sigma_z$  values are inserted in Fig. 4.1 as triangular points.

TABLE 4.4

STANDARD DEVIATIONS OF VERTICAL SPREAD AT 100 m, AS CALCULATED BY PROPOSED FORMULATION

(A) UNSTABLE ATMOSPHERIC CONDITIONS

$L,$ m	$\frac{z_0}{(-L)}$	$\frac{k^2 x}{(-L)}$	$\frac{\bar{z}}{(-L)}$	$\sigma_z,$ m	$\frac{1}{L},$ $m^{-1} \times 10^{-2}$
-10.0	0.00080	1.6	0.700	8.75	-10.00
-13.3	0.00060	1.2	0.480	8.00	-7.50
-20.0	0.00040	0.8	0.290	7.25	-5.00
-26.7	0.00030	0.6	0.210	7.00	-3.75
-50.0	0.00016	0.32	0.095	5.95	-2.00
-100.0	0.00008	0.16	0.040	5.00	-1.00

(B) NEUTRAL ATMOSPHERIC CONDITIONS

$z_0,$ m	$\frac{\bar{x}}{z_0}$	$\frac{\bar{z}}{z_0}$	$\sigma_z,$ m	$\frac{1}{L},$ $m^{-1} \times 10^{-2}$
0.008	12500	440	4.4	0.00



TABLE 4.4 (CONTD.)

## (C) STABLE ATMOSPHERIC CONDITIONS

$L$ , m	$\frac{z_0}{L}$	$\frac{k^2 \bar{x}}{L}$	$\frac{\bar{z}}{L}$	$\sigma_z$ , m	$\frac{1}{L}$ , $m^{-1} \times 10^{-2}$
10.0	0.00080	1.6	0.195	2.44	10.00
13.3	0.00060	1.2	0.160	2.67	7.50
20.0	0.00040	0.8	0.115	2.88	5.00
26.7	0.00030	0.6	0.094	3.13	3.75
50.0	0.00016	0.32	0.058	3.59	2.00
100.0	0.00008	0.16	0.034	4.25	1.00

TABLE 4.5

STANDARD DEVIATIONS OF VERTICAL SPREADS AT 100 m, AS  
CALCULATED FROM EXTENDED MONIN'S APPROACH

## (A) UNSTABLE ATMOSPHERIC CONDITIONS

$L$ , m	$\frac{z_0}{(-L)}$	$\frac{bk\bar{x}}{(-L)}$	$\frac{z_{max}}{(-L)}$	$\sigma_z$ , m	$\frac{1}{L}$ , $m^{-1} \times 10^{-2}$
-10.0	0.00080	4.80	1.00	4.65	-10.00
-13.3	0.00060	3.60	0.70	4.35	-7.50
-20.0	0.00040	2.40	0.45	4.19	-5.00
-26.7	0.00030	1.80	0.33	4.10	-3.75
-50.0	0.00016	0.96	0.17	3.95	-2.00
-100.0	0.00008	0.48	0.08	3.82	-1.00

TABLE 4.5 (CONTD.)

## (B) NEUTRAL ATMOSPHERIC CONDITIONS

$\frac{z_o}{m}$	$\frac{\bar{x}}{z_o}$	$\frac{z_{max}}{z_o}$	$\sigma_z$ , m	$\frac{1}{L}$ , $m^{-1} \times 10^{-2}$
0.008	12500	1000	3.72	0.00

## (C) STABLE ATMOSPHERIC CONDITIONS

$\frac{L}{m}$	$\frac{z_o}{L}$	$\frac{bk\bar{x}}{L}$	$\frac{z_{max}}{L}$	$\sigma_z$ , m	$\frac{1}{L}$ , $m^{-1} \times 10^{-2}$
10.0	0.00080	4.80	0.62	2.88	10.00
13.3	0.00060	3.60	0.47	2.92	7.50
20.0	0.00040	2.40	0.32	2.98	5.00
26.7	0.00030	1.80	0.25	3.10	3.75
50.0	0.00016	0.96	0.14	3.26	2.00
100.0	0.00008	0.48	0.072	3.35	1.00

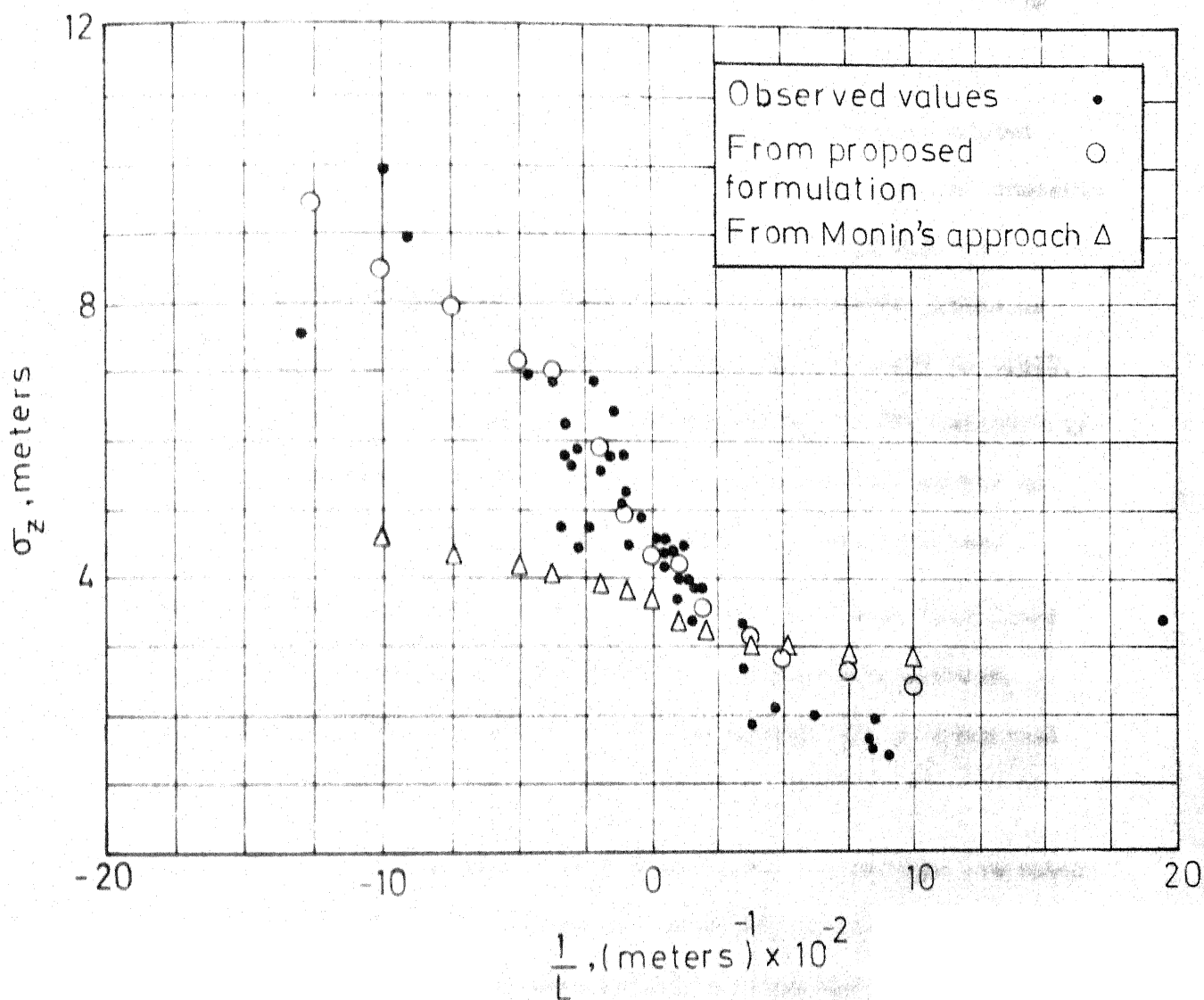


FIG. 4.1 COMPARISON OF VERTICAL SPREAD AT 100 m FROM A SOURCE,  $z_0 = 0.008 \text{ m}$

#### 4.1.6. Agreement of Observed and Computed Values of Vertical Spread

From Tables 4.2 and 4.3, and Figure 4.1, the following observations can be made :

- (i) The agreement in the values of vertical spread computed by the Extended Monin's Approach with those observed in the unstable atmospheric conditions is rather poor. The Extended Monin's Approach predicts much lower values of vertical spread, ratio of computed  $\sigma_z$  to observed  $\sigma_z$  falling in the range of 0.465 to 0.940, and the disagreement increases with the increase in the instability of the atmosphere. Thus, lower estimation of vertical spread by this method may lead to higher estimation of concentrations.
- (ii) In the neutral atmosphere, the vertical spread calculated from Monin's Approach is less than the observed one, however, the estimate is less by about 10-15% for most of the near-neutral cases.
- (iii) During stable atmospheric conditions, the spreads estimated from the Extended Monin's Approach agree well with the observed ones and also with the spreads calculated from the formulation proposed by the author for  $\bar{z}/L \leq 0.1$ . Again, beyond  $\bar{z}/L = 0.1$ , the agreement is poor and could be regarded as stemming out mainly from the inadequacy of formulation of wind profile for very stable atmosphere as further discussed in point (vi) below.
- (iv) The formulation proposed by the author for the unstable atmospheric conditions offers the estimation of vertical spread

very close to the observed values. From Table 4.2, it can be noted that the variation in the ratio of computed vertical spread to observed vertical spread is in the range of 0.875 to 1.558. Although there is some variation of the observed values, keeping in mind the statistical nature of the observed values of vertical spread, the agreement should be considered rather close. From Fig. 4.1, it can be very clearly seen that the values of vertical spread, computed from the proposed formulation for the different degrees of instability of the atmosphere, match very closely to the observed vertical spreads of pollutant. This agreement is observed for the entire range of instability considered, i.e., from near-neutral atmospheric conditions to highly unstable atmosphere with stability length as low as  $(- )5.9$ .

(v) At neutral atmospheric conditions, the vertical spread calculated from the proposed formulation agrees excellently well with the observed vertical spread.

(vi) It is observed that, during stable atmospheric conditions, the vertical spreads calculated from the proposed formulation agrees very closely with the observed spreads till the ratio of  $\bar{z}/L < 0.1$ . Beyond this, the agreement is rather poor. It should be noted here that the formulation for estimation of vertical spread is based on a wind velocity profile given by Eq. (2.14) (re-written as (3.48)), which does not hold good beyond  $z/L \approx 0.3$ , and no other appropriate formulation is available (Lumley and Panofsky, 1964). The mean value of vertical spread  $\bar{z}$  (in the ratio

of  $\bar{z}/L$ ) is the mean of particles found in the vertical section at a particular downwind distance  $\bar{x}$ . For the concentration distribution used in the derivation of the vertical spread, i.e., (Eq. 3.22),

$$\begin{aligned} c &= c_0 \exp\left(-\frac{z}{\bar{z}}\right) \\ &= c_0 \exp\left(-\frac{z/L}{\bar{z}/L}\right), \end{aligned}$$

$$z/L = 0.3, \bar{z}/L = 0.1, c/c_0 = \exp(-3) = 0.05,$$

which means that concentration at  $z/L = 0.3$  is 0.05 time axial concentration. Hence some particles are beyond the height  $z = 0.3L$ , which do not obey Eq. (2.14) and derivations therefrom. As  $\bar{z}/L$  increases more and more particles fall under this undefined region. This is probably the reason for the discrepancy in the observed and computed values. Obviously such discrepancy is only because of a proper velocity profile not having been available and not due to any flaw in the approach proposed.

## 4.2 Dispersion Study at St. Louis

This dispersion study was carried out at St. Louis, Missouri, U.S.A. from May 1963 to March 1965 with a primary objective to describe dispersion over an urban area and to relate the dispersion to meteorological parameters.

St. Louis was selected as the experimental area because it is located in a reasonably flat terrain, removed from significant topographic features that would influence the large-scale air flow.

McElroy and Pooler (1968a, 1968b) reported the data and primary analyses performed on the data collected during the dispersion study over metropolitan St. Louis.

### 4.2.1. Experimental Techniques

The fluorescent particle system utilizing zinc-cadmium sulfide was used as the tracer system. The tracer was dispersed from an aerosol disseminator, and the dissemination of the tracer from either of the two pre-selected sites near ground level was usually 1 hour long.

For each experiment, measurements of total dosage at the surface were obtained on three nearly circular arcs at distances between  $\frac{1}{2}$  and 10 miles from the dissemination site. On each arc, sampling sites were at nominal 6-degree intervals.

A meteorological network was composed of three stations on the periphery of the urban area and an instrumented television

tower (named KMOX) in the downtown area. They provided continuous records of wind, temperature and relative humidity. The TV tower was instrumented at three levels to provide information on the vertical gradients of wind and temperature. Aerovane wind transmitters recorded wind speeds and directions, while aspirated 'thermohms' operating on the resistance principle with copper-wire sensing elements transmitted temperature data electrically to a multi-point recorder. Valid turbulence data were not available during any of the tracer experiments.

Over the period of 2 years, 26 daytime and 16 evening experiments were conducted in varying meteorological conditions.

#### 4.2.2. Vertical Spreads

From the concentration data collected for the dispersion experiments, McElroy and Pooler (1968b) calculated the standard deviations  $\sigma_z$  of vertical spread for each experimental run. They assumed Gaussian distribution of concentration in the vertical to derive  $\sigma_z$  values.

For each experimental run, they analysed the meteorological data and estimated the standard deviation of horizontal wind direction fluctuations,  $\sigma_\theta$ , and the 'bulk' Richardson number,  $Ri_B$ . The  $Ri_B$  was based on temperature and wind measurements at the 127- and 459-foot levels of the TV tower, and was defined as

$$Ri_B = \frac{g}{T} \frac{[\Delta T / \Delta z + \Gamma_d] z^2}{\bar{u}^2} \quad (4.3)$$



where  $g$  is acceleration due to gravity;  $\Delta T$ , temperature difference between top and bottom of the layer;  $\Delta z$ , height difference between top and bottom of the layer;  $\bar{T}$ , mean absolute temperature through the layer;  $\Gamma_d$ , dry adiabatic temperature lapse rate;  $z$ , height of upper anemometer; and  $\bar{u}$ , the mean speed for anemometer at height  $z$ .

These  $\sigma_z$  values at different distances from the source and  $Ri_B$  values are reported in Table 4.7. Out of the total 42 experimental runs during different atmospheric conditions, results of ten experiments were considered doubtful (McElroy and Pooler, 1968b) and hence  $\sigma_z$  values for 32 experiments were reported. From these 32 sets of the results, 4 sets were considered unreliable. McElroy and Pooler grouped these useful 28 runs into four different stability categories, as shown in Table 4.6.

TABLE 4.6

## STABILITY CATEGORIES OF McELROY AND POOLER

$\sigma_\theta$ , degrees	$Ri_B$	Experiment Nos.
24 +	< - 0.01	5,7,11,19,20,25,28
18 - 22	< - 0.01	2,3,4,6,8,9,14,22,23,31,40
15 - 20	$\pm$ 0.01	16,24,35,42,43
8 - 13	> 0.01	12,18,33,37,41

They plotted values of  $\sigma_z$  versus  $\bar{x}$  for these four categories and drew best-fit lines for each category by statistical analysis. Table 4.7 reports  $\sigma_z$  values for each of the useful experiments in four categories of the atmospheric stability. This table is compiled

TABLE 4.7

SUMMARY OF DISPERSION DATA AND METEOROLOGICAL INDICES FOR  
ST. LOUIS DISPERSION STUDY(A) Category I :  $\sigma_\theta$  ,  $24^\circ +$  ;  $Ri_B < -0.01$ 

Experiment No.	$Ri_B$	$\sigma_\theta$ at 127 ft, degrees	$\bar{x}$ , m	$\sigma_z$ , m	Diurnal period
5	-0.25	33	1937	1943	Day
			4267	1672 <sup>a</sup>	
			8065	1485 <sup>a</sup>	
7	0.03 <sup>b</sup>	29	1994	997	Day
			4258	4237	
			7999	2100 <sup>a</sup>	
11	-	25	1998	323	Day
			4197	814	
			7964	1511	
19	-	25	712	149	Day
			3198	999	
			6440	3180	
20	0.00 <sup>b</sup>	26	823	480	Day
			3284	17930	
			7421	3445 <sup>a</sup>	
25	-0.02	31	698	516	Day
			3245	1204 <sup>a</sup>	
			6384	1106 <sup>a</sup>	
28	-0.40	24	2019	2148	Day
			4238	3466	
			15960	1241 <sup>a</sup>	

TABLE 4.7 (CONTD.)

(B) Category II :  $\sigma_\theta$  ,  $18^\circ - 22^\circ$  ;  $Ri_B < -0.01$ 

Experiment No.	$Ri_B$	$\sigma_\theta$ at 127 ft, degrees	$\bar{x}$ , m	$\sigma_z$ , m	Diurnal period
2	-	21	732	152	
			3152	559	Day
			6445	4134	
3	-0.05	17 <sup>b</sup>	761	56	
			3156	220	Day
			6770	890	
4	-0.03	19	882	77	
			3323	529	Day
			7590	1429	
6	-0.13	20	2022	2901	
			4286	1732 <sup>a</sup>	Day
			7938	1154 <sup>a</sup>	
8	-0.07	20	1994	263	
			4171	765	Day
			7988	952 <sup>a</sup>	
9	-0.08	21	715	101	
			3296	625	Day
			6607	1238	
14	-0.04	19	2030	123	
			4157	459	Day
			7932	637	
22	-0.51	17 <sup>b</sup>	945	104	
			3378	1771	Day
			7370	1222 <sup>a</sup>	

TABLE 4.7 (CONTD.)

Experiment No.	$Ri_B$	$\sigma_\theta$ at 127 ft, degrees	$\bar{x}$ , m	$\sigma_z$ , m	Diurnal period
23	-0.10	18	825	99	Day
			3274	984	
			7601	4112	
31	-0.11	19	940	56	Day
			3371	2535	
			13375	1982	
40	-0.05	21	733	147	Day
			3207	872	
			6445	1211	
(c) <u>Category III : <math>\sigma_\theta</math> , 15° - 20° ; <math>Ri_B \pm 0.01</math></u>					
16	0.00	17	710	64	Evening
			3241	277	
			6404	470	
24	0.01	20	949	44	Day
			3384	343	
			7434	2418	
35	-0.01	15	734	250	Day
			3245	662	
			6395	597 <sup>a</sup>	
42	0.00	15	1989	97	Evening
			4205	154	
			7501	204	
43	-0.01	15	757	63	Evening
			3186	304	
			6607	420	

TABLE 4.7 (CONTD.)

(D) Category IV :  $\sigma_\theta$ ,  $8^\circ - 13^\circ$  ;  $Ri_B > 0.01$ 

Experiment No.	$Ri_B$	$\sigma_\theta$ at 127 ft, degrees	$\bar{x}$ , m	$\sigma_z$ , m	Diurnal period
12	-	13	2032	98	Evening
			4294	86	
			8058	224	
18	0.14	8	914	24	Evening
			3377	65	
			7200	173	
33	0.03	13	959	65	Evening
			3398	144	
			7047	109	
37	0.01	13	753	68	Evening
			3162	171	
			6514	345	
41	0.12	12	627	66	Evening
			3223	102	
			7459	98	

<sup>a</sup> Values considered to be significantly affected by a limited mixing layer in the vertical.

<sup>b</sup> Values considered to be doubtful in view of other independent measures of stability during the experiment.

#### 4.2.3. Evaluation of Roughness Length

For the approach proposed in Chapter Three by the author, the establishment of roughness length  $z_0$  is very important. Since no reliable estimation of  $z_0$  was available for the urban St. Louis area, this was determined as described in the following paragraphs from the wind profile data at near-neutral conditions.

Out of total 42 experiments, those experiments were considered near-neutral ones which had bulk Richardson number  $Ri_B$  in the range of  $\pm 0.01$ . Such experiments were Nos. 16, 24, 35, 42 and 43. Wind velocity records at two heights of KMOX - TV tower were analysed for the five selected experiments and  $z_0$  was estimated.

For the neutral or very-near-neutral stability, the mean wind speed can be given as

$$\bar{u} = \frac{u_*}{k} \ln \frac{z-d}{z_0} \quad (4.4)$$

where  $d$  is the zero-plane displacement length, which depends on the average height of buildings in the area, as discussed in Section 2.2.3.2 and  $k$  is Von Karman's constant = 0.4. For St. Louis urban area,  $d$  can be estimated as 30 ft. (Hanna, 1969). Writing Eq. (4.4) for two heights

$$\begin{aligned} \bar{u}_1 &= \frac{u_*}{k} \ln \frac{(z_1-d)}{z_0}, \quad \bar{u}_2 = \frac{u_*}{k} \ln \frac{(z_2-d)}{z_0} \\ \therefore \frac{\bar{u}_1}{\bar{u}_2} &= \frac{\ln \frac{(z_1-d)}{z_0}}{\ln \frac{(z_2-d)}{z_0}} \end{aligned}$$

$$= \frac{\ln(z_1 - d) - \ln z_0}{\ln(z_2 - d) - \ln z_0}$$

$$\therefore \bar{u}_1 \ln(z_2 - d) - \bar{u}_1 \ln z_0 = \bar{u}_2 \ln(z_1 - d) - \bar{u}_2 \ln z_0$$

$$\text{or, } \ln z_0 = \frac{\bar{u}_2 \ln(z_1 - d) - \bar{u}_1 \ln(z_2 - d)}{\bar{u}_2 - \bar{u}_1}$$

$$\text{or, } \log z_0 = \frac{\bar{u}_2 \log(z_1 - d) - \bar{u}_1 \log(z_2 - d)}{\bar{u}_2 - \bar{u}_1} \quad (4.5)$$

Here  $\bar{u}_1$  and  $\bar{u}_2$  can be taken as half-hourly averages at two heights.

The wind speed data at KMOX - TV tower, as reported by McElroy and Pooler (1968a), are 10-min averages. These data were used to obtain half-hourly averages of wind speeds at two heights. These average wind speeds are in miles per hour and are reported in Table 4.8. It was observed from comparison of wind speed data found from KMOX - TV tower with that from pilot balloon measurements that the wind speed data during experiment No. 43 were inconsistent, and hence were not included in the analysis. Out of the four experiments used for this analysis, wind data of anemometers fitted at 127 ft and 255 ft were used for experiment nos. 24, 35 and 42, whereas during experiment no. 16, anemometer at 255 ft was not fitted (McElroy and Pooler, 1968a), and hence wind speed records of 127 ft and 459 ft were used. Using  $d = 30$  ft in all cases, value of roughness length  $z_0$  was calculated for each half-hourly interval. These values of  $z_0$  are reported in Table 4.8.

TABLE 4.8

EVALUATION OF  $z_0$  FROM HALF-HOURLY WIND DATA, USING EQ.(4.5)

Experiment No.	Time	$\bar{u}_1$ at 127 ft, mph	$\bar{u}_2$ at 255 ft, mph	$z_0$ , ft
16	20.20 - 20.50	14.50	21.00 <sup>a</sup>	3.46
	20.50 - 21.20	14.25	21.75 <sup>a</sup>	5.75
	21.20 - 21.50	13.50	21.75 <sup>a</sup>	8.12
	21.50 - 22.20	13.50	21.50 <sup>a</sup>	7.50
	22.20 - 22.50	16.50	24.00 <sup>a</sup>	3.55
	22.50 - 23.20	17.75	24.25 <sup>a</sup>	1.70
	23.20 - 23.50	17.25	24.75 <sup>a</sup>	3.02
24	10.00 - 10.30	16.00	20.75	5.45
	10.30 - 11.00	15.50	20.00	5.40
	11.00 - 11.30	17.00	22.25	6.30
	11.30 - 12.00	17.00	22.75	7.40
	12.00 - 12.30	17.25	22.25	5.25
35	12.00 - 12.30	14.00	16.25	0.49
	12.30 - 13.00	14.00	16.75	1.28
	13.00 - 13.30	15.00	19.00	3.98
	13.30 - 14.00	14.25	17.00	1.28
42	20.00 - 20.30	11.25	15.00	7.84
	20.30 - 21.00	11.75	16.00	9.75
	21.00 - 21.30	14.25	19.25	8.70
	21.30 - 22.00	14.50	19.75	9.35
	22.00 - 22.30	16.50	19.75	1.33
	22.30 - 23.00	14.25	16.50	0.49

a : These were at height of 459 ft.



TABLE 4.9  
MEAN AND STANDARD DEVIATION OF  $z_o$

SR. No.	$z_o$ , ft	$z_o - \text{Mean } z_o$ , ft	$(z_o - \text{Mean } z_o)^2$ , ft <sup>2</sup>
1	3.46	-1.42	2.016
2	5.75	0.87	0.757
3	8.12	3.24	10.500
4	7.50	2.62	6.864
5	3.55	-1.33	1.769
6	1.70	-3.18	10.112
7	3.02	-1.86	3.460
8	5.45	0.57	0.325
9	5.40	0.52	0.270
10	6.30	1.42	2.016
11	7.40	2.52	6.350
12	5.25	0.37	0.137
13	0.49	-4.39	19.272
14	1.28	-3.60	12.960
15	3.98	-0.90	0.810
16	1.28	-3.60	12.960
17	7.84	2.96	8.762
18	9.75	4.87	23.720
19	8.70	3.82	14.592
20	9.35	4.47	20.000
21	1.33	-3.55	12.603
22	0.49	-4.39	19.272

$$\Sigma z_o = 107.39$$

$$\Sigma (z_o - \text{Mean } z_o)^2 = 189.527$$

$$\text{Mean } z_o = \frac{107.39}{22} = 4.88 \text{ ft} \approx 1.488 \text{ m}$$

$$\begin{aligned}
 \therefore 95\% \text{ confidence interval} &= \text{Mean } z_0 \pm 2.08 \sigma_{\bar{x}} \\
 &= 4.88 \pm 2.08 \times 0.64 \\
 &= 4.88 \pm 1.33 \text{ ft} \\
 &= 6.21 \text{ ft or } 3.55 \text{ ft} \\
 \text{i.e.} \quad &1.895 \text{ m or } 1.082 \text{ m}
 \end{aligned}$$

This shows that there is 95% probability of the value of  $z_0$  falling in the range of 1.082 to 1.895 m.

The surface roughness length,  $z_0$ , is sometimes calculated with the assumption that displacement length  $d = 0$ . The Eq. (4.5) becomes

$$\log z_0 = \frac{\bar{u}_2 \log z_1 - \bar{u}_1 \log z_2}{\bar{u}_2 - \bar{u}_1} \quad (4.8)$$

Using  $\bar{u}_1$  and  $\bar{u}_2$  values from Table 4.8,  $z_0$  was calculated for each half-hourly interval. The arithmetic average value of  $z_0$  worked out to be 10.3 ft (= 3.14 m). This shows that the estimation of  $z_0$  from wind data assuming  $d = 0$  leads to over-estimation of  $z_0$  value.

It is interesting to compare the mean value  $z_0$  computed from the wind data during near-neutral atmospheric conditions, and  $z_0$  value given directly by approximation formulæ given by Kutzbach (1961, quoted by Hanna, 1969). According to Kutzbach, as discussed in Section 2.2.3.2, Eqs. (2.6a and 2.6b),

$$\frac{d}{h} = (A)^{-0.3} \quad (4.9)$$

$$\frac{z_o}{h} = (\Lambda)^{-1.1} \quad (4.10)$$

where  $d$  is zero-plane displacement length,  $h$  is the average height of the buildings, and  $\Lambda$  is the ratio of the total area of a given region to the area of the buildings in that region. Value of  $\Lambda$  lies usually in the range of 2 to 10 for urban areas.

McElroy and Pooler (1968a) have shown (their Fig. 15) the land usage in vicinity of KMOX - TV tower. From this, it can be assumed that the average height of the buildings in the area is around 60 ft. With  $d = 30$  ft, from Eq. (4.9), ratio  $\Lambda$  can be worked out, as

$$\begin{aligned} \frac{d}{h} &= \frac{30}{60} = (\Lambda)^{-0.3} \\ \therefore \Lambda &= (2)^{\frac{1}{0.3}} = 10 \end{aligned}$$

Using  $\Lambda = 10$  in Eq. (4.10),

$$\begin{aligned} \frac{z_o}{h} &= \frac{z_o}{60} = (10)^{-1.1} \\ \therefore z_o &= 60 \times \frac{1}{12.6} = 4.75 \text{ ft} = 1.45 \text{ m} \end{aligned}$$

It is observed that roughness length  $z_o$  calculated from Eq. (4.10) is of the same order of the value of  $z_o$  found from wind data. The former value lies within the 95% confidence interval of  $z_o$  derived from wind data, and is very close to mean  $z_o$ .

For the present study of diffusion, average value of roughness length given in Table 4.9, as 1.488 m (= 4.88 ft) can be approximated to 1.50 m and used.

#### 4.2.4. Stability Lengths

For the St. Louis dispersion study, the stability length  $L$  for any of the experiment has not been derived. It was necessary to establish  $L$  for the present study.

As described in Section 4.2.2, McElroy and Pooler (1968b) used  $Ri_B$  and  $\sigma_\theta$  as the stability parameters and derived relationship between  $\sigma_z$  and downwind distance  $\bar{x}$  for four different categories of atmospheric stability. Studying these graphs (Fig. 2 of McElroy and Pooler, 1968b), it can be observed that there is a considerable scatter of data points about best-fit lines. Hence, instead of establishing stability length  $L$  and then evaluating  $\sigma_z$  from theoretical considerations to compare with  $\sigma_z$  derived by McElroy and Pooler for each individual experiment, more meaningful comparison could be done with the best-fit lines of  $\sigma_z$  vs  $\bar{x}$  plot for each of the four categories of atmospheric stability. Thus, stability lengths  $L$  representing each of the four stability categories are established as shown below.

As stated in Section 2.2.4.2, the standard deviation  $\sigma_\theta$  of wind direction fluctuations can be taken as a predictor of turbulence. In the present case, it is used to establish stability length  $L$ . Following Inoue (1959), Eq. (2.24a),

$$\sigma_{\theta} = \frac{\beta u_*}{\bar{u}} \quad (4.11)$$

where  $\beta$  is a constant and  $\sigma_{\theta}$  is in radians. The average values of  $\sigma_{\theta}$  for the four categories of stability were taken as shown in Table 4.10.

TABLE 4.10  
AVERAGE VALUES OF  $\sigma_{\theta}$  FOR FOUR STABILITY CATEGORIES

Category	$Ri_B$	Stability conditions	Average $\sigma_{\theta}$ , degree
I	$< -0.01$	Unstable	27
II	$< -0.01$	Unstable	20
III	$\pm 0.01$	Neutral	18
IV	$> 0.01$	Stable	12

The Eq. (4.11) modifies to

$$\sigma_{\theta} \times \frac{\pi}{180} = \frac{\beta u_*}{\bar{u}} \quad (4.12)$$

for  $\sigma_{\theta}$  in degrees.

For the neutral stability condition, the mean wind speed  $\bar{u}$  in Eq. (4.12) can be substituted from Eq. (4.4), so that

$$\sigma_{\theta} \times \frac{\pi}{180} = \frac{\beta u_*}{\frac{u_*}{k} \ln \left( \frac{z-d}{z_0} \right)}$$

where  $d$  is the zero-plane displacement length ( $= 30$  ft) and  $k$  is Von Karman's constant ( $= 0.4$ ).

$$\therefore \sigma_{\theta} \times \frac{\pi}{180} = \frac{\beta k}{2.3 \log \left( \frac{z-d}{z_0} \right)}$$

$$\therefore \beta = 2.3 \times \frac{\pi}{180} \times \frac{1}{k} \times \sigma_{\theta} \log \left( \frac{z-d}{z_0} \right)$$

$$\text{or } \beta = 0.1 \sigma_{\theta} \log \left( \frac{z-d}{z_0} \right) \quad (4.13)$$

The standard deviation  $\sigma_{\theta}$  of wind direction fluctuation was measured at the height of 127 ft. Substituting numerical values of  $z, d$  and  $z_0$ , for  $\sigma_{\theta} = 18^\circ$

$$\beta = 0.1 \times 18 \times \log \left( \frac{127 - 30}{5.53} \right)$$

$$= 1.8 \log 17.55$$

$$= 2.25$$

It can be recalled that, for any stability condition, mean wind at any height  $z$  is given by Eq. (2.16) as

$$\bar{u} = \frac{u_*}{k} [f(z/L) - f(z_0/L)] \quad (4.14)$$

Substituting Eq. (4.14) in Eq. (4.12)

$$\begin{aligned} \sigma_{\theta} \times \frac{\pi}{180} &= \frac{\beta u_*}{\frac{u_*}{k} [f(z/L) - f(z_0/L)]} \\ &= \frac{\beta k}{f(z/L) - f(z_0/L)} \end{aligned} \quad (4.15)$$

For known values of  $\sigma_{\theta}$  (at height  $z$ ),  $\beta$  and  $z_0$ , stability length  $L$  can be established. For unstable case, knowing that at height 127 ft where  $\sigma_{\theta}$  is measured free convection conditions

would be prevailing ( $z/(-L) > 0.08$  ; Sec. 2.2.3.3),  $\bar{u}$  is given by Eq. (3.39) as

$$\bar{u} = \frac{u_*}{k} [0.48 - 2.3 \log (z_o/(-L)) - 1.3 (z/(-L))^{-1/3}] \quad (4.16)$$

Taking  $z$  in the Eq. (4.16) as above the zero-plane, its effective value =  $(z-d)$

$$\therefore \bar{u} = \frac{u_*}{k} [0.48 - 2.3 \log (z_o/(-L)) - 1.3 ((z-d)/(-L))^{-1/3}] \quad \dots (4.17)$$

$$\text{or, } f\left(\frac{z}{L}\right) - f\left(\frac{z_o}{L}\right) = 0.48 - 2.3 \log (z_o/(-L)) - 1.3 ((z-d)/(-L))^{-1/3} \quad \dots (4.18)$$

Substituting Eq. (4.18) in Eq. (4.15), for unstable atmospheric conditions

$$\sigma_\theta \times \frac{\pi}{180} = \frac{\beta k}{0.48 - 2.3 \log (z_o/(-L)) - 1.3 ((z-d)/(-L))^{-1/3}}$$

Inserting values of  $\beta = 2.25$ ,  $z = 127$  ft,  $d = 30$  ft,  $(z-d) = 97$  ft = 29.6 m,  $z_o = 4.88$  ft  $\approx 1.50$  m, and  $k = 0.4$

$$\begin{aligned} \sigma_\theta \times \frac{\pi}{180} &= \frac{2.25 \times 0.4}{[0.48 - 2.3 \log (1.50) + 2.3 \log (-L) - 1.3 (29.6/(-L))^{-1/3}]} \\ &= \frac{0.9}{0.48 - 0.405 + 2.3 \log (-L) - \frac{1.3(-L)^{1/3}}{(29.6)^{1/3}}} \end{aligned}$$

$$= \frac{0.9}{0.075 + 2.3 \log (-L) - 0.42 (-L)^{1/3}} \quad (4.19)$$

For stability category I,  $\sigma_\theta = 27^\circ$ ,

$$\therefore 27 \times \frac{\pi}{180} = \frac{0.9}{0.075 + 2.3 \log (-L) - 0.42 (-L)^{1/3}}$$

$$\therefore 0.075 + 2.3 \log (-L) - 0.42 (-L)^{1/3} = 1.91$$

$$\text{or, } 2.3 \log (-L) - 0.42 (-L)^{1/3} = 1.835 \quad (4.20)$$

Solving Eq. (4.20) by trial-and-error, the stability length  $L$  works out to be -20 m.

Similarly for stability category II,  $\sigma_\theta = 20^\circ$ ; substituting this in Eq. (4.19), and simplifying

$$2.3 \log (-L) - 0.42 (-L)^{1/3} = 2.495 \quad (4.21)$$

which on trial solutions gave  $L = -65$  m.

For stable atmospheric conditions,  $\bar{u}$  is given by Eq. (2.14)

as

$$\bar{u} = \frac{u_*}{k} \left( \ln \frac{z}{z_0} + \alpha \frac{(z-z_0)}{L} \right) \quad (4.22)$$

where  $\alpha$  is a constant = 6. Putting Eq. (4.22) in Eq. (4.15), for stable atmospheres, with zero-plane adjustment

$$\sigma_\theta \times \frac{\pi}{180} = \frac{\beta k}{2.3 \log \frac{z-d}{z_0} + \alpha \left( \frac{z-d-z_0}{L} \right)} \quad (4.23)$$



As  $\sigma_\theta = 12^\circ$ ,  $\beta = 2.25$ ,  $z = 127$  ft,  $d = 30$ ,  $(z-d) = 97$  ft = 29.6 m,  $\alpha = 6$ ,  $z_0 = 4.88$  ft  $\approx 1.50$  m and  $k = 0.4$ , the stability length  $L$  works out from Eq. (4.23), as 128 m.

Table 4.11 summarizes the stability lengths for the four stability categories.

TABLE 4.11  
STABILITY LENGTHS FOR FOUR STABILITY  
CATEGORIES

Category	$\sigma_\theta$ , degrees	L, m
I	27	-20
II	20	-65
III	18	$\infty$
IV	12	128

#### 4.2.5. Vertical Spreads from Proposed Formulation

Having established the values of  $z_0$  and  $L$ , the vertical spreads for any distance downwind can be derived from the theory described in Chapter Three. These values of vertical spread can be compared with the observed spreads. Figures 4.2 through 4.5 show the comparison between these values. In each category of stability, the  $\sigma_z$  values obtained by McElroy and Pooler (1968b) are shown corresponding to their downwind distances,  $\bar{x}$ . McElroy-Pooler also showed best-fit lines for each category,

which are shown by solid lines.

For known values of  $z_0$  and  $L$ , the standard deviations of vertical spread,  $\sigma_z$ , were calculated from the proposed formulation as well as from the extension of Monin's approach. The procedure of finding out these value was the same as described in Sec. 4.1.5. These values are shown in the graphs.

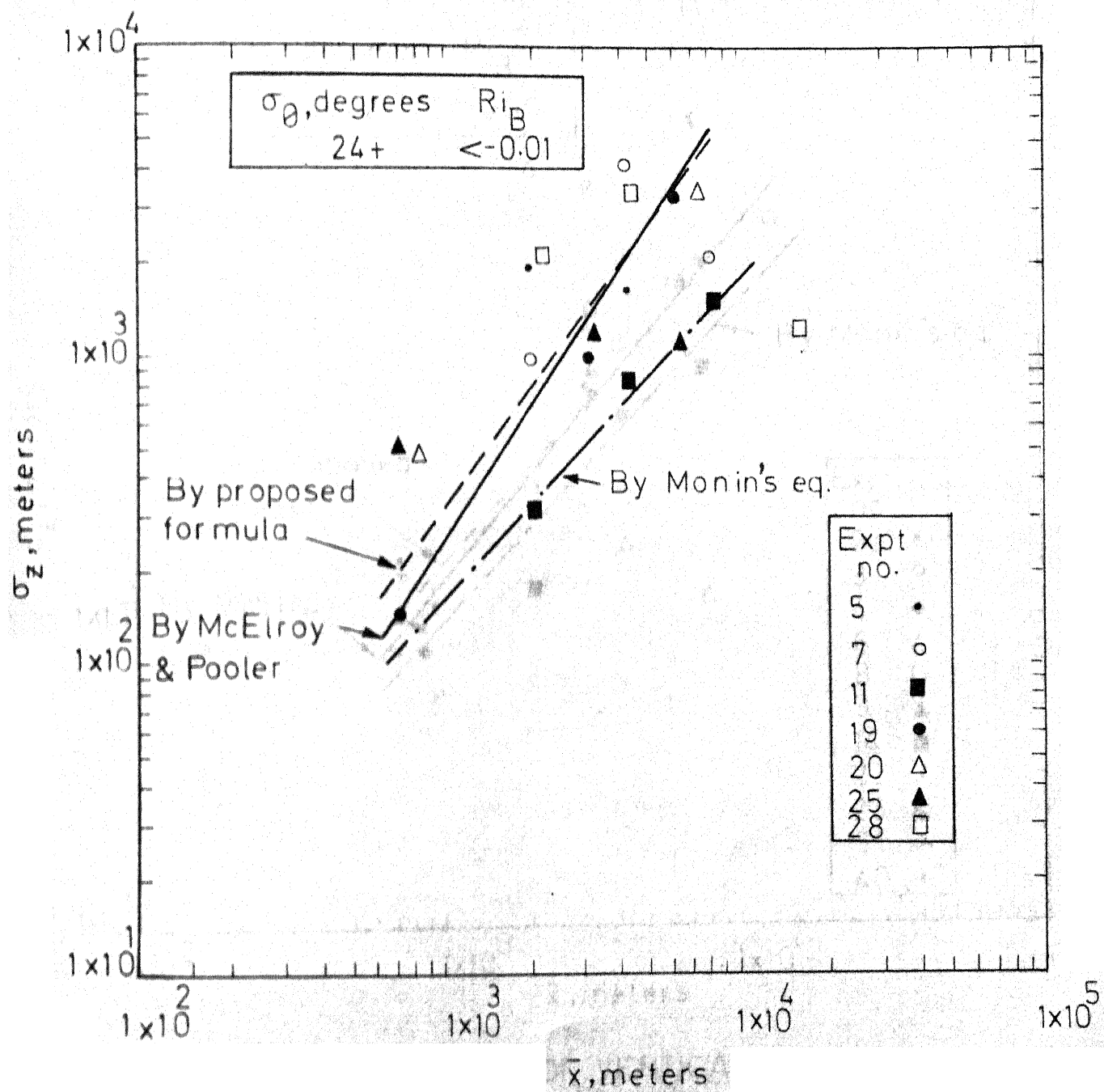


FIG. 4.2 COMPARISON OF VERTICAL SPREAD AT ST. LOUIS

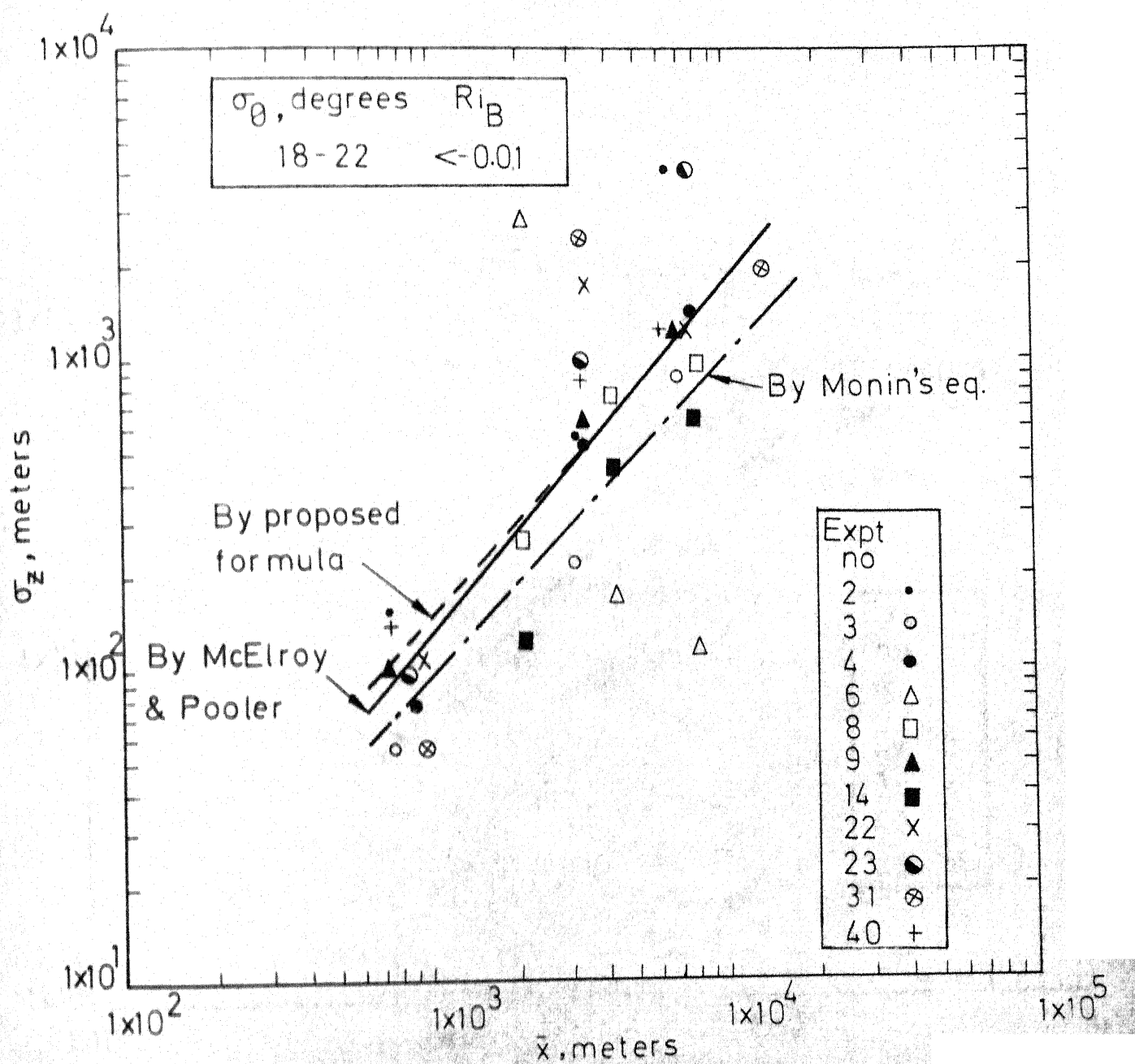


FIG. 4.3 COMPARISON OF VERTICAL SPREAD AT ST. LOUIS

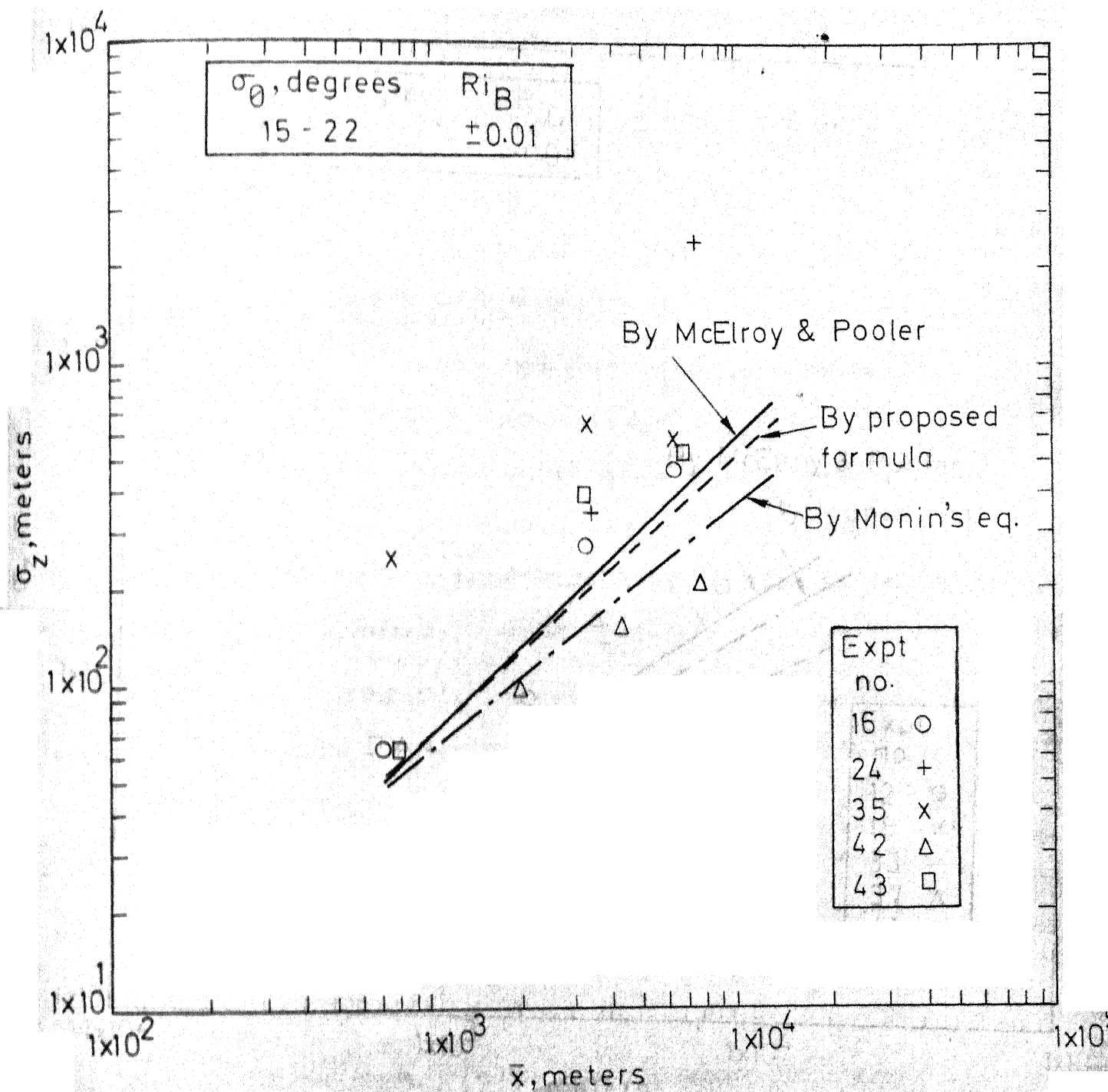


FIG. 4.4 COMPARISON OF VERTICAL SPREAD AT ST. LOUIS

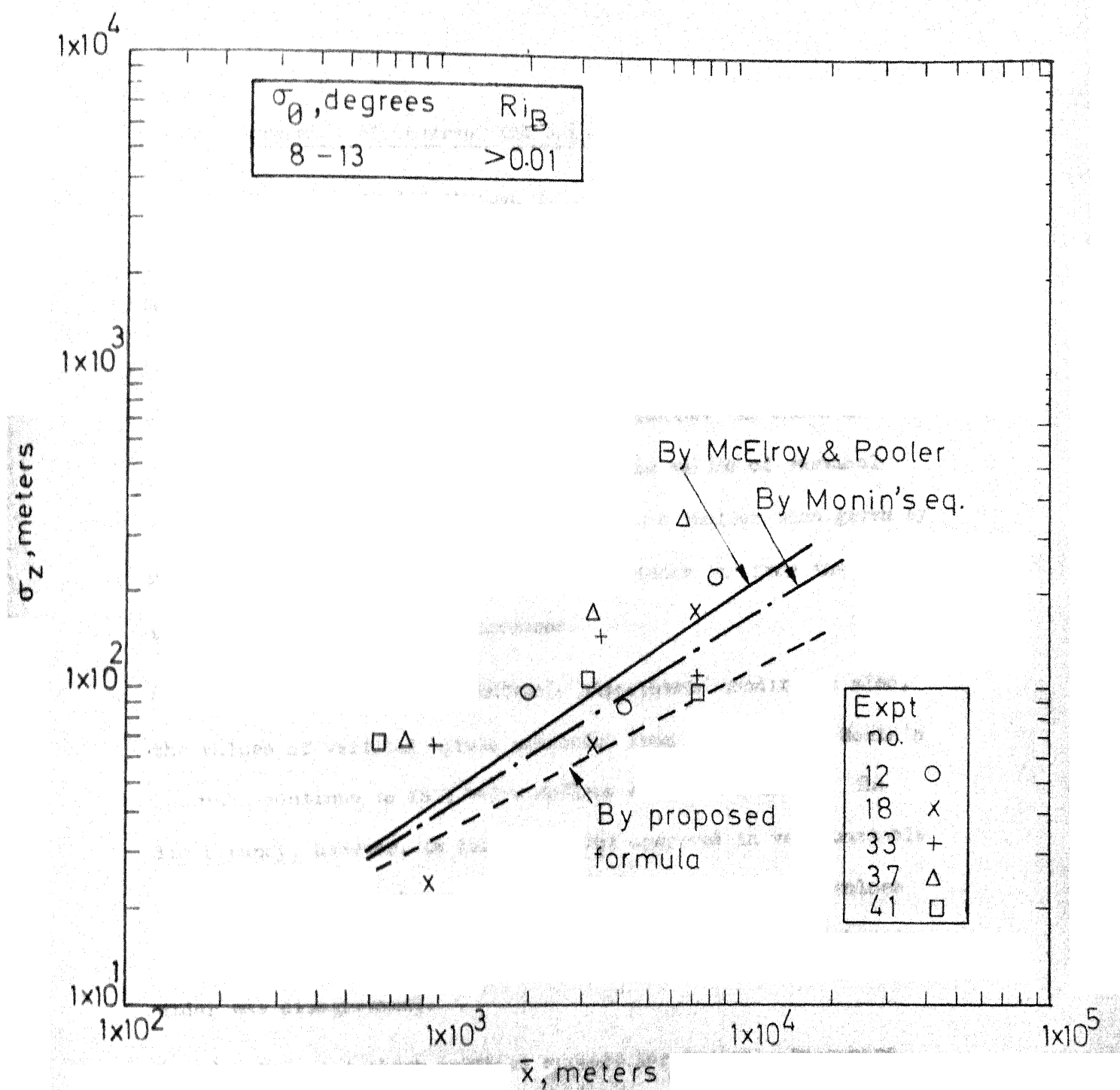


FIG. 4.5 COMPARISON OF VERTICAL SPREAD AT ST. LOUIS

#### 4.2.6 Agreement of Observed and Computed Values of Vertical Spread

From Figures 4.2 through 4.5, the comparison of observed vertical spreads and computed vertical spreads can be made. The following observations should be noted:

(i) The Extended Monin's Approach gives smaller values of vertical spreads for all atmospheric conditions. As shown in Fig. 4.2, for very unstable atmosphere, the values of vertical spread computed by Monin's approach are much smaller than given by McElroy and Pooler. As the downwind distance  $\bar{x}$  from the source increases, the divergence increases.

(ii) For the moderately unstable atmospheric conditions also, the values of vertical spread predicted from the Extended Monin's Approach continue to fall below McElroy-Poolers' values. The discrepancy, however, is less than that observed in very unstable atmosphere. This observation is in confirmation of PPG values where also, Monin's approach showed that higher the instability, wider was disagreement.

(iii) Fig. 4.4 shows vertical spreads for neutral atmosphere. Monin's approach, here again, gives smaller values of vertical spreads, which was also in line with the observation made for PPG values. The discrepancy increases with the downwind distance  $\bar{x}$ .

(iv) Monin's approach applied to stable atmospheric conditions at St. Louis, gives results which are closer to McElroy-Poolers'

values, as shown in Fig. 4.5. However, as discussed earlier, applicability of mathematical formulation for very stable atmospheres is doubtful. Although Monin's values are better in comparison in this case, his values for very stable cases of PPG site were poor in agreement.

(v) For very unstable atmospheric conditions shown in Fig. 4.2, the vertical spreads computed from the proposed formulation agrees closely with the ones given by McElroy and Pooler (1968b). At a distance of around 600m from the source, the discrepancy is maximum, viz., observed spread is 120m whereas computed value is nearly 160m. As the distance downwind increases the agreement between computed and observed spreads improves, and beyond 1500m, the agreement is excellent.

(vi) It is observed from Fig. 4.3 that for moderately unstable atmosphere the formulation proposed by the author gives vertical spreads which are very closely in agreement with McElroy-Poolers' values.

(vii) The proposed formulation gives values of vertical spread for neutral conditions of the atmosphere which are in excellent agreement with McElroy-Poolers' values, as shown in Fig. 4.4.

(viii) For the stable atmospheric conditions, the estimation of vertical spreads by the proposed formulation is rather poor. This is, again, due to the fact that the wind profiles beyond  $z/L=0.3$  has



not been properly expressed mathematically. Looking to the nature of slope of the times drawn in Fig. 4.5, it is observed that for  $\bar{x} < 600\text{m}$ ,  $\sigma_z$  values given by the formulation would be comparable, but as distance  $\bar{x}$  increases, more and more particles of pollutants reach the undefined region beyond  $z/L=0.3$  and the poorer is the agreement.

(ix) For the case of stable atmosphere, the implications of urban heating are not properly investigated as yet, and hence it is not very surprising that the vertical spread predicted by the proposed formulation is not in good agreement of McElroy-Poolers' values.

## Chapter Five

### PROCEDURE FOR PREDICTION OF CONCENTRATIONS OF POLLUTANTS IN AIR UNDER DIFFERENT METEOROLOGICAL CONDITIONS

The mathematical equations (and tables and charts) developed in Chapter Three can be used to predict vertical spreads and hence air pollutant concentrations at various points. As seen in Chapter Four, such predicted spreads and concentrations closely agree with the field observations. It would hence be useful to enumerate the steps involved in the prediction of concentration of air pollutants at any point downwind from a source, following the proposed mathematical models.

#### 5.1 Micrometeorological Data

According to the proposed mathematical model, determination of surface roughness length  $z_0$  and Monin-Obukhov stability length  $L$  is very essential. The procedures for their determination depend upon the type of available micrometeorological data.

Three sets of micrometeorological instrumentation are considered.

(1) Case one: Instrumentation consists of wind speed records at two heights, temperature records at two heights and continuous wind direction records at one height.

(ii) Case Two: Temperature recording instruments are available at two heights, along with continuous wind speed and wind direction records at one height.

(iii) Case Three: The minimum of micrometeorological instrumentation is required in this case, viz., temperature records at two heights,  $z_1$  and  $z_3$  and wind velocity records at one intermediate height  $z_2$ . The height  $z_2$  is so selected that it is a geometric mean of  $z_1$  and  $z_3$ , i.e.  $z_2 = \sqrt{z_1 \cdot z_3}$ . In a practical case  $z_1 = 1\text{m}$ ,  $z_3 = 4\text{m}$  and hence  $z_2 = 2\text{m}$ .

Using data from any one of these three cases, surface roughness length  $z_0$  and stability length  $L$  can be evaluated as described below.

## 5.2 Zero-plane Displacement Length

Check the type of the surface roughness found at the site of diffusion study. If the site is open unobstructed level terrain, the zero-plane displacement length  $d = 0$ . If the area contains moderate to large obstructions, the surface roughness would be large, and the zero-plane displacement should be taken into considerations and can be approximated by Eq. (4.9), i.e.,

$$\frac{d}{h} = (A)^{-0.3} \quad (5.1)$$

where  $h$  is the average height of the obstructions (including

buildings, trees, etc.) found in the area,  $A$  is a constant which depends on the amount of area occupied by the obstructions in that region and for urban areas lies between 2-10. When the area occupied by buildings in the area is large, value of  $A$  would be smaller. Localities like very thickly populated residential or commercial complexes have  $A$  nearing 24, while relatively less-thickly populated areas have higher values of  $A$ .

It is imperative that the heights at which wind and temperature records are obtained should be more than  $d$ . This is very important in micrometeorological observations within the urban area. (Wind velocity profiles and all the formulation derived in the previous chapters apply only above the zero-plane. Below the zero-plane, i.e., at height  $z < d$ , the wind velocity profiles treated earlier and formulation for spread do not apply. Pollutant distribution in the local geometry of streets, lanes and by-lanes cannot be estimated by the procedure described here.)

### 5.3 Determination of Surface Roughness Length.

Surface roughness length  $z_0$  for the site can be determined as shown below.

#### 5.3.1 Instrumentation as Case one.

(1) Select periods during which neutral to very-near-neutral conditions of atmosphere prevailed. This is done as follows.

At neutral or adiabatic conditions of atmosphere, the temperature lapse rate is  $1.0^{\circ}\text{C}/100\text{ m} \approx 5.5^{\circ}\text{F}/1000\text{ ft.}$  (Magill et al, 1956). If the heights at which two temperatures are available are  $z_1$  and  $z_2$  ( $z_2 > z_1$ ), for this interval of height, adiabatic lapse rate of temperature corresponds to

$$1.0 \times \frac{(z_2 - z_1) \text{ (m)}}{100 \text{ (m)}} \quad (5.3a)$$

in degrees Centigrades, or

$$5.5 \times \frac{(z_2 - z_1) \text{ (ft)}}{1000 \text{ (ft)}} \quad (5.3b)$$

in degrees Fahrenheit.

When the fall in actually observed temperature between these two heights is very-nearly this value, neutral to very-near-neutral conditions of atmospheric stability are assumed.

(ii) Obtain the wind velocity records of such periods of neutral to very-near-neutral conditions. Calculate the half-hourly averages of wind velocity for these periods, and denote them as  $\bar{u}_1$  at height  $z_1$  and  $\bar{u}_2$  at height  $z_2$ . Then, the surface roughness length is given by Eq. (4.5), rewritten here as

$$\log z_0 = \frac{\bar{u}_2 \log(z_1 - d) - \bar{u}_1 \log(z_2 - d)}{\bar{u}_2 - \bar{u}_1} \quad (5.2)$$

### 5.3.2 Instrumentation as Case Two and Case Three

In these cases data to compute wind profiles are not available. The surface roughness length  $z_0$  has to be approximately estimated from Eq. (4.10)

$$\frac{z_0}{h} = (A)^{-1.1} \quad (5.4)$$

where  $h$  and  $A$  are appropriately assumed as discussed in Section 5.2.

## 5.4 Determination of Stability Length

At the time of any diffusion study, stability conditions of the atmosphere are to be quantitatively specified. This can be done in terms of Monin-Obukhov stability length  $L$ . The method of determination of  $L$ , again, depends on the type of the micrometeorological instrumentation available.

### 5.4.1 Instrumentation as Case One

(i) For the periods of neutral to very-near-neutral conditions of atmospheric stability (as decided in Sec. 5.3.1), take the wind direction fluctuation records. Calculate the

arithmetic mean direction of the wind, the deviations of individual readings from the mean direction. Square the deviations and sum up. The standard deviation,  $\sigma_\theta$ , is given by

$$\sigma_\theta = \left[ \frac{\sum (\theta - \text{Mean } \theta)^2}{N} \right]^{1/2} \quad (5.5)$$

where  $\theta$  is the individual value of wind direction, and  $N$  number of observations for the period.

(ii) Evaluate the constant  $\beta$  given by Eq. (4.13) under neutral stability conditions, as

$$\beta = 0.1 \times \sigma_\theta \times \log \left( \frac{z-d}{z_0} \right) \quad (5.6)$$

$\sigma_\theta$  being in degrees, and  $z$  being the height at which wind-direction is recorded.

(iii) Similar to step (i), determine  $\sigma_\theta$  (in degrees) for the period at which stability length  $L$  is required.

(iv) If it is a day time experiment, unstable conditions may be expected, and the following equation can be used to determine  $L$  by trial solution

$$\sigma_\theta \times \frac{\pi}{180} = \frac{\beta \times k}{0.48 - 2.3 \log(z_0/(-L)) - 1.3((z-d)/(-L))^{-1/3}} \quad (5.7)$$

$k$  being a universal constant of value 0.4.

For the evening or night time experiment, inversion conditions may be prevailing, the equation can be used as

$$\sigma_{\theta} \times \frac{\pi}{180} = \frac{\beta \times k}{2.3 \log \left( \frac{z-d}{z_0} \right) + \alpha \left( \frac{z-d}{L} \right)} \quad (5.8)$$

where  $\alpha = 6$  and  $k = 0.4$ .

Substitute appropriate values of  $\beta$ ,  $\sigma_{\theta}$ ,  $z$  and  $d$ , and obtain value of stability length  $L$ .

#### 5.4.2 Instrumentation as Case Two

Here also wind-direction fluctuation data are available and steps to be followed to evaluate stability length  $L$  are the same as enumerated in Sec. 5.4.1.

#### 5.4.3 Instrumentation as Case Three.

Here wind direction records being not available, the following procedure is adopted.

- (i) Obtain temperature records,  $t(z_1)$  and  $t(z_3)$ , at heights  $z_1 = 1\text{m}$  and  $z_3 = 4\text{m}$  and wind records,  $\bar{u}(z_2)$ , at height  $z_2 = 2\text{m}$ . Find the average values of each of these. Find absolute mean temperature  $\bar{T}$  between height  $z_1$  and  $z_3$ .
- (ii) Evaluate stability parameter  $B$  as given by

$$B = \frac{g}{\bar{T}} \cdot \frac{t(z_1) - t(z_3)}{\bar{u}^2(z_2)} \quad (5.9)$$

where  $g$  is the acceleration due to gravity.



(iii) By trial solutions, obtain stability length  $L$  from the equation (Takeuchi, 1961)

$$B = -\frac{1}{L} \frac{3 \frac{\alpha}{L} + 1.368}{\left(2 \frac{\alpha}{L} + 2.3 \log \frac{z}{z_0}\right)^2} \quad (5.10)$$

where  $\alpha$  is a constant, which can be taken as 0.6 for unstable atmosphere and as 6.0 for stable atmosphere (Sec. 2.2.3.3).

The above procedure is only for open country with  $d = 0$ . If  $d \neq 0$ ,  $z_1$ ,  $z_2$ ,  $z_3$  can be taken as  $(z_1 - z_0 - d)$ ,  $(z_2 - z_0 - d)$  and  $(z_3 - z_0 - d)$  respectively. Hence temperature records should be at  $z_1 = (z_0 + d + 1)$  m, and  $z_3 = (z_0 + d + 4)$  m, whereas wind anemometer should be placed at  $z_2 = (z_0 + d + 2)$  m.

### 5.5 Estimation of Vertical Spread

Once the surface roughness length  $z_0$  and stability length  $L$  are known, the vertical spread of pollutant at any downwind distance  $\bar{x}$  from the source can be estimated from the formulation given in Chapter Three.

- (i) Calculate the ratios  $z_0/|L|$  and  $k^2 \bar{x}/|L|$  where  $k = 0.4$ .
- (ii) For the pair of values of  $z_0/|L|$  and  $k^2 \bar{x}/|L|$ , selecting appropriate graphs of Figs. (3.6) or (3.7), value of  $\bar{z}/|L|$  can be read off.
- (iii) Obtain  $\bar{z}$  from the ratio  $\bar{z}/|L|$ .

As the surface roughness length  $z_0$  for a particular site remains almost constant, the Figs. (3.6) and (3.7) can re-drawn by denoting  $\bar{z}/z_0$  as ordinate and  $\bar{x}/z_0$  as abscissa. Figs. (5.1) and (5.2) show the re-evaluated graphs for different conditions of  $z_0/|L|$ . For a known value of  $z_0$ , values of  $\bar{x}$  corresponding to values of the ratio  $\bar{x}/z_0$  and similarly for  $\bar{z}$  can be permanently recorded on Figs. (5.1) and (5.2). This can facilitate the use of the graphs. Then for any ratio of  $z_0/|L|$ , at a particular  $\bar{x}$ , value of  $\bar{z}$  can be directly read.

## 5.6 Estimation of Lateral Spread

(1) From the known values of  $\bar{u}(z_1)$ ,  $L$  and  $z_0$ , obtain the value of  $u_*$  from

$$\bar{u} = \frac{u_*}{k} [0.48 - 2.3 \log (z_0/(-L)) - 1.3((z_1-d)/(-L))^{-1/3}] \quad (5.11)$$

$$\text{or } \bar{u} = \frac{u_*}{k} [2.3 \log \frac{z_1-d}{z_0} + \alpha \frac{(z_1-d)}{L}] \quad (5.12)$$

where Eq. (5.11) is for day time unstable and Eq. (5.12) is for night time stable atmospheric conditions.

(ii) At any height  $z$  where concentration of pollutant is required to be computed, evaluate  $\bar{u}(z)$  from Eq. (5.11) or (5.12) depending upon stability conditions.

(iii) If the micrometeorological instrumentation is of case One or Case Two  $\sigma_\theta$  value at height  $z_1$  would be known (Sec. 5.4.1).

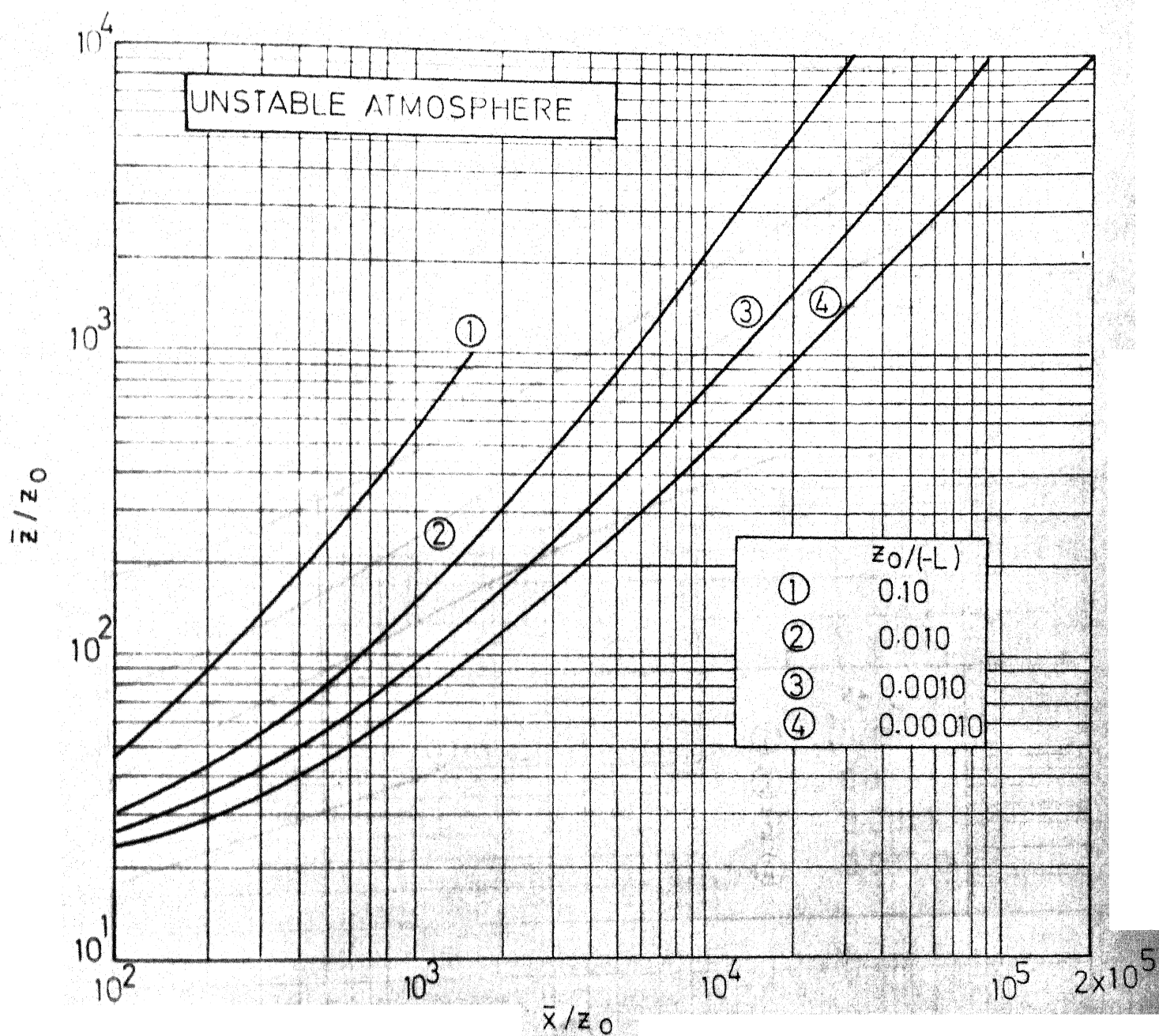


FIG. 5.1 PLOT OF  $\bar{x}/z_0$  Vs  $\bar{z}/z_0$  FOR UNSTABLE ATMOSPHERE

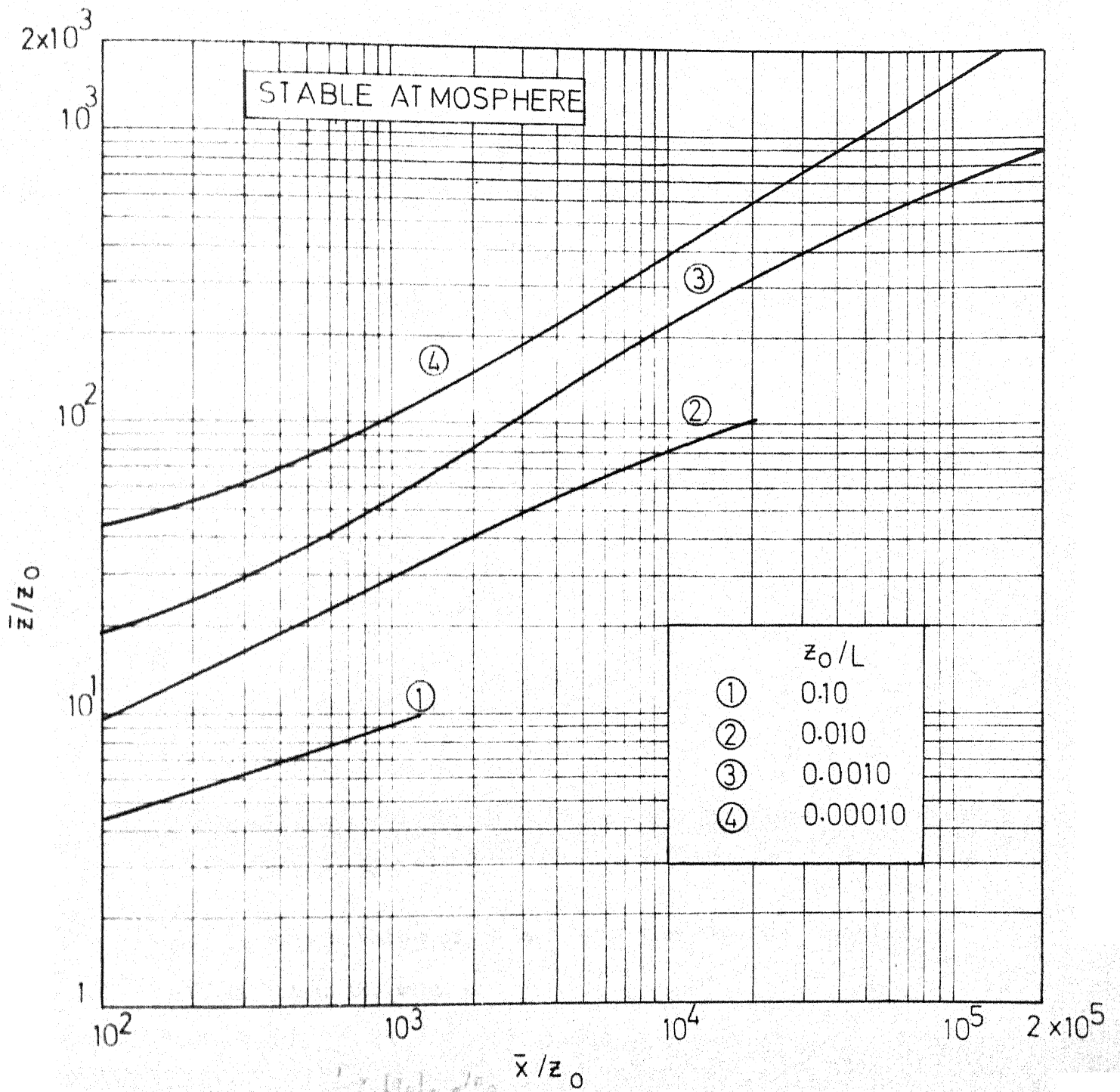


FIG. 5.2 PLOT OF  $\bar{x}/z_0$  VS  $\bar{z}/z_0$  FOR STABLE ATMOSPHERE

The value of  $\sigma_\theta$  at height  $z$  is

$$\sigma_\theta(z) = \frac{\sigma_\theta(z_1) \bar{u}(z_1)}{\bar{u}(z)} \quad (5.13)$$

For instrumentation of case Three, the  $\sigma_\theta$  value can be given by

$$\sigma_\theta(z) = \frac{\beta u_*}{\bar{u}(z)} \quad (5.14)$$

where  $\beta$  can be assumed as 2.25.

(iv) Find the averaging time  $s$  for reaching upto distance  $\bar{x}$  by

$$s = \frac{\bar{x}}{\bar{u} \cdot \beta} \quad (5.15)$$

Here  $\bar{u}$  is what is calculated in Step (ii) above, and  $\beta = 4$  (Hino, 1968b).

(v) Find the sampling time  $\tau$  for which the sample of pollutant would be collected.

(vi) For the values of  $s$  and  $\tau$ , from Fig. 5.3 (after Hino, 1968b), obtain the value of

$$\frac{1}{2} \times [\sigma_\theta]_{\tau, s} / \sigma_\theta$$

(vii) From Eq. (3.59)

$$\sigma_y = \bar{x} [\sigma_\theta]_{\tau, s} \quad (5.16)$$

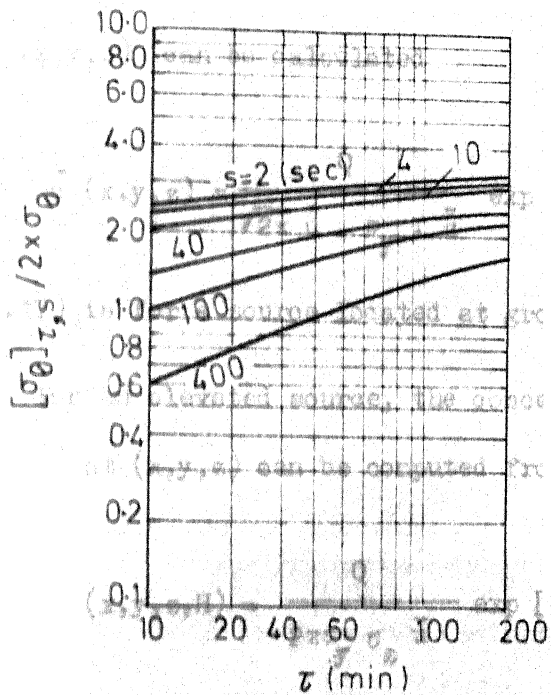


FIG. 5.3 RELATION BETWEEN THE RATIO OF HALF WIDTH OF MAXIMUM FLUCTUATIONS THE r.m.s VALUE AND THE SAMPLING TIME  $\tau$  (AFTER HINO, 1968 b)

### 5.7 Estimation of Concentration Distribution

From Eq. (3.70), for any known value of quantity of pollutant released per unit time,  $Q$ , the concentration at any point  $(x,y,z)$  can be calculated

$$\bar{c}(x,y,z) = \frac{Q}{\sqrt{2\pi} \bar{u} \cdot \sigma_y \cdot z} \exp \left[ -\frac{1}{2} \frac{y^2}{\sigma_y^2} - \frac{z}{z} \right] \quad (5.17)$$

Eq. (5.17) is for a source located at ground-level.

For an elevated source, the concentration of pollutant at any point  $(x,y,z)$  can be computed from (Turner, 1970)

$$\bar{c}(x,y,z,H) = \frac{Q}{2\pi\sigma_y \sigma_z \bar{u}} \exp \left[ -\frac{1}{2} \frac{y^2}{\sigma_y^2} \right] \times$$

$$\left\{ \exp \left[ -\frac{1}{2} \left( \frac{z-H}{\sigma_z} \right)^2 \right] + \exp \left[ -\frac{1}{2} \left( \frac{z+H}{\sigma_z} \right)^2 \right] \right\} \quad (5.18)$$

where  $H$  is the effective height of the source.

Thus for any given meteorological conditions and pollutant source data, the pollutant concentrations at various points in the air can be predicted. The effect of various source control measures or of changed meteorological conditions can also be predicted to enable planning of a successful pollution control programme.

## Chapter Six

### FIELD STUDIES DONE AT KANPUR

#### 6.1 Introduction

The formulation developed by the author is for a source at or very near ground level. The field data used to validate the formulation were also for sources at or near ground level. If there is a point source at moderate height above the ground level, this method may still give practically comparable results. Theoretically, however, some modifications are warranted, but without going into much of theoretical modifications, applicability of this formulation on the spreads at relatively short distance away from moderately elevated sources was checked. For this purpose, some diffusion studies were carried out in the city of Kanpur.

Kanpur city is situated on the right bank of the river Ganga. Its geographical location is around the latitude of  $26^{\circ} 30'N$ , and the longitude of  $80^{\circ} 20'E$ . It is situated in the gangatic plains, having flat terrain of very moderate slope.

The population of Kanpur is nearly 13 lacs, which makes it the eighth most populous city of the country. It is one of the important industrial centres of India. The campus of Indian Institute of Technology at Kanpur is located at a distance of about 5 km from the outskirts of the city.



## 6.2 Planning of Pollution Studies

For the present study, two sites with different surface roughnesses were selected. Site One was near a power-house situated near the bank of river (hence, named Riverside Power-House). The prevailing winds are from the river side, and smoke emitted by the power-house spreads on to the built-up area of the city around Leather Research Institute. Second site, named Site Two, was within the campus of Indian Institute of Technology near the boiler house in the Southern Laboratories.

It was decided to use sulphur-dioxide as the tracer, as the coal burnt by the power-house has 0.4% sulphur content, and smoke contains easily measurable concentrations of sulphur-dioxide.

The proposed method of estimating vertical spread is valid only in the surface layer of the atmosphere, which has as stated in Sec. 2.2.2, a thickness in the range of 50-200 m. The plume of smoke emitted from the moderately high chimneys in the surface layer would spread vertically as well as laterally and after travelling some distance downwind may spread into the region above the surface layer of the atmosphere. Hence downwind distances selected for the study were relatively short.

It was decided to use hydrogen gas-filled tethered balloon to measure the vertical temperature profile and collecting samples

of air at different heights. As no other micrometeorological information was available for the urban area, vane anemometer was used to record wind speeds. Thus, instrumentation of case three, as described in Sec. 5.1, i.e. temperature records at two heights and wind speed record at one intermediate height were obtained.

The observed concentrations of sulphur-dioxide at different points were compared with those computed using procedure outlined in the preceding chapter.

### 6.3 Materials and Methods

#### 6.3.1 The Source

##### (a) Site One

The cluster of five chimneys of the Riverside Power-House was taken as the source of  $\text{SO}_2$ -pollutant. The power-house has a power generating capacity of 1.1. million units per day. It has 15 boilers, fed on coal from Ranigang series of coal mines. Table 6.1 gives the details of the chimneys. Table 6.2 gives the particulars of the boilers.

TABLE 6.1

## DETAILS OF CHIMNEYS OF RIVERSIDE POWER-HOUSE, KANPUR

Sr. No.	Height, ft	Diameter, ft	Type	Boilers attached
1	186.33	10	Brick	1,2,3,4
2	204.5	12	Brick	5,6,7,8
3	204.5	12	Brick	9,10,11,12
4	213.25	8.86	Steel	12A,14
5	200.0	8.86	Steel	15

TABLE 6.2

## PARTICULARS OF BOILERS OF RIVERSIDE POWER-HOUSE, KANPUR

Sr. No.	Type	Steam-fbw rate, lb/hr	Coal-burning rate, tons/hr
1	LP	20,000	1.5
2	LP	20,000	1.5
3	LP	20,000	1.5
4	LP	20,000	1.5
5	LP	40,000	2.5
6	LP	40,000	2.5
7	LP	40,000	2.5
8	LP	60,000	2.5
9	HP	100,000	6.0
10	HP	100,000	6.0
11	HP	120,000	6.0
12	HP	120,000	6.0
12A	HP	120,000	6.0
14	HP	120,000	6.0
15	HP	120,000	6.0

The sulphur content of the coal used was 0.4%, as given from the analysis of coal supplied by the power-house authorities.

On the days of experiments, the boilers nos. 1,5,6,9 and 14 were not operating, but remaining 10 were in operation.

(b) Site Two

The chimney of the boiler-house at the end of the Southern Laboratories, I.I.T. Campus, was used to emit known amount of sulphur-dioxide. Sulphur-dioxide was produced by burning sulphur at the bottom of the chimney.

The chimney height is 15.2 m and diameter is 75 cm. The rate of burning of sulphur was maintained at 5.0g/min.

### 6.3.2 Vertical Temperature Measurements

As described in Sec. 5.1, different sets of micrometeorological instruments can be used for estimation of spreads of the pollutant, but it was difficult to go for continuous wind speed and direction records. Hence it was decided to go for the Case Three of Instrumentation. This requires temperature measurements at two heights. For this purpose, a hydrogen gas-filled balloon along with a temperature sensor was used.

#### 6.3.2.1. Materials

(a) Balloons

Rubber balloons, specification No. White S.R. 875, of Swastik Rubber Products Ltd. Poona-3, were used for this study.

These balloons when fully inflated with hydrogen gas assume a diameter of about 150 cm. The price (1973) of the balloon was Rs. 30/- each. For each filling, it requires about 1.5 cubic meters (at atmospheric pressure) of hydrogen gas.

Hydrogen gas obtained in cylinders from Indian Oxygen Co. at the cost of Rs. 350/- per 100 cubic meters was used.

(b) Thermistors

A thermistor was used as a temperature sensor. Different types of thermistors are available for the different types of the uses. Thermistors were purchased from M/s. Tempo Semiconductors (18, Laranjape B Scheme, Subhash Road, Vile Parle (East), Bombay-57AS). Two different types of the thermistors were tried:

(i) Rugged beads (Price: Rs. 12/- each)

(ii) Glass mini-probes (Price: Rs. 20/- each)

6.3.2.2. Methods

(a) Filling the Balloon

Commercial hydrogen gas was used to fill in the rubber balloon. A pressure-rubber tubing was attached to the hydrogen gas cylinder and the other end of the 2-m long tube was put well inside the balloon, and tightened with a piece of cord.

soldered to the thermistor, were about 100 m long. The micro-ammeter was used to measure the unbalanced current, and was protected by putting 1 kilo-ohms resistance in series. A 9-volt battery powered the circuit.

The calibration of the meter was carried out in the accurately-maintained hot water-bath of a Warburg apparatus. The thermistor probe and a mercury thermometer reading upto  $0.1^{\circ}\text{C}$  were put in a test-tube kept in the hot water-bath. Unbalanced current passing through the ammeter was correlated with the temperature.

Out of the two different types of the thermistors, it was found that the rugged-bead type was more suitable for the out-of-door work as it was in the present case.

#### (1) Field Test Layout

Once the thermistor was calibrated, the thermistor sensor and the lead wires were connected to the nylon cord of the balloon. As it was also proposed to collect samples of air at different heights, a plastic tube of 3 mm diameter was also attached to the cord. Thus the combined cord was made up of the plastic tube, two insulated copper wires as the

lead to thermistor circuit, and a nylon cord. All these were connected by light transparent adhesive tape at every 30 cm or less. Tags carrying distance (or height) mark from the probe (and the mouth of the plastic tube) were also attached to the combined cord at every one meter.

The nylon cord attached to the inflated balloon was extended upto about 2m and there it was tied to the combined cord. The balloon was slowly allowed to rise lifting the combined cord along with it. If the atmosphere is not very turbulent and the balloon is properly filled in with the hydrogen gas, the sway of the balloon is almost negligible. The balloon ascends straight up. The box containing the complete circuit of the thermistor was kept on the ground (and so was the instruments for collecting samples of the air through the plastic tube).

The balloon was slowly sent upwards. As the thermistor probe (and also the mouth of the plastic tube) reached specified heights, the balloon was kept floating at that height and the sample of air was collected and the reading in the Wheatstone bridge circuit was recorded. The same procedure was repeated at different heights.

### 6.3.3. Measurement of Wind Velocity

A vane anemometer, was used to record the average wind velocity at a specified height. The recording was done in a cumulative way for every 15 minutes.

#### 6.3.4. Measurement of Sulphur-Dioxide Concentrations

##### (a) Collection of Sample

As it was decided to collect samples of air at different heights, a plastic tube of 3 mm diameter was sent up along with the tethered balloon, as described in the preceding section.

A hand-operated midget vacuum pump was used to suck samples of air. The absorbing solution was put in a midget impinger and the rubber tubing provided at the end of the plastic tube was connected to the impinger. The vacuum pump connection was made at the other outlet of the impinger. The vacuum pump was re-calibrated to know the rate of flow of air through the entire length of the plastic tube (as the head loss increases with the length). The pump was operated for 10 minutes at each sampling. As the rate of flow and period of sampling were known, the total volume of air sampled could be calculated.

##### (b) Analysis

The exposed absorbing sample was analysed by the standard West and Gaeke method which is described in Appendix A-2.

#### 6.4. Results and Discussions

##### 6.4.1. Zero-plane Displacement Length

##### (a) Site One

The average height of buildings around that area is about 40 ft  $\approx$  12 m, making  $h = 12$  m in Eq. (5.1). The value



of  $A$  in Eq. (5.1) is the ratio of total area of a given region to the area of the buildings in that region. Lesser the density of buildings, higher the value of  $A$ . It was observed that the buildings around the Site One were relatively sparsely situated, the ratio of built up area being around 12%, hence value  $A$  was assumed as 9. The value of  $d$  is given by

$$\frac{d}{h} = (A)^{-0.3}$$

where  $h = 12$  m

$$\therefore d = 12 \times (9)^{-0.3}$$

$$\text{or, } d = 6 \text{ m}$$

(b) Site Two

The obstructions were mainly trees and single-storeyed buildings with average height around 6 m. The obstructions are not very thickly located the area occupied by obstructions being around 5-7%, and  $A$  value, consequently, was assumed as 13.

$$d = h(A)^{-0.3}$$

$$= 6(13)^{-0.3}$$

$$\approx 3 \text{ m}$$

#### 6.4.2. Surface Roughness Length

(a) Site One

From Eq. (5.4), the surface roughness length  $z_0$  can be calculated.

$$\frac{z_o}{h} \approx (A)^{-1.1}$$

$$\therefore z_o = 12 \times (9)^{-1.1}$$

$$\approx 1.0 \text{ m}$$

(b) Site Two

The surface roughness length is given by

$$\frac{z_o}{h} \approx (A)^{-1.1}$$

$$= 6 \times (13)^{-1.1}$$

$$\approx 0.4 \text{ m}$$

These values fall well within the independently derived values of  $z_o$  for different roughnesses, shown in Table 2.1.

### 6.4.3. Micrometeorological Measurements

(a) Site One

As discussed in Sec. 5.4.3, temperatures were measured at heights  $z_1 = d + z_o + 1 = 6 + 1 + 1 = 8 \text{ m}$  and  $z_3 = d + z_o + 4 = 6 + 1 + 4 = 11 \text{ m}$ . Wind velocity record was obtained at height  $z_2 = d + z_o + 2 = 6 + 1 + 2 = 9 \text{ m}$ .

For the temperature measurements, the thermistor was calibrated. The calibration graph of the current (in  $\mu\text{A}$ ) versus temperature (degrees, C) showed that for the range of the temperature of interest, i.e.  $10^\circ\text{C}$  to  $50^\circ\text{C}$ , the plot was linear. The slope of the line was  $0.1^\circ\text{C}$  per  $\mu\text{A}$ .

Every time when the thermistor was at 1 m above the surface of the earth, the ammeter was adjusted to the central reading of 50 A. The corresponding actual temperature at that height was noted down with the help of a mercury thermometer (reading upto  $0.1^{\circ}\text{C}$ ). When the thermistor sensor was sent up in the air, the change in the ammeter reading was noted down and was converted into difference in temperature in  $^{\circ}\text{C}$ . This could avoid the use of calibration curve for every time converting the ammeter reading to corresponding temperature reading.

Temperature readings for 8 m and 11 m were interpolated from temperature profile obtained upto height of 40 m.

#### (b) Site Two

The temperatures were measured at heights  $z_1 = d + z_0 + 1 = 3 + 0.4 + 1 = 4.4$  m, and  $z_3 = d + z_0 + 4 = 3 + 0.4 + 4 = 7.4$  m, whereas wind velocity was measured at a height of  $z_2 = d + z_0 + 2 = 3 + 0.4 + 2 = 5.4$  m.

At each site, three different runs were carried out at three different distances from the source, as shown in Table 6.3. During each run, concentrations and temperatures at three different heights were measured. Stability conditions were different for these three runs of study. Table 6.3 reports the temperatures and wind speed measurements.

TABLE 6.3

## WIND SPEED AND VERTICAL TEMPERATURES FOR KANPUR STUDY

Run No.	Downwind distance $\bar{x}$ , m	Temp. @ $z_1$ m, °C	Temp. @ $z_3$ m, °C	Wind Speed @ $z_2$ m, m/sec.	Period, hrs
(a) Site One					
1	700	19.40	18.60	0.780	Noon
2	400	16.90	16.84	0.304	Late afternoon
3	200	15.10	15.12	0.122	Evening
(b) Site Two					
4	100	28.15	28.025	0.480	Noon
5	200	27.60	27.63	0.360	Late evening
6	100	32.50	32.51	0.265	Early evening

Substituting these values in Eq. (5.9), the values of stability parameter B were calculated; from which, using Eq. (5.10) values of stability length L were derived, as reported in Table 6.4.

TABLE 6.4  
VALUES OF STABILITY PARAMETERS FOR KANPUR STUDY

(a) Site One			(b) Site Two		
Run No.	$B, \frac{-1}{m}$	$L, m$	Run No.	$B, \frac{-1}{m}$	$L, m$
1	0.042	-70	4	0.0178	-30
2	0.022	-130	5	-0.0075	70
3	-0.046	45	6	-0.0046	115

#### 6.4.4. Calculation of Vertical Spreads

From the estimated values of  $z_0$  and  $L$ , the vertical spreads can be calculated from Figs. 5.1 and 5.2, for appropriate values of  $\bar{x}$ . Here,  $z_0$  being 1 m, the figures 5.1 and 5.2 represent  $\bar{x}$  and  $\bar{z}$  values, for Site One.

The results are shown in Table 6.5.

TABLE 6.5  
VERTICAL SPREADS  $\bar{z}$  FOR KANPUR STUDY

(a) Site One		(b) Site Two	
Run No.	$\bar{z}, m$	Run No.	$\bar{z}, m$
1	115	4	20.0
2	62	5	11.2
3	15	6	9.2

### 6.4.5. Calculation of Lateral Spreads

According to the steps given in Sec. 5.6, the lateral spreads were calculated. The results of important steps are shown in Table 6.6.

TABLE 6.6

LATERAL SPREADS  $\sigma_y$  FOR KANPUR STUDY

Run No.	$u_*$ m/Sec.	Height $z$ , m	$\bar{u}(z)$ , m/sec.	$\sigma_\theta$ , radians	$\tau$ , min	$s = \frac{x}{\bar{u}(z)\beta}$	$\sigma_y$ , m
(a) Site One							
1	0.461	20	2.890	0.358	10	60.5	650
		30	3.300	0.314	10	53.0	595
		40	3.540	0.292	10	49.5	573
2	0.178	20	1.160	0.345	10	86.2	330
		30	1.360	0.294	10	73.5	294
		40	1.475	0.282	10	67.8	288
3	0.122	20	0.575	0.200	10	87.0	96
		30	0.810	0.142	10	52.0	77
		40	1.060	0.108	10	47.0	61
(b) Site Two							
4	0.123	10	0.918	0.300	10	27.2	102
		20	1.250	0.220	10	20.0	79
		30	1.450	0.191	10	17.3	71
5	0.081	10	0.700	0.260	10	71.5	130
		20	1.050	0.174	10	47.6	97
		30	1.325	0.138	10	37.8	80
6	0.062	10	0.500	0.279	10	50.0	76
		20	0.717	0.194	10	34.8	57
		30	0.870	0.160	10	28.8	54

#### 6.4.6. Computation of Concentrations

Firstly, the quantity of  $\text{SO}_2$  emitted at the source is computed in each case, and reported as  $Q$ , g/sec. As the distances at which the concentrations are measured are very short, the correction for the plume rise need not be applied (Turner, 1970). The actual heights of the chimneys are taken as the effective heights.

For Site One, the total quantities of fuel burnt on those days worked out to be 39.5 tonnes/hr. Taking 0.4% as the sulphur content, 64 molecular weight of  $\text{SO}_2$ , 32 molecular weight of S, the quantity of  $\text{SO}_2$  being released per second works out as

$$Q = \frac{39.5(\text{tonnes}) \times 10^6(\text{g/tonnes}) \times 0.004(\text{g/g}) \times 64(\text{mol.wt of SO}_2)}{1(\text{hr}) \times 3600(\text{sec/hr}) \times 32(\text{mol. wt. of S})}$$

$$= 88 \text{ g/sec of SO}_2.$$

For Site Two, the 5 g of sulphur was burnt per min. Hence

$$Q = \frac{5(\text{g/g}) \times 64(\text{mol. wt. of SO}_2)}{1(\text{min}) \times 60(\text{sec/min}) \times 32(\text{mol. wt. of S})}$$

$$= 0.167 \text{ g/sec of SO}_2.$$

Results of the computed and observed concentrations are given in Table 6.7.

Sampling stations were selected as near as possible to the anticipated mean center line; hence,  $y \approx 0$ , for each sun.

TABLE 6.7  
POLLUTANT CONCENTRATION VALUES FOR KANPUR STUDY

Run No.	z, m	Observed concentration, $C_o$ , ppm	Computed concentration, $C_c$ , ppm	$\frac{C_c}{C_o}$
(a) Site One				
1	20	0.0420	0.0427	1.020
	30	0.0375	0.0420	1.120
	40	0.0380	0.0417	1.100
2	20	0.3170	0.2780	0.877
	30	0.3620	0.2770	0.766
	40	0.2800	0.2760	0.986
3	20	0.1510	0.1620	1.070
	30	0.6000	0.7650	1.280
	40	1.4210	2.3900	1.680
(b) Site Two				
4	10	0.0067	0.0075	1.120
	20	0.0055	0.0065	1.170
	30	0.0050	0.0047	0.930
5	10	0.0120	0.0098	0.816
	20	0.0105	0.0093	0.880
	30	0.0000	0.0040	-
6	10	0.0330	0.0293	0.890
	20	0.0312	0.0290	0.930
	30	0.0900	0.0790	0.880



#### 6.4.7 Discussion of Results

From the values of pollutant concentrations given in Table 6.7, the following points can be observed:

- (i) Based on the proposed formulation, the vertical and horizontal spreads and thence the pollutant concentrations can be calculated which are generally comparable to the observed concentrations.
- (ii) During unstable atmospheric conditions, for both the sites of investigation, concentrations computed agreed very closely with observed ones. The variation of the ratio of computed to observed concentrations was within the range of 0.766 to 1.17, which for the statistical variation of the entity may be considered as reasonably narrow.
- (iii) Stable atmospheric conditions gave generally close agreement between computed and observed concentrations for the area of low surface roughness like Site Two was. The ratio of computed to observed values of concentrations was between 0.816 to 0.93.
- (iv) At the area having large surface roughness, like Site One, the agreement between computed and observed concentrations was rather poor, during very stable atmospheric conditions. The ratio of computed to observed concentrations lies in the range of 1.07 to 1.68. As discussed earlier, this may be regarded mainly due to inadequate wind profile formulation during very stable atmospheric

conditions and also due to effects of urban heating.

(v) Applicability of the formulation during neutral atmospheric conditions could not be verified in this study at Kanpur, as none of the experimental run was conducted in such conditions.

From this study, it appears that the proposed formulation may be used to predict concentrations at any point downwind from a source either at or near the ground-level. The procedure used here to compute concentrations of pollutant requires the micrometeorological data which can be relatively easily collected. The procedure incorporates, in a quantitative manner, effects of different surface roughnesses and of different atmospheric stability conditions.

## Chapter Seven

### CONCLUSIONS

Lagrangian similarity theory has been applied to diffusion phenomenon to predict the vertical spreads of pollutants released from a source situated in the surface layer of the atmosphere.

Based on the investigations given in the preceding chapters, the following conclusions can be drawn:

- (1) Extended Monin's Approach to represent plume boundaries by his equations generally yields lower estimation of vertical spreads for all atmospheric conditions, and is hence not reliable.
- (ii) Mathematical equations can be developed to represent the vertical spread of the mean of the ensemble of particles at any mean downwind distance from the source, as has been done by the author in Chapter Three.
- (iii) For both low as well as high surface roughnesses, the formulations proposed by the author give very good predictions of vertical spreads in unstable as well as neutrally stable atmospheric conditions.
- (iv) For stable atmospheric conditions, the formulation gives comparable results upto  $\bar{z}/L \leq 0.1$ . Beyond this level, the divergence between observed vertical spread and computed vertical

spread becomes considerable. This is probably due to inadequacies in the present-day knowledge to express wind profiles mathematically in very stable atmospheric conditions.

(v) Unlike other available formulations, the proposed mathematical formulation (and tables and charts prepared therefrom) can be successfully used to predict the quantitative effects of different surface roughnesses and different stability conditions of the atmosphere.

(vi) This formulation can be used with even minimum micrometeorological instrumentation (viz., temperature records at two predetermined heights and wind velocity at one height) without recourse to the use of a number of empirical coefficients, as is necessary in various existing formulations.

(vii) Very little micrometeorological information is presently available which can be useful for the prediction of concentrations of pollutants even in urban and industrial complexes where air pollution potential is very high. During planning of air quality management of a region, along with instrumentation for monitoring extent of air pollution, instrumentation for collecting micrometeorological data should also be planned. Instruments for recording turbulence field would be ideal, but if they are not available, as shown by the present investigations, at least instruments for recording wind velocity, wind directions and temperature profile

should be installed, and such records must be routinely collected for all the urban and industrial areas.

#### Limitations of the Proposed Approach and Direction for Future Research

The major limitation of the proposed formulation is that it applies strictly in the surface layer of the atmosphere. Although many of the sources of air pollution are located within this layer, tall chimneys of industrial complexes may emit pollutants in the region beyond this layer and diffusion phenomenon for such cases does not lend itself to easy mathematical formulation.

The proposed formulation applies to the case of a single point source. To extend its use to a multiple-source urban diffusion problem would be a little unwieldy, because contribution from each source located upwind has to be calculated separately and formulation proposed here does not relate  $\bar{x}$  and  $\bar{z}$  by a simple form.

Hence, it would be interesting to investigate, in future, the usefulness of the proposed formulation to the study of multiple-source diffusion problem, and to suggest, if possible, simple relation between  $\bar{x}$  and  $\bar{z}$ .

The problem of diffusion in very stable atmospheric conditions also needs further investigations. Valid mathematical formulation for the vertical wind profile during such stable conditions of atmosphere is very much essential for any work of the type proposed here.

More exploration is required for this purpose. Looking to the fact that the very stable atmospheric conditions impede the capacity of the air to disperse pollutants and hence the pollutant concentrations build up, adequate mathematical relations are required to predict concentrations during such conditions of the atmosphere for the successful management of air quality in any region.

APPENDIX A-1

COMPUTER PROGRAMME FOR NUMERICAL INTEGRATION USING  
GAUSS-LEGENDRE QUADRATURE

```
C      SIMILARITY THEORY
C      SOLVING (DX/DZ) NUMERICALLY
C      GAUSS-LEGENDRE QUADRATURE WITH FOUR POINTS
C      INT=INTERVAL
C      LF=FINAL LIMIT
C      M=NUMBER OF POINTS IN GAUSS-LEGENDRE QUADRATURE=4
C      NZ=NUMBER OF STEPS
C      A=INITIAL LIMIT
C      AO=AREA OF INTERVAL,ORIGINAL
C      AN=NEW AREA
C      NZO=NUMBER OF ZO/L
      COMMON AI,I
      DIMENSION ZO(10),AI(10)
      READ 100,INT,LF,M,NZO
100    FORMAT(4I5)
      READ 110,(AI(I),I=1,NZO)
110    FORMAT(7F7.3)
      READ 120,(ZO(I),I=1,NZO)
```

```

120  FORMAT(7F7.4)

      AO=0.0

      A=0.0

      NS=LF/INT

      DO 2 I=1,NZO

        IPRINT 200,ZOL(I)

200  FORMAT (1H,15X,5HZO/L=,2X,F7.4)

      IPRINT 201

201  FORMAT (1H,10X,3HZ/L,22X,5HKBX/L,15X,4HZ/ZO,15X,4HX/ZO)

      DO 1 J=1,100

        B=A+FLOAT( INT)

        AREA=GAUSS(A,B,M)

        AN=AO+AREA

        IF (J.EQ.100) GO TO 10

        AO=AN

        A=B

        GO TO 11

10   A=0.0

      AO=0.0

11   B1=B/(ZOL(I))

      A1=(AN/(ZOL(I)))/0.48

      IPRINT 202,B,AN,B1,A1

202  FORMAT(/1H,5X,F10.3,10X,F15.6,10X,F15.6,10X,F15.6)

1    CONTINUE

```



2 CONTINUE

STOP

END

FUNCTION FUNCTN(X)

COMMON AI,I

DIMENSION AI(10)

FUNCTN=(AI(1)-1.3/(X\*\*(1./3.)))/((1.+7.\*X)\*\*(1./6.))

RETURN

END

FUNCTION GAUSS (A,B,M)

C=(B-A)/2.0

D=(B+A)/2.0

SUM=0.65214\*(FUNCTN(0.33998\*C+D)+FUNCTN(-0.33998\*C+D)) +

1 0.34786\*(FUNCTN(0.86113\*C+D)+FUNCTN(-0.86113\*C+D))

GAUSS=C\*SUM

RETURN

END

## APPENDIX A-2

### STANDARD WEST AND GAEKE METHOD FOR MEASUREMENT OF SULPHUR DIOXIDE IN AIR (Indian Standard IS : 5182 (Part II) - 1969)

#### 1. Reagents

- (a) Absorbing solution 0.1 M sodium tetrachloromercurate.

Dissolve 27.2 g mercuric chloride and 11.7 g sodium chloride in 1 litre of distilled water.

- (b) p-Rosaniline hydrochloride.

Dissolve 0.20 g of p-rosaniline hydrochloride in 100 ml of distilled water and filter the solution after 48 hrs. Pipette 20 ml of this into a 100-ml volumetric flask. Add 6 ml of concentrated hydrochloric acid. Allow to stand for 5 minutes, then dilute to mark with distilled water.

- (c) Formaldehyde solution.

Dilute 5 ml of 40% formaldehyde solution to 1 litre with distilled water.

- (d) Sodium sulphite solution

Dissolve 640 mg of sodium metabisulphite in 1.0 litre of water. Standardize. 1 ml = 150  $\mu$ l of  $\text{SO}_2$ .

#### 2. Procedure

- (a) Preparation of standard curve

(i) Pipette exactly 2 ml of standard sulphite solution into a 100-ml volumetric flask and dilute to mark with absorbing reagent. This final solution contained 3.0  $\mu$ l of  $\text{SO}_2$  per ml.

(ii) Add accurately 0.5, 1.0, 1.5 and 2.0 ml portions of the dilute standard sulphite solution to a series of 10-ml volumetric flasks and dilute to the marks with absorbing reagent. Continue with the analysis procedure given in 2(b).

(iii) Plot the absorbance as the ordinate against the  $\mu\text{l}$  of  $\text{SO}_2$  per 10 ml of absorbing solution.

### (b) Analysis

(i) Set up a sampling train consisting of absorber, metering device, and air pump in this order.

(ii) Pipette exactly 10 ml of absorbing reagent into the absorber. Aspirate the air sample at a rate of 0.2 to 2.5 litres per min. At the end of the sampling time, stop the pump and detach the absorber for titration.

(iii) Add 1.0 ml of p-rosaniline solution and 1.0 ml of formaldehyde solution and mix well.

(iv) After 20 min read the absorbance at 560 m $\mu$  in a spectrophotometer with a 10-ml unexposed absorbing solution as the blank for reference.

### 3. Calculation

(i) Concentration of  $\text{SO}_2$  in air is :

$$\text{SO}_2, \text{ ppm by volume} = \frac{\mu\text{l of SO}_2}{\text{Volume of air sampled}}$$

$$(ii) \quad \text{SO}_2, \text{ ppm by volume} \times \frac{64 \times 10^6}{24470} = \text{SO}_2, \mu\text{g/m}^3.$$

## REFERENCES

- Anisimova, E.P., A.A. Pivovarov, and N.A. Okhanova, 1965 : Dependence of the roughness parameter of the sea surface on wind velocity. Izvestiya Atmos. Oceanic Phys., 1, 640-642.
- A.S.M.E. Committee, 1968 : Recommended Guide for the Prediction of Dispersion of Airborne Effluents. Am. Soc. Mech. Engr., New York, N.Y., 85 pp.
- Barad, M.L., and D.A. Haugen, 1959: A preliminary evaluation of Sutton's hypothesis for diffusion from a continuous point source. J. Meteorol., 16, 12-20.
- Batchelor, G.K., 1953: The conditions for dynamical similarity of motions of a frictionless perfect-gas atmosphere. Quart. J. Roy. Meteorol. Soc., 79, 224-235.
- Batchelor, G.K., 1959 : Some reflections on the theoretical problems raised at the symposium. In Atmospheric Diffusion and Air Pollution, edited by F.N. Frenkiel and P.A. Sheppard, Advances in Geophysics, 6, Academic Press, New York, N.Y., 449-452.
- Bosanquet, C.H., and J.L. Pearson, 1936 : The spread of smoke and gases from Chimneys. Trans. Faraday Soc., 32, 1249-1263.
- Bowne, N.E., 1969 : A simulation model for air pollution over Connecticut. J. Air. Poll. Control Assoc., 19, 570-574.

- Busch, N. and H.A. Panofsky, 1968 : Recent spectra of atmospheric turbulence. Quart. J. Roy. Meteorol. Soc., 94, 132-148.
- Businger, J.A., J.C. Wyngaard, Y. Izumi, and E.F. Bradley, 1971: Flux profile relationships in the atmospheric surface layer. J. Atmos. Sc., 28, 181-189.
- Calder, K.L., 1949 : Eddy diffusion and evaporation in flow over aerodynamically smooth and rough surfaces: a treatment based on laboratory laws of turbulent flow with special references to conditions in the lower atmosphere. Quart. J. Mech. and Applied Math., 2, 153-176.
- Carnahan, B., H.A. Luther, and J.O. Wilkes, 1969 : Applied Numerical Methods. John Wiley & Sons, New York, N.Y., 604 pp.
- Cermak, J.E., 1963 : Lagrangian similarity hypothesis applied to diffusion in turbulent shear flow. J. Fluid Mech., 15, 49-64.
- Clarke, J.F., 1964: A simple diffusion model for calculating point concentrations from multiple sources. J. Air Poll. Control Assoc., 14, 347-52.
- Cohen, L.D., S. Barr, R. Krablin, and H. Newstein, 1972 : Steady-state vertical turbulent diffusion of Radon. J. Geophys. Res., 77, 2654-2664.
- Cramer, H.E., 1959 : Engineering estimates of atmospheric disposal capacity. Am. Ind. Hyg. Assoc. J., 20, 183-197.

- Davenport, A.G., 1961 : The spectrum of horizontal gustiness near the ground in high winds. Quart. J. Roy. Meteorol. Soc., 87, 194-202.
- Davies, D.R., 1950 : Three-dimensional turbulence and evaporation in the lower atmosphere. Quart. J. Mech. & Applied Math., 3, 64-73.
- Deacon, E.L., 1949: Vertical diffusion in the lowest layers of the atmosphere. Quart. J. Roy. Meteorol. Soc., 75, 89-103.
- Deacon, E.L., 1957: Wind profiles and the shearing stress-an anomaly resolved. Quart. J. Roy. Meteorol. Soc., 83, 537-540.
- Downie, N.M., and R.W. Heath, 1965: Basic Statistical Methods. Harper and Low, Pub. New York, N.Y., 325 pp.
- Ellison, T.H., 1957 : Turbulent transport of heat and momentum from an infinite rough plane. J. Fluid Mech., 2, 456-466.
- Ellison, T.H., 1959: Meteorology. Science Progress, 47, 495-506.
- Erdelyi, A., W. Magnus, F. Oberhettinger, and F.G. Tricomi, 1954: Tables of Integral Transforms, Volume I. McGraw-Hill Book Co., New York, N.Y., 391 pp.
- Fortak, H.G., 1970 : Numerical solution of temporal and spatial distributions of urban air pollution concentration. In Proc. Symp. Multiple-Source Urban Diffusion Models, U.S.E.P.A.

- Frenkiel, F.N., 1953 : Turbulent Diffusion. In Advances in Applied Mechanics, edited by Von Mises, R. and T. Von Karman, Vol. III, Academic Press, New York, N.Y. 61-107.
- Gifford, F.A., 1961 : Uses of routine meteorological observations for estimating atmospheric dispersion. Nuclear Safety, 2, 47-51.
- Gifford, F.A., 1962 : Diffusion in the diabatic surface layer. J. Geophy. Res. 67, 3207-3212.
- Gifford, F.A., 1968: An outline of theories of diffusion in the lower layers of the atmosphere. In Meteorology and Atomic Energy, edited by Slade D., U.S. Atomic Energy Commission, 65-116.
- Gifford, F.A., 1970: Atmospheric diffusion in an urban area, 2nd Int. Radiation Protection Assoc. Conf. Brighton, England, 5 pp.
- Gifford, F.A. and S.P. Hanna, 1970: Urban air pollution modelling. 2nd International Clean Air Congress, Washington, 6 pp.
- Godson, W.L., 1958: The diffusion of particulate matter from an elevated source. Archiv. f. Met. Geoph. und Biokl., A, 10, 305-312.
- Godstein, S., 1938: Modern Developments in Fluid Dynamics. University Press, Oxford, 687 pp.

Gurvich, A.S., 1965: Vertical temperature and wind velocity profiles in the atmospheric surface layer. Izvestiya Atmos. Oceanic Phys., 1, 31-36.

Hanna, S.R., 1968: A method of estimating vertical eddy transport in the planetary boundary layer using characteristics of the vertical velocity spectrum. J. Atmos. Sc., 25, 1026-1033.

Hanna, S.R., 1969: Urban micrometeorology. American Nuclear Safety Meeting, San Francisco, 10 pp.

J Hanna, S.R., 1971: A simple method of calculating dispersion from urban area sources. J. Air Poll. control Assoc., 21, 774-777.

J Haugen, D.A., M.L. Barad, and P. Antanaitis, 1961: Values of parameters appearing in Sutton's diffusion models. J. Meteorol., 18, 368-372.

Hay, J.S. and F. Pasquill, 1957: Diffusion from a fixed source at a height of a few hundred feet in the atmosphere. J. Fluid Mech., 2, 299-310.

Hay, J.S., and F. Pasquill, 1959: Diffusion from a continuous source in relation to the spectrum and scale of turbulence. In Atmospheric Diffusion and Air Pollution, edited by F.N. Frenkel and P.A. Sheppard, Advances in Geophysics, 6, Academic Press, New York, N.Y., 345-365.



- Heins, T.S. and L.K. Peters, 1973: The effects of a horizontal impervious layer caused by a temperature inversion aloft on the dispersion of pollutants in the atmosphere. Atmos. Environ., 7, 39-48.
- Hewson, E.W., 1955: Meteorological problems in air pollution control. Procd. 1st Int. Congress of Air Poll., 50-63.
- Hino, M., 1968a: Computer experiment on smoke diffusion over a complicated topography. Atmos. Environ., 2, 541-558.
- Hino, M., 1968b: Maximum ground-level concentration and sampling time. Atmos. Environ., 2, 149-165.
- Inoue, E., 1959: The effects of thermal stratification on turbulent diffusion in the atmospheric surface layer. In Atmospheric Diffusion and Air Pollution, edited by F.N. Frenkiel and P.A. Sheppard, Advances in Geophysics, 6, Academic Press, New York, N.Y., 319-330.
- Jaffe, S., 1967: A three-layer diffusion model as applied to unstable atmospheric conditions. J. Appl. Meteorol., 6, 297-300.
- Kapur, J.N., and H.C. Saxena, 1972: Mathematical Statistics. S. Chand & Co., New Delhi, 519 pp.
- Kazanskii, A.B., 1965: On the critical Richardson number. Izvestiya Atmos. Oceanic Phys., 1, 507-508.

- Khamis, S.H., 1965: Tables of the Incomplete Gamma Function Ratio  
Justus Von Liebig Verlag Darmstadt, Germany, 412 pp.
- Koogler, J.B., R.S. Sholtes, A.L. Danis, and C.I. Harding, 1967:  
A multivariate model for atmospheric dispersion prediction.  
J. Air Poll. Control Assoc., 17, 211-214.
- Lamb, R.G., 1973: Note on the application of K-theory to diffusion  
problems involving nonlinear chemical reactions. Atmos.  
Environ., 7, 257-263.
- Leonard, R.P., 1959: Long range cloud diffusion in the lower atmosphere.  
J. Air Poll. Control Assoc., 9, 77-82.
- Lumley, J.L., and H.A. Panofsky, 1964: The Structure of Atmospheric  
Turbulence. Interscience, New York, N.Y., 239 pp.
- ✓ Magill, P.L., F.R. Holden, and C. Ackley (eds), 1956: Air Pollution  
Hand book, McGraw-Hill Book Co., New York, N.Y.
- Martin, D.O., 1971: An urban diffusion model for estimating long  
term average values of air quality, J. Air Poll. Control  
Assoc., 21, 16-19.
- Matveev, L.T., 1967: Physics of the Atmosphere. Israel Program for  
Scientific Translation, Jerusalem, 699 pp.
- ✓ McElroy, J.L., and F. Pooler, 1968a: St. Louis Dispersion Study,  
Volume I. National Air Poll. Control Admi., Durham ,  
N.C., 352 pp.
- ✓ McElroy, J.L., and F. Pooler, 1968b: St. Louis Dispersion Study, Volume II.  
National Air Poll. Control Admi., Durham, N.C., 51 pp.

- Miller, M.E., and G.C. Holzworth, 1967: Air atmospheric model for metropolitan areas. J. Air Poll. Control Assoc., 17, 46-50.
- Monin, A.S., and A.M. Obukhov, 1954: Basic regularity in turbulent mixing in the surface layer of the atmosphere. Tr. Geofiz. Inst. Akad. Nauk SSSR, 151, 163-187.
- Monin, A.S., 1959a: General survey of atmospheric diffusion. In Atmospheric Diffusion and Air Pollution, edited by F.N. Frenkiel and P.A. Sheppard, Advances in Geophysics, 6, Academic Press, New York, N.Y., 29-40.
- Monin, A.S., 1959b: Smoke propagation in the surface layer of the atmosphere. In Atmospheric Diffusion and Air Pollution, edited by F.N. Frenkiel and P.A. Sheppard, Advances in Geophysics, . Academic Press, New York, N.Y., 331-343.
- Monin, A.S., 1962: Empirical data on turbulence in the surface layer of the atmosphere. J. Geophy. Res., 67, 3103-3109.
- Monin, A.S., 1965: On the symmetry properties of turbulence in the surface layer of air. Izvestiya Atmos. Oceanic Phys., 1, 25-29.
- O'Brien, J.J., 1965: An investigation of the diabatic wind profile of the atmospheric boundary layer. J. Geophy. Res., 70, 2277-2290.

- O'Brien, J.J., 1970: A note on the vertical structure of the eddy exchange coefficient in the planetary boundary layer. J. Atmos. Sc. 27, 1213-15.
- Tagurova, V.I., 1961: Tables of the Exponential Integral. Pergamin, Oxford, 151 pp.
- Pandolfo, J.P., 1966: Wind and temperature profiles for constant-flux boundary layer in lapse conditions with a variable eddy conductivity to eddy viscosity ratio. J. Atmos. Sc., 23, 495-502.
- Danofaley, H.A., A.K. Blackadar, and G.E. McVehil, 1960: The diabatic wind profile. Quart. J. Roy. Meteorol. Soc., 86, 390-398.
- Iansfsky, H.A., and R. McCormick, 1960: The spectrum of vertical velocity near the surface. Quart. J. Roy. Meteorol. Soc., 86, 495-503.
- Iansfsky, H.A., and B. Irasad, 1965: Similarity theories and diffusion. Int. J. Air and Water Poll., 9, 419-430.
- Pasquill, F., 1961: The estimation of the disprsn of wind borne material. Meteorol Mag., 90, 33-49.
- Pasquill, F., 1962a: Atmospheric Diffusion. D. Van Nostrand Co., London, 297 pp.
- Pasquill, F., 1962b: Recent broad-band spectral measurement of turbulence in the lower atmosphere. J. Geophy. Res., 67, 3025-3028.

- Pasquill, F., 1966: Lagrangian similarity and vertical diffusion from a source at ground level. Quart. J. Roy. Meteorol. Soc., 92, 185-195.
- Pasquill, F., 1970a: Prediction of diffusion over an urban area—current practice and future prospects. In Proc. Symp. Multiple-Source Urban Diffusion Models, U.S.E.P.A.
- Pasquill, F., 1970b: Discussions. In Proc. Symp. Multiple-Source Urban Diffusion Models U.S.E.P.A.
- Pasquill, F., 1971: Wind structure in the atmospheric boundary layer. Phil. Trans. Roy. Soc., London, A, 269, 439-456.
- Peters, L.K., and G.E. Klinzing, 1971: The effect of variable diffusion coefficients and velocity on the dispersion of pollutants. Atmos. Environ., 5, 497-504.
- Prandtl, L., and O.G. Tietjens, 1934: Applied Hydro and Aeromechanics, McGraw-Hill Co., New York, N.Y., 311 pp.
- Priestley, C.H.B., 1959: Turbulent Transfer in the Lower Atmosphere. Uni. of Chicago Press, Chicago, 130 pp.
- Randerson, D., 1970: A numerical experiment in simulating the transport of sulfur dioxide through the atmosphere. Atmos. Environ., 4, 615-632.
- Richardson, L.F., 1926: Atmospheric diffusion shown on a distance-neighbour graph. Proc. Roy. Soc., London, A, 110, 709-737.

- Rider, N.E., 1954: Eddy diffusion of momentum, water vapour and heat near the ground. Phil. Trans. Roy. Soc., London, A, 246, 481-501.
- Roberts, J.L., E.J. Croke, and A.S. Kennedy, 1970: An urban atmospheric dispersion model. In Proc. Symp. Multiple-source Urban Diffusion Models, U.S.E.I.A.
- Rounds, W., 1955: Solutions of the two-dimensional diffusion equations. Trans. Am. Geophys. Union, 36, 395-405.
- Rouse, H., 1959: Advanced Mechanics of Fluids. John Wiley & Sons, New York, N.Y., 444 pp.
- Shieh, L.J., B. Davidson, and J.F. Friend, 1970: A model of diffusion in urban atmospheres:  $\text{SO}_2$  in Greater New York. In Proc. Symp. Multiple-source Urban Diffusion Models, U.S.E.P.A.
- Shir, C-C., 1970: A pilot study in numerical techniques for predicting air pollutant distribution downwind from a line stack. Atmos. Environ., 4, 387-407.
- Shive, J.N., 1960: The Properties, Physics, Design of semi-conductor Devices. D. Van Nostrand Co., London, 487 pp.
- Singer, I.A., J.A. Frizzola, and M.E. Smith, 1966: A simplified method of estimating atmospheric diffusion parameters. J. Air Poll. Control Assoc., 16, 594-596.
- Singer, I.A., and M.E. Smith, 1966: Atmospheric dispersion at Brookhaven National Laboratory. Int. J. Air Water Poll., 10, 125-135.

Smith, F.B., 1957: The diffusion of smoke from a continuous elevated point-source into a turbulent atmosphere.

J. Fluid Mech., 2, 49-76.

Sutton, O.G., 1934: Wind structure and evaporation in a turbulent atmosphere. Iroc. Roy. Soc., A, 146, 701-716.

Sutton, O.G., 1953: Micrometeorology. McGraw-Hill, New York, N.Y., 333 pp.

Swinbank, W.C., 1962: Wind profile in thermally stratified flow.

Nature, 186, 463-464.

Swinbank, W.C., 1964: The exponential wind profile. Quart. J. Roy.

Meteorol. Soc., 90, 119-135.

Takeuchi, K., 1961: On the structure of the turbulent field in the surface boundary layer. J. Meteorol. Soc. Japan, 39, 346-367.

Taylor, G.I., 1921: Diffusion by continuous movements. Iroc. London Maths. Soc., Ser. 2, 20, 196-207.

Taylor, R.J., 1960: Similarity theory in the relation between fluxes and gradients in the lower atmosphere. Quart.

J. Roy. Meteorol. Soc., 86, 67-78.

Turner, D.B., 1964: A diffusion model for an urban area. J. Appl. Meteorol., 3, 83-91.

Turner, D.B., 1970: Workbook of Atmospheric Dispersion Estimates. U.S.E.I.A., 84 pp.

Walters, T.S., 1962: Diffusion into a turbulent atmosphere from a continuous point source, and from an infinite across-wind line source at ground level. Int. J. Air Water Poll. 6, 349-352.

Wanta, R.C., 1968: Meteorology and Air Pollution. In Air Pollution Vol. I, edited by A.C. Stern, Academic Press, New York, N.Y., 187-226.



## APPEND A

### Replies to the comments of Thesis Examiners

#### Examiners' Report No. 1

- (1) The point observed is correct, as  $z$  in Eq. (2.4a) is from the Earth's surface, whereas  $z$  in Eq. (2.4b) is from a basis where  $\bar{u} = 0$ .
- (2) Although it is true that Pasquill (1966) has proposed that  $z$  in equations (2.50), (2.52) and (2.53) is the mean height of an ensemble of particles, he could not get validation of his proposal in stratified flow. Thus, Pasquill (1966) concluded as :

'If the apparent failure of the current application of similarity theory in stratified flow does indeed arise as suggested above, it is difficult to see how to represent the vertical spread in terms of  $\bar{z}$  alone. A possible alternative is to revert to the type of representation used by Monin (1959).'

In view of the observation made it is suggested that line 10 of the synopsis be read as

'Besides, unlike Monin's approach, where he assumed that the equations of motion represented boundaries of the plume, the author assumes, following Pasquill's suggestion, that the equations of motion be taken to represent the mean height of ensemble of particles.'

- (3) The integral in Eq. (3.35) was evaluated using the Table of Integral Transforms (Erdelyi et al., 1954). It is correct that Laplace Transforms as such were not used.

- (4) The values of  $\bar{z}/(-L)$  for each pair of  $z_0/(-L)$  and  $k^2\bar{x}/(-L)$  could be derived from equations (3.42), (3.43) and (3.47). But within the

engineering limitations of accuracy of measurements of various parameters, the values of  $\bar{z}/(-L)$  derived from the graphs as shown in Fig. 3.6 will be normally good enough.

(5) All these misprints are noted and corrected.

(6) Within the region of  $0 < z < z_0$ , the velocity profile is undefined and hence it is not theoretically correct to evaluate the integrals as indicated in equations just after (3.30), (3.34b), (3.39), (3.51), (3.54) from the boundary 0 to  $\infty$ , but they should have been integrated from  $z_0$  to  $\infty$ . However, the region of 0 to  $z_0$  being very small, the difference in the numerical values is not expected to be significant.

As suggested by the examiner, the evaluation of integral in the range of  $z_0$  to  $\infty$  is carried out below for neutral stability conditions for equations following Eq. (3.30) :

$$\begin{aligned} \frac{d\bar{x}}{dt} &= \frac{\int_{z_0}^{\infty} c \bar{u} dz}{\int_{z_0}^{\infty} c dz} \\ &= \frac{\int_{z_0}^{\infty} c_0 \exp\left(-\frac{z}{\bar{z}}\right) \left(\frac{u_*}{k} \ln \frac{z}{F}\right) dz}{\int_{z_0}^{\infty} c_0 \exp\left(-\frac{z}{\bar{z}}\right) dz} \end{aligned}$$

Writing  $z = z' + z_0$ , i.e., measuring height from  $z_0$  basis and denoting it as  $z'$ ,

$$\frac{d\bar{x}}{dt} = \frac{u_*}{k} \left[ \frac{\int_0^{\infty} \exp\left(-\frac{z'+z_0}{\bar{z}}\right) \left(\ln \frac{z'+z_0}{z_0}\right) dz'}{\int_0^{\infty} \exp\left(-\frac{z'+z_0}{\bar{z}}\right) dz'} \right]$$

Table

$\frac{\bar{z}}{z_0}$	$\frac{\bar{x}}{z_0}$ (new)	$\frac{\bar{x}}{z_0}$ (old)	$\frac{\bar{z}}{z_0}$	$\frac{\bar{x}}{z_0}$ (new)	$\frac{\bar{x}}{z_0}$ (old)
1	1.94	-	50	764	740
5	27.0	-	60	976	950
10	80	55	70	1205	1180
15	143	114	80	1445	1405
20	217	187	90	1690	1650
30	379	350	100	1935	1890
40	563	536			

These calculations indicate that for larger values of  $\bar{z}/z_0$ , (such as 440 in the PPG studies) the values of  $\bar{x}/z_0$  obtained from the procedure followed above will be within 1% of the values computed as in the thesis.

Thus, in Table 4.2 of thesis, the values in columns 3,4 and 5 would remain unchanged.

In the case of other stability conditions, both those stable and unstable ones, the influence of this change would be even smaller and neglecting it would be permissible.

Examiners' Report NO. 2

- (1) The integration on page 65 was checked again and it was found that the result reported in the thesis was correct.
- (2) The suggestion is good, but the assumption of 95% conversion of S to SO<sub>2</sub> is also arbitrary as is of 100%.

Examiners' Report No. 3

Under the heading 'Comments' :

- (1) The values of  $\alpha$  depend on the stability conditions.

For unstable atmosphere, O'Brien (1965) analysed over 2800 wind profiles and arrived at the value of  $\alpha = 0.6$ , which was the same as suggested originally by Monin-Obukhov. This value was adopted for the present study.

For stable atmosphere, however, the variation in the values of  $\alpha$  reported by different authorities was wider. In 1955, Swinbank arrived at  $\alpha = 0.6$ , but later Taylor (1960) reanalysed the numerous wind profiles reported by Swinbank, Monin-Obukhov, etc. and arrived at the value of  $\alpha = 6$  for stable atmosphere, which is adopted here for the present study.

- (2) Equation 2.15 should read

$$\bar{u} = \frac{u_*}{k} [-c(-z/L)^{-1/3} + \text{constant}]$$

- (3) The basis of 0.48 and 2.3 in the expression for  $\bar{u}$  in section 3.3.1 is given on pages 75-76.

Under the heading 'Concentration Distribution' :

(1) It is true that Pasquill suggested a general profile of vertical distribution of concentration as  $\exp(-b z^s)$ ; however, the values  $s$  has not been uniquely offered. Pasquill (1962, p. 188) himself observed:

'When the source is at ground level the vertical distribution evidently requires a different value of  $s$ , which has yet to be generally determined, but which on preliminary evidence is nearer unity.'

Bosanquet-Pearson (1936) and Calder (1952) also observed and adopted  $s = 1$ . As such the simple exponential distribution with  $s = 1$  was adopted.

Similarly, the assumption of Gaussian distribution in the horizontal is also empirical, but there is more evidence for  $s$  nearing 2, and hence Gaussian distribution was adopted.

(2) In Table 4.2, values of  $\bar{z}/(-L)$ ,  $\bar{z}/z_0$  or  $\bar{z}/L$  were read from the appropriate graphs. From these values,  $\bar{z}$  was calculated. To compare these computed  $\bar{z}$  with observed Gaussian  $\sigma_z$  values,  $\bar{z}$  was converted to  $\sigma_z$  by Eq. (4.1) assuming Gaussian distribution. Thus the last column in Table 4.2 gives the ratio of computed  $\bar{z}/0.8$  and observed Gaussian  $\sigma_z$ .

Although there are several models existing, none of them incorporates the effects of both the inhomogeneous turbulence field of different stability conditions of the atmosphere as also of different aerodynamic roughnesses of the underlying surface. In the model proposed here, attempts have been made to incorporate both these

effects and in this respect, it definitely differs from the other existing models.

(4) The experiments carried out at Kanpur were really meant to be only pilot study, to assess the possibility of using the proposed formulation to a point source at moderate height above the ground surface. There were many shortcomings in the experimental work. The vertical profile of temperature and measurement of pollution concentration at different heights were difficult to get. The recourse was to use meteorological balloons which are helpful for the purpose only during relatively low wind speed conditions.

The map of location of powerhouse in Kanpur city is attached.

The background concentration of  $\text{SO}_2$  was negligible in both the sites.

-----  
List of Misprints

Sr. No.	Page	Line	In place of	Read
1	11	Last	Eq. (2.5)	Eq. (2.4)
2	13	11	$z/L = (K_H/K_M) R_1(z/L)$	$z/L = (K_H/K_M) R_1 \phi(z/L)$
3	13	12	$(z/L)$	$\phi(z/L)$
4	72	10, first term in numerator	$\int_0^\infty$	$\int_0^{z^*}$
5	73	2 denominator	$-z$	$-\bar{z}$
6	75	1	Eqs. (3.32a) and (3.32b)	Eqs. (3.33a) and (3.33b)
7	89	3	$ku_* \bar{z}$	$ku_* / \bar{z}$
8	109	3	0.00149	0.00136